RHODES UNIVERSITY

Where leaders learn

Pre-concentration of heavy metals in aqueous environments using electrospun polymer nanofiber sorbents

A thesis submitted to Rhodes University in fulfillment of the requirements for the degree of Doctor of Philosophy (Science)

Godfred Darko

Supervised by

Professor Nelson Torto

Dedication

To Cee; It's all for you... ... .

Acknowledgements

I would like to express my sincere thanks to everyone who was involved or helped in this project. First, I would like to thank the Boss, Prof. Nelson Torto, for his guidance throughout this project. I would also like to convey my appreciation to Prof. James Darkwa and Prof. Aboagye-Menyeh for recommending me to the Boss. I would like to thank Prof. James Hawkins Ephraim, Dr. Maria Baeza Romero, Dr. Sylvester Twumasi, Dr. Evans Adei, Mr. Enos Kwame Adepa, Mr. Ernest Apau and Mr. Osei Akoto whose encouragements whetted my appetite to undertake this study. I would also like to thank Prof. Tebello Nyokong, Prof. Karen De Clerck, Prof. Philippe Westbroek, Ms. Annelies Goethals, Dr. Bert De Schoenmaker and Ms. Sheilla Odhiambo (Host II) for their support during my visit to Ghent. I am grateful to Kwame Nkrumah University of Science and Technology for granting me study leave. I am also grateful to the members in my research group (F12) especially Mr. Samuel Chigome and Ms. Bellah Pule. I would like to express my appreciation to Rhodes University and the staff in the Department of Chemistry especially Ms. Benita Tarr, Mr. John Fourie, Mr. Francis Chindeka, Ms. Nombasa Ntengenya, Ms. Barbara Ah Yui, Mr. V. Dondashe, Mr. E. Sukula, Mr R. Douglas and Mr. A. Adriaan. Finally, I would like to acknowledge my parents, family and friends for their continuous support and encouragement.

Abstract

This thesis presents an alternative approach for pre-concentrating heavy metals in aqueous environments using electrospun polymer nanofiber sorbents. The conditions for electrospinning polyethersulfone, polystyrene, polysulfone and polyamide-6 were optimized. The morphologies and porosities of the electrospun nanofibers were studied using SEM and BET nitrogen gas adsorptions. The nanofibers had mesoporous morphologies with specific surface areas up to 58 m^2/g. The electrospun nanofiber sorbents were characterized in terms of their tunability for both uptake and release of heavy metals. The usability of the sorbent was also assessed. The sorbents showed fast adsorption kinetics for heavy metals (< 20 min for As, Cu, Ni and Pb) in different aqueous environments. The adsorption characteristics of the sorbents best fitted the Freundlich isotherm and followed the first order kinetics. The efficiencies of adsorption and desorption of heavy metals on both imidazolyl-functionalized polystyrene and amino-functionalized polysulfone sorbents were more than 95% up to the fifth cycle of usage. Reusability improved dramatically (up to 10 runs of usage) when mechanically stable amino-functionalized nylon-6 electrospun nanofibers were used. The capacity of the amino-functionalized nylon-6 sorbent to pre-concentrate heavy metals compared very favourably with those of aqua regia and HNO_3+H_2O_2 digestions especially in less complex matrices. Due to their highly porous nature, the electrospun nanofibers exhibited high adsorption capacities (up to 50 mg/g) for heavy metal ions. The loading capacities achieved with the imidazolyl-functionalized sorbent were higher than those for amino-functionalized mesoporous silica and biomass-based sorbents. The electrospun nanofiber sorbents presents an efficient and cost effective alternative for pre-concentrating heavy metals in aqueous environments.

Table of contents

List of papers

I. Darko, G., Chigome, S., Tshentu, Z., Torto, N. (2011). Enrichment of Cu(II), Ni(II), and Pb(II) in aqueous solutions using electrospun polysulfone nanofibers functionalized with 1-[bis[3-(dimethylamino)-propyl]amino]-2-propanol. Analytical Letters, 44: 1855-1867.

II. Chigome, S., Darko, G., Buttner, U., Torto, N. (2010). Semi-micro solid phase extraction with electrospun polystyrene fiber disks. Anal. Methods, 2: 623-626.

III. Chigome, S., Darko, G., Torto, N. (2011). Electrospun nanofibers as sorbent material for solid phase extraction. Analyst, 136: 2879-2889.

IV. Rammika, M., Darko, G., Tshentu, Z., Sewry, J., Torto, N. (2011). Dimethylglyoxime based ion-imprinted polymer for the determination of Ni(II) ions from aqueous samples. Water SA, 37(3): 1-10.

V. Rammika, M., Darko, G., Torto, N. (2011). Incorporation of Ni(II)-dimethylglyoxime ion-imprinted polymer into electrospun polysulfone nanofibers for the determination of Ni(II) ions from aqueous samples. Water SA, 37(4): 537-546.

VI. Darko, G., Chigome, S., Lillywhite, S., Tshentu, Z., Darkwa, J., Torto, N. (2011). Sorption of heavy metal ions in aqueous environments using electrospun polystyrene nanofibers functionalised with diazole ligands. International Journal of Envorinmental Analytical Chemistry (Under Review).

VII. Darko, G., Sobola, A., Chigome, S., Adewuyi, S., Okonkwo, J.O., Torto, N. (2012). Pre-concentration of heavy metals using electrospun amino-functionalized nylon-6 nanofiber sorbent. S. Afr. J. Chem., 65: 14-22.

VIII. Darko, G., Zugle, R., Nyokong, T., De Clerck, K., Westbroek, P., Goethals, A., De Schoenmaker, B. Torto, N. (2011). Steady states electrospinning of polyethersulfone (In preparation).

IX. Pakade, V.E., Cukrowska, E.M., Darkwa, J., Darko, G., Torto N., Chimuka, L. (2012) Simple and efficient ion imprinted polymer for recovery of uranium from environmental samples. Water Sci. Technol., 65(4): 728-736.

List of Patents

I. Ruphino, Z., Darko, G., Litwinski, C., Nyokong, T., Torto, N. (2012) Polymer bound metallophthalocyanines. International Patent. WO 2012 / 023 100 A1.

List of abbreviations

AC	Alternating current
AFM	Atomic Force Microscope
BET	Brunauer- Emmet-Teller
C	Equilibrium concentration
CNTs	Carbon nanotubes
d	Diameter
DC	Direct current
DCE	Dichloroethene
DMF	*N,N*-dimethylformamide
DTAB	Dodecyl trimethyl ammonium bromide
E	Applied voltage
E°	Standard redox cell potential
Eqn	Equation
eV	Electron volts
FT-IR	Fourier transform infrared
g	gram
h	Length of the capillary
HA	Hyalauronic acid
HFP	Hexafluoropropylene
I	Current
ICP-OES	Inductively couple plasma-optical emission spectroscopy
K	Conductivity

keV	kilo electron volts
kV	kilovolts
LOD	Limits of detection
LOQ	Limits of quantification
m^2	metre squared
MEK	Methyl ethyl ketone
mg	milligrams
mg/L	milligram per litre
min	minute
ml	millilitre
MPa	mega Pascal
NIST	National Institute of Standards and Technology
nm	nanometre
NMP	N-Methyl-2-pyrrolidone
P	Pressure
PA-6	Polyamide-6 (Nylon-6)
PCEMA	Poly(methyl methacrylate)
PCL	Poly(L-caprolactone)
PES	Polyethersulfone
PET	Polyethylene terephthalate
PLGA	poly(lactic-co-glycolic acid)
PLLA	Poly(L-lactic) acid
PMMA	Poly(methyl methacrylate)
P_o	Saturated vapour pressure

PS	Polystyrene
PSU	Polysulfone
Q	Surface charge
Q_R	Maximum charge
r	Radius
SEM	Scanning electron microscope
rpm	Revolutions per minute
TEBAC	Triethyl benzyl ammonium chloride
tg	Glass transition temperature
THF	Tetrahydrofuran
TMACl	Tetramethylammonium chloride
UK	United Kingdom
US	United States
V_C	Critical or minimum voltage
V_m	Molar volume
WHO	World Health Organisation
wt%	Weight percent
x	Mass of adsorbate adsorded
ε	Dielectric constant
μ	Velocity
ρ	Density
σ	Statistical error
γ	Surface tension

List of figures

List of schemes

List of tables

1

Introduction

1.1 Heavy metal pollution in water

Many different definitions based on density, atomic weights (Fu and Wang, 2011) and toxicities (Boran and Altınok 2010) have been proposed for heavy metals. The term is therefore used for a loosely-defined subset of elements that exhibit metallic properties including the transition metals, some metalloids, lanthanides and actinides (Duffus 2002). They are generally classified as elements having atomic weights between 63.5 and 200.6, and a specific gravity greater than 5.0 (Srivastava and Majumder 2008). The heavy metals cannot be degraded and destroyed unlike their organic counterparts. They are stable and persistent environmental contaminants (Fu and Wang 2011). They are widespread, typically in concentrations less than 1 mg/L, in surface water resources (Zolotov *et al.,* 1987).

Although their concentrations in natural water sources are low (mg/L range), metal ions tend to bio-accumulate through the food chain (Gundacker 2000; Pourang 1995) and exert various health effects on humans and animals. The impact of heavy metals on human health is becoming a challenge to public health (Demirbas 2008; Muhammad *et al.,* 2011). Heavy metals are ranked high among the most important pollutants in natural and treated water resources. There is therefore the need for a regular, quick and accurate determination of the heavy metal ion in water resources. The direct quantification of metals in natural water samples has, however, proven to be a challenge as their concentrations are usually below the detection limits of many analytical instruments (Mohammadi *et al.,* 2010). Hence, the need for an efficient sample pre-concentration step to bring their concentrations to detectable levels for accurate measurements.

1.2 Sources of heavy metals in water

Heavy metals in water could originate from natural sources (such as weathering and erosion of bed rocks and ore deposits) or anthropogenic sources such as mining, industries, wastewater irrigation and agriculture activities (Chanpiwat *et al.,* 2010). Industrial waste constitutes the major source of metal pollution in natural water (Celik and Demirbas 2005; Demirbas *et al.,* 2006; 2005; Pastircakova, 2004). Heavy metals are found in the wastewater from several industrial processes such as electroplating, metal finishing, metallurgical, tanning, mining and chemical manufacturing industries (Acar and Malkoc 2004; Al-Rub 2006). Heavy metals from these sources eventually leach into surface and underground water reserves and pollute them (Kang *et al.,* 2007). Figure 1.1 illustrates some of the major sources of heavy metals in aquatic enviroments

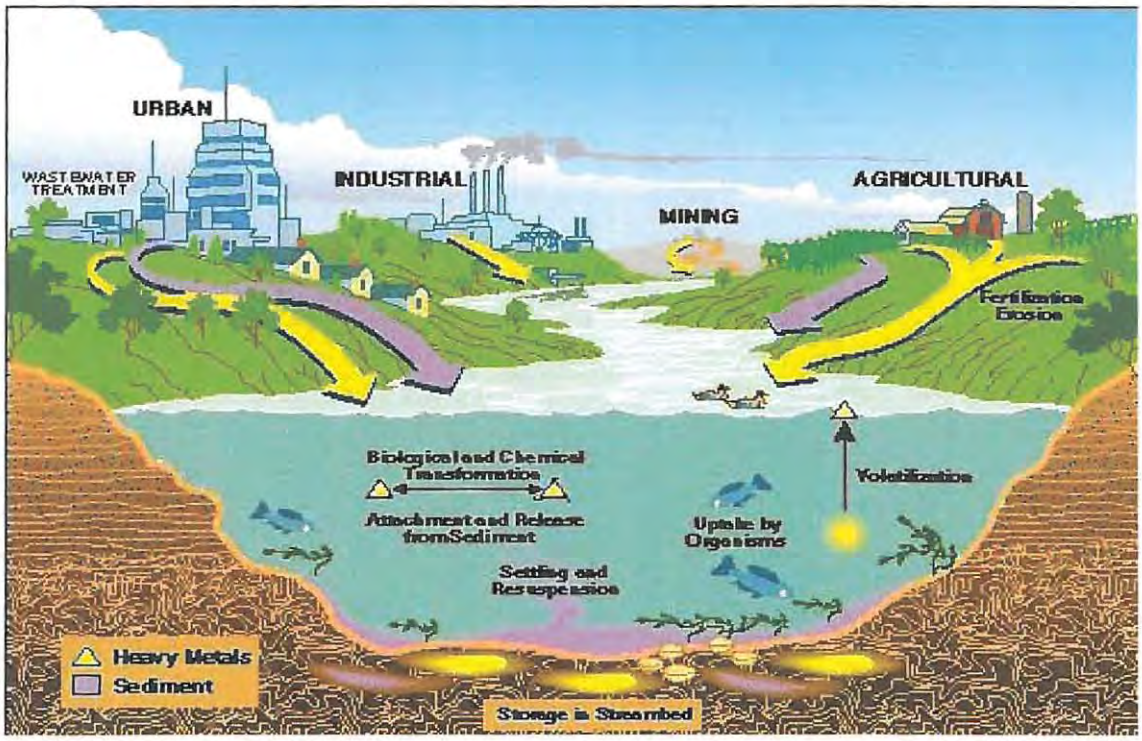

Figure 1.1: Sources of heavy metals in aquatic environments (Garbarino *et al.,* 1995).

1.3 Toxicities of heavy metals in water

Heavy metals are among the most harmful elemental pollutants in water and are of particular concern because of their toxicities to human (Fu and Wang 2011). Some of the heavy metals such as copper, cobalt, iron, magnesium and zinc are required (in trace concentrations) in human diet for normal body functions and as such, dietary allowances have been set for them (Table 1.1).

Table 1.1: Recommended (daily) dietary allowances and overdose effects of some essential heavy metals (Ohno *et al.*, 2010; WHO 1996)

	Recommended daily intake (mg)	Over dosage (mg)	Effect
Cu	2	10	Intestinal distress
Fe	15	20	Stomach upset
Zn	15	25	Anaemia

However, these same elements can cause health effects in humans when their tolerance levels are exceeded. For example, zinc is important for the physiological functions of living tissue and regulates many biochemical processes. However, excess of zinc in the body can cause health problems such as stomach cramps, skin irritations, vomiting, nausea and anemia (Oyaro *et al.*, 2007). Copper is essential for metabolic activities in the body and forms an active component of haemoglobin (Paulino *et al.*, 2006). However, excess copper in the blood stream can get deposited in the brain, liver and pancreas myocardium (Palanivelu *et al.*, 2006) and initiates intestinal distress, kidney damage and anemia (Al-Rub *et al.*, 2006).

The presence of some toxic heavy metals such as cadmium, lead and mercury in the body has a potentially damaging effect on human physiology (Demirbas 2008). Nickel exceeding its critical

level in the human system may cause lung and kidney failure, gastrointestinal distress, pulmonary fibrosis and skin dermatitis (Borba *et al.*, 2006). Nickel is also known to be a human carcinogen (Fu and Wang 2011). Mercury is a neurotoxin and can impair the functions of the kidney (Namasivayam and Kadirvelu, 1999). Exposure to high levels of mercury will also result in death (Godt *et al.*, 2006). Cadmium exposes human health to several risks. Chronic exposure to cadmium results in kidney dysfunction, mucous membrane destruction, diarrhea and vomiting as well as bone damage. It also affects the production of progesterone and testosterone. Lead is one of the most toxic heavy metals that have latent long-term negative impacts on human health; causing anemia, encephalopathy, hepatitis and nephritic syndrome (Deng *et al.*, 2006). Lead can also damage the brain, kidneys and the liver as well as the nervous and the reproductive systems (Naseem and Tahir, 2001). In view of their high toxicities, the exact concentrations of heavy metals in water samples ought to be known. Also, effort ought to be made to reduce their concentrations in water to lowest possible levels or remove them completely.

1.4 Methods for treating heavy metals in water

Many methods, including chemical precipitation, ion-exchange, adsorption, membrane filtration, electrochemical treatment have been explored for removing heavy metals from water. Each of these methods has their own advantages and limitations (Kurniawan *et al.*, 2006). Some of these methods could be explored to pre-concentrate heavy metals in water.

1.4.1 Ion exchange

Ion exchange is a reversible process where an ion from a solution is exchanged for a similarly charged ion attached to an immobile solid particle. Ion-exchange process is widely used in water purification and softening. The most common ion exchangers used in water treatment are the

strongly acidic resins with sulfonic acid groups (-SO_3H) and the weakly acidic with carboxylic acid groups (-COOH). As a solution containing heavy metal passes through cations column, metal ions are exchanged for hydrogen ions on the resin as depicted in equations 1.1 and 1.2 below:

$$nR-SO_3H + M^{n+} \rightarrow (R-SO_3^-)_n M^{n+} + nH^+ \qquad 1.1$$

$$nR-COOH + M^{n+} \rightarrow (R-COO^-)_n M^{n+} + nH^+ \qquad 1.2$$

Ion-exchange processes have high levels of efficiencies and fast kinetics (Alyüz and Veli 2009). However, their efficiencies for heavy metal uptake are affected by many variables such as pH, temperature, initial metal concentration and contact time (Abo-Farha *et al.*, 2009; Gode and Pehlivan, 2006).

1.4.2 Membrane filtration

Membrane filtration processes have high efficiencies for removing heavy metals and are easy to operate. The major drawback of these processes is the high power consumption due to the pumping pressures, and fouling of the membranes (Fu and Wang 2011). Membrane processes that could be applied to remove heavy metals from water are ultrafiltration, reverse osmosis and nanofiltration.

In ultrafiltration, hydrostatic pressure is used to force the water sample through a semipermeable membrane. Suspended solids are retained, while water and low-molecular-weight solutes (such as ions) pass through the membrane. The method is effective in removing suspended matter. However, some of the dissolved ions like the hydrates that have smaller sizes than the pore of the membrane can also pass through (Landaburu-Aguirre 2009; Sampera *et al.*, 2009).

Reverse osmosis is effective in removing a wide range of dissolved species from wastewater. It has been used extensively in the desalination industry (Shahalam *et al.*, 2002) but has not been applied on the other water types (such as wastewater) because of its high cost of operation (Zhang *et al.*, 2009).

Nanofiltration is a membrane filtration process used mostly in treating polyvalent cations in surface and fresh ground water sources that contain low levels of dissolved solids (Hillie and Hlophe 2007; Letterman 1999). Nanofiltration is a promising technology for removing heavy metal ions such as nickel (Murthy and Chaudhari, 2008), chromium (Muthukrishnan and Guha, 2008), copper (Cséfalvay *et al.*, 2009) and arsenic (Figoli *et al.*, 2010; Nguyen *et al.*, 2009) from waste water. The nanofiltration process benefits from ease of operation, reliability and comparatively low energy consumption (Erikson, 1988). The transmembrane pressure (pressure drop across the membrane) required in nanofiltration is lower (up to 3 MPa) than those used in conventional membrane filtration, reducing the operating cost significantly. However, nanofiltration membranes are still subject to scaling and fouling.

1.4.3 Coagulation and flocculation

Coagulation and flocculation followed by sedimentation and filtration is also used in water treatment. Many coagulants such as aluminium, ferrous sulfate and ferric chloride are available for removal of particulates and impurities by forming hydroxide precipitates (Chang and Wang, 2007). Generally, coagulation and flocculation cannot completely treat the heavy metals in water (Chang and Wang, 2007). Therefore, coagulation and flocculation must be followed by other treatment techniques (Bojic *et al.*, 2009; Plattes *et al.*, 2007, Tokuyama *et al.*, 2010).

1.4.4 Electrochemical treatment

This method involves plating-out the metal ions onto a cathode surface. The electrodeposited metal can be recovered from the cathode in their elemental states. Electrochemical wastewater technologies have not been widely applied because they involve relatively large capital investment and electricity supply (Wang *et al.*, 2007).

1.4.5 Adsorption

Adsorption is recognized as an effective and economic method for treatment of heavy metals in water. The adsorption process offers flexibility in design and operation and, in many cases, produces high-quality treated water (Fu and Wang 2011). In addition, it allows for the regeneration and reuse of the sorbents after they have been desorbed. The effectiveness of the adsorption process depends on the characteristics of the sorbent used. The adsorption process could therefore be explored to pre-concentrate heavy metals in water samples. Several different kinds of adsorbents, including activated carbons, bioadsorbents and carbon nanotubes have been used (Hamissa *et al.*, 2010).

Activated carbon sorbents: Activated carbon sorbents have been widely used in removing heavy metals from water (Jusoh *et al.*, 2007). However, the depleted source of commercial coal-based activated carbon has resulted in a sharp increase in price. To make progress in heavy metals adsorption, alternative adsorbents that are cheaper and effective ought to be explored (Guo *et al.*, 2010; Yanagisawa *et al.*, 2010).

Biosorbents: The major advantage of biosorption lies in the use of readily available and inexpensive materials. Biosorbents are derived from three main sources (Apiratikul and

Pavasant, 2008), namely; (i) non-living biomass such as bark, lignin and shells (ii) algal biomass and (iii) microbial biomass such as bacteria, fungi and yeast. Several different forms of inexpensive, materials such as potato peels (Aman *et al.,* 2008), sawdust (Kaczala *et al.,* 2009), black gram husk (Saeed *et al.,* 2005), eggshell (Jai *et al.,* 2007), seed shells (Amudaa *et al.,* 2009), coffee husks (Oliveira *et al.,* 2008), sugar-beet (Mata *et al.,* 2009) and citrus peels (Schiewer and Patil, 2008), kaolinite and montmorillonite (Gu and Evans, 2008; Sud et al. 2008), zeolites (Apiratikul and Pavasant, 2008), clay and peat (Al-Jlil and Alsewailem, 2009) have been investigated for adsorption of heavy metals from water. However, the process seems to be grappling with difficulties of reusability of the sorbents.

Carbon nanotubes: Carbon nanotubes (CNTs) have been widely studied for their excellent properties in adsorption applications. They have proven to possess great potential for removing heavy metal ions such as cadmium (Kuo and Lin, 2009), chromium (Pillay *et al.,* 2009), copper (Li *et al.,* 2010), lead (Kabbashi *et al.,* 2009; Wang *et al.,* 2007), and nickel (Kandah and Meunier, 2007) from water. The mechanisms by which the metal ions are adsorbed on CNTs are not well understood but they appear attributable to surface electrostatic attraction, sorption-precipitation and chemical interaction between the metal ions and the CNTs (Rao *et al.,* 2007). Both functionalized and unfunctionalized CNTs have superior adsorption capabilities compared with activated carbons (Pillay *et al.,* 2009). However, CNTs could be harmful to human health (Karlsson *et al.,* 2008; Simon-Deckers *et al.,* 2008) and their widespread use will result in their eventually discharge into the human environment (Fu and Wang, 2010). An environmentally friendly adsorbent that have capacities comparable to those of CNTs will therefore be a better

alternative (Li *et al.*, 2010). This is why electrospun nanofibers are receiving attention as a new platform for adsorption of heavy metals from water.

Electrospun nanofiber sorbents: Electrospun nanofibers are currently receiving worldwide attention in adsorption applications (Greiner and Wendorff 2006) because they have the ability to overcome the limitations (low adsorption capacity, reusability) of the other kinds of adsorbents. A major limitation of activated carbons and bioadsorbents is their inability to desorb the heavy metals they adsorb back into solution for quantification. Their applications are therefore limited to mopping up the metals ions from water and not for sample preparation or pre-concentration purposes.

The electrospun nanofibers have high specific surface areas and porosities that impart on them very high adsorption capacities (Huang *et al.*, 2003). The electrospinning process offers the flexibility for surface functionalizing the nanofibers with moieties that have high affinities for the heavy metals. For example, heavy metals are known to interact strongly with ligands such as the amino, thiol and hydroxyl groups (Aguado *et al.*, 2009; Yoshitake 2003). The binding abilities of the electrospun nanofibers for metals are dramatically enhanced when they are surface functionalized with ligands (Kang *et al.*, 2007). Functionalized electrospun nanofibers could therefore make excellent adsorbent for quantitative pre-concentration of heavy metals from aqueous environments. The metal ions adsorbed could easily be leached back into solutions by pH adjustments in order to avail the metals for quantification without affecting the integrity of the sorbent. These remarkable features of electrospun nanofibers make them the preferred

sorbent materials for development of a platform for pre-concentration of heavy metals from water.

1.5 Scope of the thesis

The aim of this study was to develop electrospun nanofiber sorbents that have tunable characteristics for uptake of metals from water samples and releasing them into solutions, upon adjustment of pH, for quantification. The study focused on optimizing parameters for electrospinning different polymers into nanofibers and characterizing the sorbents developed from the nanofibers in terms of their tunabililty for uptake and release of heavy metals from aqueous environments, reusability and loading capacities.

Electrospinning conditions were optimized for four different polymers (polyamide-6, polyethersulfone, polysulfone and polystyrene). The nanofibers were fully characterized in terms of their average diameters, morphologies and porosities. The nanofiber mat were then stamped out into optimized masses and applied as adsorbents for uptake of heavy metals. Parameters affecting adsorption such as initial concentration, contact time and pH were also investigated. The capacity of the functionalized electrospun fibers to pre-concentrate heavy metals from tap water, river water, sea water, treated and untreated sewage was assessed. The loaded sorbents were then desorbed and their efficiencies of adsorptions/desorption as well as cycles of usage determined. The capacities of the sorbents to pre-concentrate heavy metals were compared with the extraction efficiencies of two standard wet ashing or acid digestion (aqua regia and HNO_3+H_2O_2) protocols.

2

Nanofiber sorbents

2.1 Overview

This chapter discusses the various methods for producing nanofibers. Methods such as drawing, template synthesis, phase separation, self-assembly and melt blowing will be discussed in this chapter. Electrospinning will be considered in detail in Chapter 3.

2.2 Methods for producing nanofibers

Production of nanofibers has centered around organic polymers and inorganic materials. The synthesized nanofibers can be tailored for specific purposes. Several methods for producing nanofibers have been outlined in literature (Ramakrishna *et al.*, 2005) but they could all be categorized into 5 groups; drawing, template synthesis, phase separation, self-assembly and electrospinning.

2.2.1 Drawing

A micropipette or the tip of an atomic force microscope (AFM) is dipped into a droplet of a viscous polymer solution near the contact line. The micropipette or the AFM tip is smoothly withdrawn slowly from the solution (Fig 2.1). Nanofibers are formed provided the solution is viscous enough. Drawing a nanofiber requires a viscoelastic material that can undergo strong deformations.

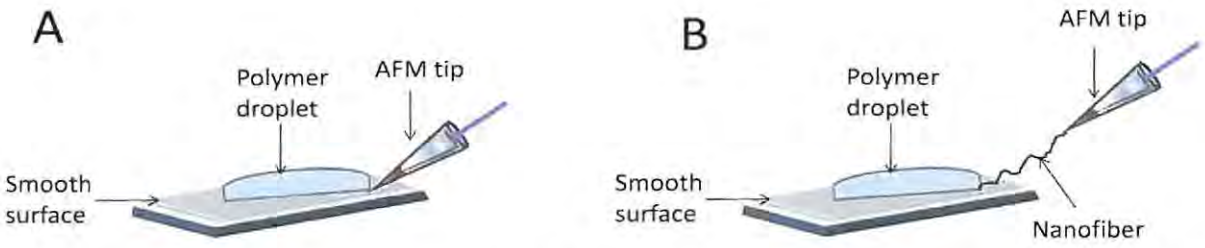

Figure 2.1: Drawing process in which (A) AFM tip is in contact with polymer droplet and (B) AFM tip is drawn away to generate nanofibers

The drawing method was applied successfully in fabricating sodium citrate nanofibers using chloroauric acid as the solvent (Ondarcuhu and Joachim 1998). Even though the drawing process gives a good level of repeatability, control of fiber dimensions is limited. The drawing process is only suitable for laboratory production of nanofibers as it cannot be scaled up for industrial or commercial production.

2.2.2 Template synthesis

In the template synthesis, the polymer solution is extruded through a metal oxide membrane having pore diameters in the nano range. Upon coming into contact with a solidifying solution, the extruded solution forms nanofibers whose diameters are determined by the pores in the template. Fibers of specified diameter can easily be made using a template of an appropriate diameter. Feng *et al.,* (2002) used a setup similar to the one illustrated (Fig 2.2) to synthesize PAN nanofibers. Nanofibers having diameters of about 100 nm were obtained from a PAN solution using dimethylformamide (DMF) as the solvent.

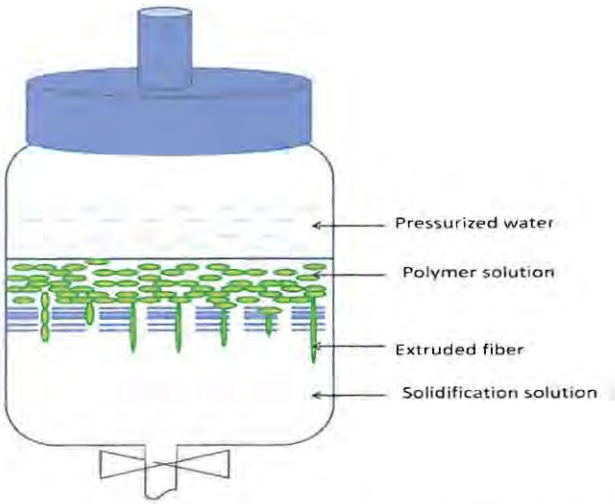

Figure 2.2: A schematic setup for producing fibers through template synthesis

2.2.3 Phase separation

In phase separation, a polymer solution is allowed to form a gel and then the solvent is extracted leaving behind the residual porous solid phase (Fig 2.3).

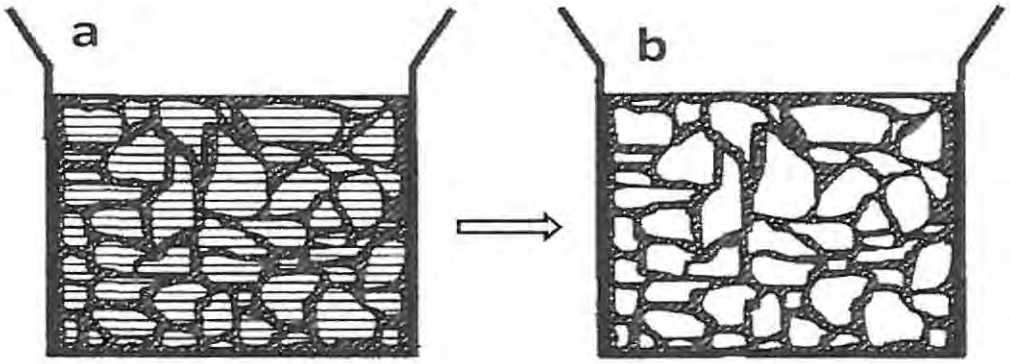

Figure 2.3: A phase separation process in which (a) polymer solution is allowed to gel out and (b) nanofibers are formed after extracting the solvent (Ramakrishna *et al.*, 2005)

This method has a minimal equipment requirement, batch-to-batch consistency is achieved easily and the mechanical properties of the matrix can be tailored by adjusting polymer concentration (Ramakrishna *et al.*, 2005). However, it is limited to a few polymer types and there is only little control over the diameters of fibers formed. Nanofibers have been successfully generated from poly(L-lactic) acid (PLLA) using this method (Ma and Zhang, 1999).

2.2.4 Self-assembly

In self-assembly, smaller molecules are used as building blocks to create nanofibers (Liu *et al.*, 1996). This method has been used extensively in synthesis of genetic materials such as DNA (Hartgerink *et al.*, 2001; Liu *et al.*, 1996, 1999; Yan *et al.*, 2001). This method has also been applied on PCEMA core-PS shell (Liu, 1997), and many other copolymers (Yan *et al.*, 2004). Self-assembly requires no machinery to move or orient components. Self-assembly can be used to produce atomically precise nanosystems. The fundamental disadvantage of pure self-assembly

is that for every product, the structure of the parts must encode the structure of the whole (Ramakrishna *et al.*, 2005)

2.2.5 Melt blowing

Melt blowing is a process for producing fibers directly from polymers using high-velocity air. It is a single-step process that converts polymer raw material directly into nanofibers. The polymer is melted in an extruder and then pumped through die holes into a high speed, hot air chamber. The fibers formed are collected on a rotating collector (Bresee 2004). Figure 2.4 is a schematic diagram of a melt blowing setup. The process has a high productivity and has been used to generate nanofibers from polymers such as polypropylene, polyethylene, polybutylene terephthalate, Nylon 6 and polystyrene (Chen *et al.*, 2005; Ellison *et al.*, 2007).

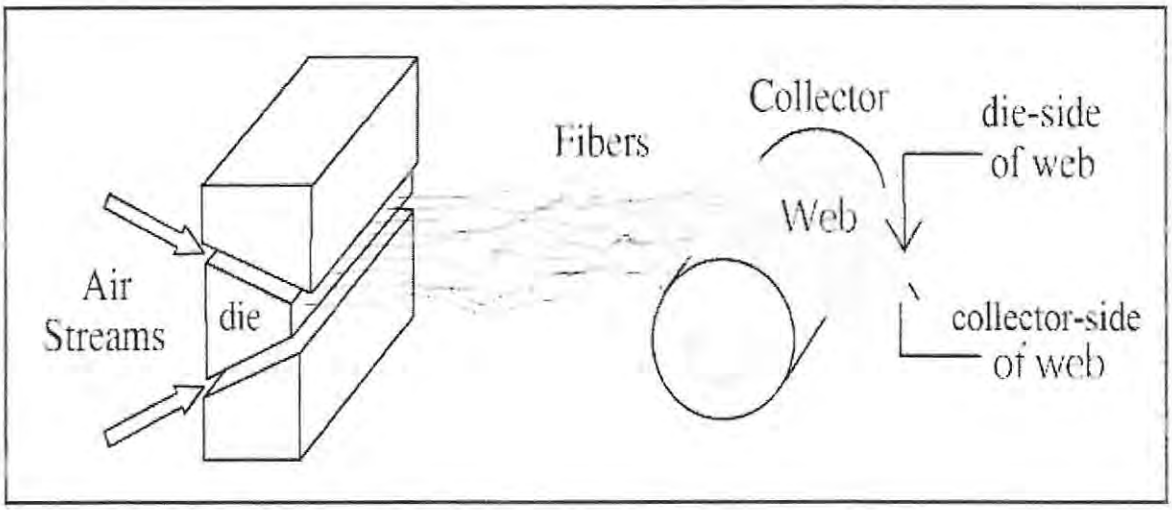

Figure 2.4: Typical melt blowing setup (Bresee 2004).

3

Electrospinning

3.1 Overview

Electrospinning is the most versatile of all the methods for making nanofibers. The method could be applied to virtually every soluble or fusible polymer and the polymer solutions can be modified with additives prior to or after electrospinning for special purposes (Bhardwaj and Kundu 2010; Greiner and Wendorff 2007). The chapter discusses the electrospinning process in detail.

3.2 Historical background of electrospinning

The first documented accounts on electrospinning were put forward by J. F. Cooley and W. J. Morton in 1902 (Table 3.1). They described the electrospinning process as "the deposition of a viscous polymer solution as a cobweb-like mass from a positively charged orifice onto a negatively charged electrode". A year later, in 1903, Cooley patented electrospinning as "an introduction of the viscous polymer solution near the terminus of a charged electrode to yield fibers". Between 1934 and 1944, Anton Formhals patented five different versions of the electrospinning apparatus. Formhals was the first to document methods for electrospinning multi-component nanofibers and introduced a moving collecting system that allows some degree of fiber orientation.

Table 3.1: Chronological development of electrospinning patents (Andrady, 2008)

Holder	Year	U.S. Patent Reference #
Cooley, J.F.	1902	692,631
Morten, J.W.	1902	705,691
Cooley, J.F.	1903	745,276
Formhals, A.	1934–1944	1,975,504; 2,077,373; 2,109,333; 2,116,942; 2,123,992; 2,158,415; 2,158,416; 2,160,962; 2,187,306; 2,323,025; 2,349,950
Hagiwara, K.	1929	1,699,615
Norton, C.L.	1936	2,048,651
Gladding, E.K.	1939	2,168,027
Manning, F.W.	1943	2,336,745
Simons, H.L.	1966	3,280,229
Simm, W., *et al.*,	1976	3,944,258
Martin, G.E., *et al.*,	1977/1978	4,043,331; 4,044,404; 4,127,706
Simm, W., *et al.*,	1978	4,069,026
Fine, J., *et al.*,	1980	4,223,101
Guignard, C.	1980/1981	4,230,650; 4,287,139
Bornat, A.	1982	4,323,525
How, T.V.	1985	4,552,707
Bornat, A.	1987	4,689,186
Martin, G.E., *et al.*,	1989	4,878,908
Berry, J.P.	1991	5,024,789
Scardino, F.L. and Balonis, R.J.	2000	6,106,913
Chu, B., *et al.*,	2004	6,713,011

In the 1960s, Sir Geoffrey Taylor contributed immensely towards the fundamental understanding of the behaviour of droplets placed in electric fields (Taylor 1964, 1969). Taylor's findings helped develop the electrospinning process further. Around the same period, H. L. Simons (Table 3.1) identified conductivity, dielectric constant, viscosity and volatility of solvent as the key parameters that determine electrospinnability, fiber morphology and fiber diameter. In 1971, Peter Baumgarten demonstrated the dependence of fiber diameter on viscosity (and hence on polymer concentration) and the electric field applied (Baumgarten 1971). Table 3.1 shows the

chronological development of patents on electrospinning from 1902 to 2004 (Andrady, 2008). There are currently over 70 patents filed on various aspects of electrospinning.

3.3 Description of the electrospinning process

In electrospinning, a high electric field is generated between the polymer solution contained in a syringe and a metallic collection plate by connecting the needle of the syringe to a high voltage power supply as shown in Figure 3.1. At a certain threshold voltage (depending on a number of factors to be discussed later) when the repulsive electrostatic force overcomes the surface tension of the polymer solution, a droplet draws out into a cone-shaped terminus and sprays downwards towards the grounded collector (usually an aluminum foil). As the jet travels towards the collector plate, the solvents dry off and the jet deposits as a mesh of nanofibers on the collector.

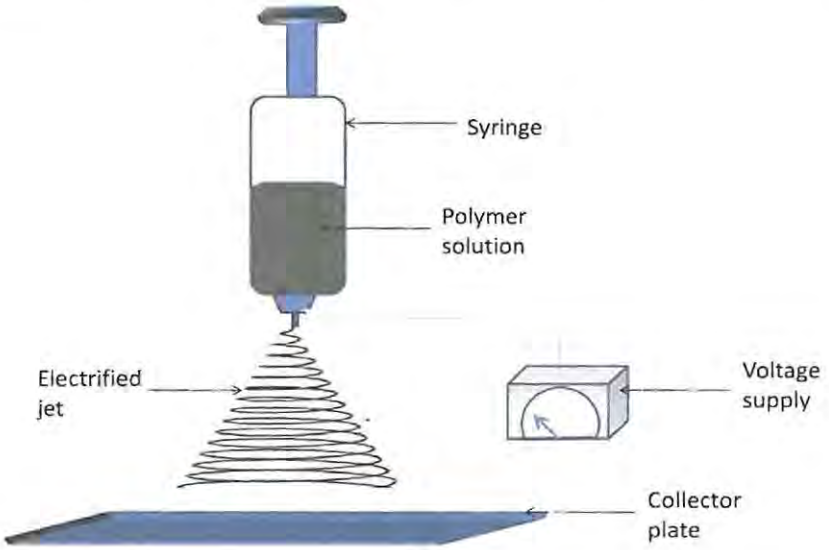

Figure 3.1: A schematic diagram of a typical electrospinning setup.

3.4 Physical principles of the electrospinning process

The polymer solution undergoes a number of processes, during electrospinning, before it transforms into nanofibers. For the convenience of description, Reneker and Fong (2006) divided the electrospinning process into 4 key stages: launching the jet, jet elongation, whipping instability and solidification.

3.4.1 Launching the jet

The jet launching is the first stage of the electrospinning process. The jet launching stage comprises droplet generation and Taylor cone formation. In the absence of an applied electric field, a polymer solution pumped through a capillary will just form droplets and fall off under the influence of gravity. Assuming that the only forces working on the meniscus of the droplets of polymer solution having density (ρ) are surface tension (ϒ) and gravity (g), then the radius of the droplet, r_0, produced by a capillary of internal radius R is given by the expression

$$r_0 = \left(\frac{3R\gamma}{2\rho g}\right)^{\frac{1}{3}} \qquad 3.1$$

When a high enough voltage is applied to the droplets (having a finite conductivity), the electrical force (E_f) and the gravitational force (G_f), will both work against the surface tension and only a sustainable droplet size will be maintained at the capillary tip when these forces balance out.

$$\text{i.e., } \gamma = E_f + G_f \qquad 3.2$$

Based on the equation first postulated by Loeb *et al.*, (1941), Bugarski *et al.*, (1994); DeShon and Carson (1968) as well as Lee (2003) proposed that the magnitude of the electric force at a capillary tip carrying a positive voltage (V) held at a distance (L) from a grounded metal surface is given as

$$E_f = \frac{(4\pi\varepsilon V^2)}{\ln\left(\frac{4L}{R}\right)^2} \qquad 3.3$$

ε is the permittivity of the gas in which the process was carried out (usually, air).

Equation 3.3 depicts that as the voltage increases, the diameter of the droplet becomes progressively smaller until instability sets in at a critical value of the electric field (V_C) where electrospraying and therefore bead formation starts. To maintain a constant flow of the charged droplets, the outward electrical force must be higher than the inward surface tension.

$$\text{i.e. } E_f \geq g\rho\left[\left(\frac{r^2}{\beta}\right) - V\right] \qquad 3.4$$

Instability of the electrically charged electrospinning jet has been explained using the Rayleigh condition (Rayleigh 1882). Rayleigh proposed that the maximum charge, Q_R, that the surface of a droplet can accommodate in vacuum is determined by the surface tension (γ) and the radius of the droplet (r)

$$Q_R = 8\pi\left(\varepsilon\gamma r^2\right)^{\frac{1}{2}} \qquad 3.5$$

According to Rayleigh (1882), the electrically charged polymer droplet becomes unstable when the electrical force exerted on it exceeds its surface tension. Rayleigh, again, espoused that when the electrostatic force overcomes the surface tension (which acts in the opposite direction to the electrostatic force) the unstable charged droplet breaks up into a series of charged droplets at this point and the polymer solution ejects into fine jets. The droplet first deforms in the electric field and then explodes into a number of smaller droplets due to coulombic repulsion of the charges accumulated on its surface. In practice, this limit can be reached by either gradually increasing the electric field or by systematically reducing the droplet's diameter through evaporation (Abbas and Latham 1967; Kalayci *et al.*, 2005).

According to Taylor's theory, it is the instability induced on the surface of the electrically charged droplet that causes the nanofiber formation (Taylor, 1964;1969). Taylor hypothesized that a spherical droplet of polymer forms at the capillary tip and elongates as the applied voltage increases. The elongated droplet assumes a cone-like shape and a narrow jet of liquid ejects from this point (Taylor 1964, 1969). It is the change in shape of the droplet into conical shape that defines the onset of the fiber formation. Accordingly, it was proposed that the Taylor cone forms at a critical voltage (V_c) given as

$$V_c^2 = \left[\left(\frac{2L}{h}\right)^2 \ln\left(\frac{2h}{r}\right) - 1.5\right](0.117\pi r T) \qquad 3.6$$

where h and r are length of the capillary and radius of the drop respectively.

Equation 3.6 suggests that the critical voltage required for electrospinning to occur is dependent on the surface tension of the solution. The Taylor's equation does not take into consideration the conductivity and the viscosity of the solution. In practice, however, both conductivity and viscosity heavily influence cone formation (Hendricks *et al.*, 1964). The Taylor cone may not necessarily be maintained throughout the electrospinning process. Maintenance of the Taylor cone is dependent on the ratio of the feed rate and the rate of mass transfer onto the collector (Wang *et al.*, 2006) and that electrospinning can occur from an essentially flat surface of a solution subjected to a strong enough electric field (Yarin and Zussman 2004).

The pendant electrically charged Taylor cone does not explode because of the chain entanglement in the concentrated polymeric solution. The surface area of the Taylor cone also increases to accommodate the charge build-up and this leads to stretching out of the cone and fiber formation (Burger *et al.*, 2006; Shenoy *et al.*, 2005). According to Deitzel *et al.*, (2006), the jet initiation occurs from the surface layers of the cone. By conservation of mass, feed rate and the speed of the launched jet can be described as

$$\text{Feed rate} = \left(\frac{\pi d \rho \mu}{4}\right) \qquad 3.7$$

where d is the diameter of the jet, ρ is the density, and μ its velocity.

By conservation of charge, (He *et al.*, 2005a, 2005b) the current flowing in the jet (I) relates to the applied voltage (E) as

$$I = \pi d^2 Q \mu + \left(\frac{k \pi d^2 E}{4} \right) \qquad 3.8$$

where Q is the surface charge and k the conductivity of the solution.

3.4.2 Jet elongation

Jet elongation occurs when a voltage (V_C) exceeding the strength of surface tension of the polymer solution is applied. Buer *et al.,* (2001) revealed that the velocity of the jet increases as it travels towards the collector. As a result of solvent evaporation and polymer stretching, the jet diameter decreases rapidly.

3.4.3 Whipping instability

The initially straight jet segment eventually becomes unstable and displays bending and undulating movements as it travels towards the collector. This undulating motion of the charged jet is primarily due to the competition between several different modes of instabilities such as axis symmetric, bending and Raleigh instabilities (Hohman *et al.,* 2001b; Reneker *et al.,* 2000; Spivak and Dzenis 1998; Spivak *et al.,* 2000; Yarin *et al.,* 2001a, 2001b).

The predominant mode of instability exhibited is dependent on the electric field, with stronger fields favouring whipping instability. Whipping instability is known to be the primary mechanism responsible for reducing nanofiber dimensions during electrospinning (Shin *et al.,* 2001a, 2001b). However, it has been pointed out that suppressing this instability using either a secondary electric field or a short gap distance (between the tip of the needle and the collector) does not change the average fiber diameter significantly (Dzenis 2004). It is, therefore, the interplay of these different forces that determines the diameter of the jet and not just one of them. Consequently, no mathematical model has singly explained the entire electrospinning process

adequately. Understanding of the process is far from complete, and not all the factors that govern the fiber formation are well understood.

3.4.4 Jet solidification

The time available to the jet to undergo whipping instability is determined by the rate of evaporation of the solvent. The microstructure, morphology and mechanical integrity of the electrospun nanofibers are affected by the volatility characteristics of the solvent mixture used (Wei *et al.*, 2006a). Solvent volatility is therefore a key consideration in controlling fiber diameter and morphology. With appropriate selection of solvents and process parameters, extremely fine nanofibers can be electrospun (Koombhongse *et al.*, 2001; Larsen *et al.*, 2004a; Reneker *et al.*, 2002).

3.5 Types of electrospinning

Though the electrospinning technique can be scaled up for commercial production, its productivity has been a challenge (Greiner and Wendorff 2007). There have therefore been many attempts to improve on the productivity of the process. Improved and more efficient versions of electrospinning have recently evolved but they all operate on the basic principles of the techniques. The different versions can be categorized under mono nozzle, multi nozzle and needleless electrospinning.

3.5.1 Mono nozzle electrospinning

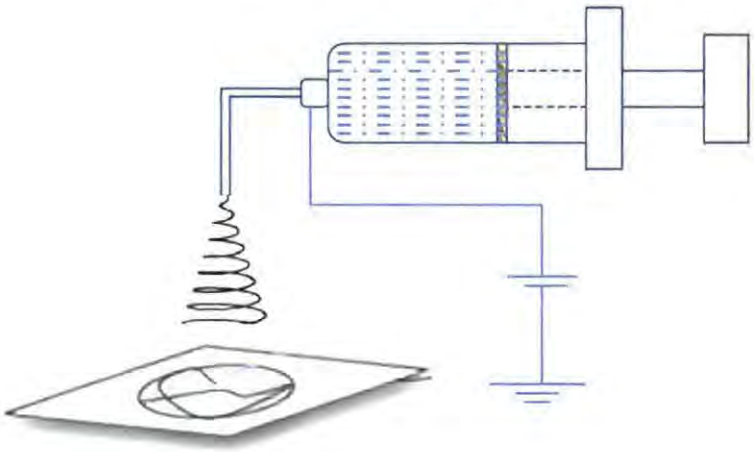

Figure 3.2: A mono nozzle electrospinning setup

The mono nozzle is the simplest type of electrospinning setup in which only one nozzle/needle discharges the polymer solution (Fig 3.2). It is by far the most common and popular type of electrospinning especially in research laboratories. Mono nozzle electrospinning is simple and does not require a lot of capital investment. Its major limitation is the low productivity.

3.5.2 Multi nozzle electrospinning

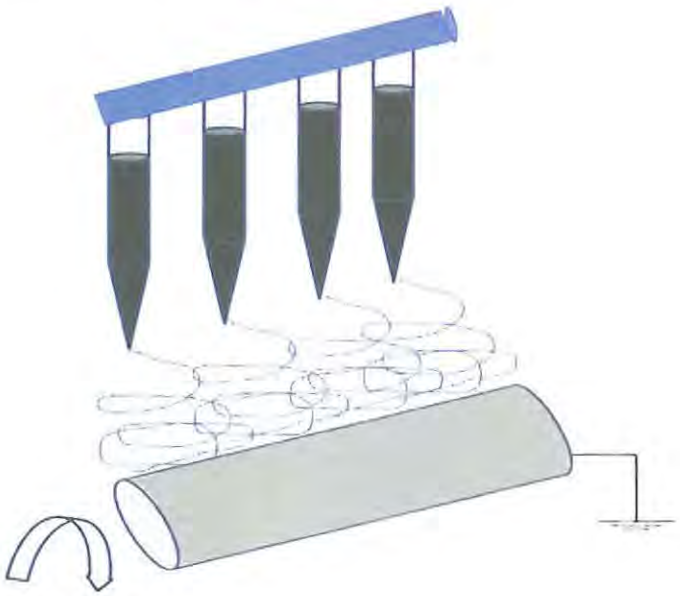

Figure 3.3: A multi nozzle electrospinning setup

In the multi nozzle electrospinning, the polymer solution is fed into an array of nozzles or needles which are either static or moving. If the array of needles is the moving type, then they must be programmed to move in unison. The multi nozzle setup allows for the deposition of multi-component structures if different polymer solutions are electrospun concurrently. It is a straightforward way of increasing the productivity of electrospinning by just increasing the number of nozzles discharging the polymer solution (Ding *et al.,* 2004; Kidoaki *et al.,* 2005; Madhugiri *et al.,* 2003; Theron *et al.,* 2005). The average fiber diameter may increase as a result of the fluctuation of the electric field between the nozzles and the collector. Figure 3.3 shows a schematic diagram of a multiple spinneret electrospinning setup.

3.5.3 Needleless electrospinning

In the needleless electrospinning, the needles are replaced with holes, but the underlying principles of electrospinning remain the same. The system consists of a porous polyethylene tube placed inside a coaxial cylindrical drum (Fig 3.4). The polymer solution is pushed through the holes in the porous polyethylene tube using air pressure. When optimal electrical charges are induced on the polymer through the use of the electrode situated inside the porous tube, nanofibers extrude through the pores. The needleless method is said to be hundred times more efficient than the conventional electrospinning methods (Yarin and Zussman 2004). Maintenance of an even distribution of polymer solution and air pressure over the different holes in the porous drum is the main challenge of the needleless electrospinning. Reproducibility could therefore be low.

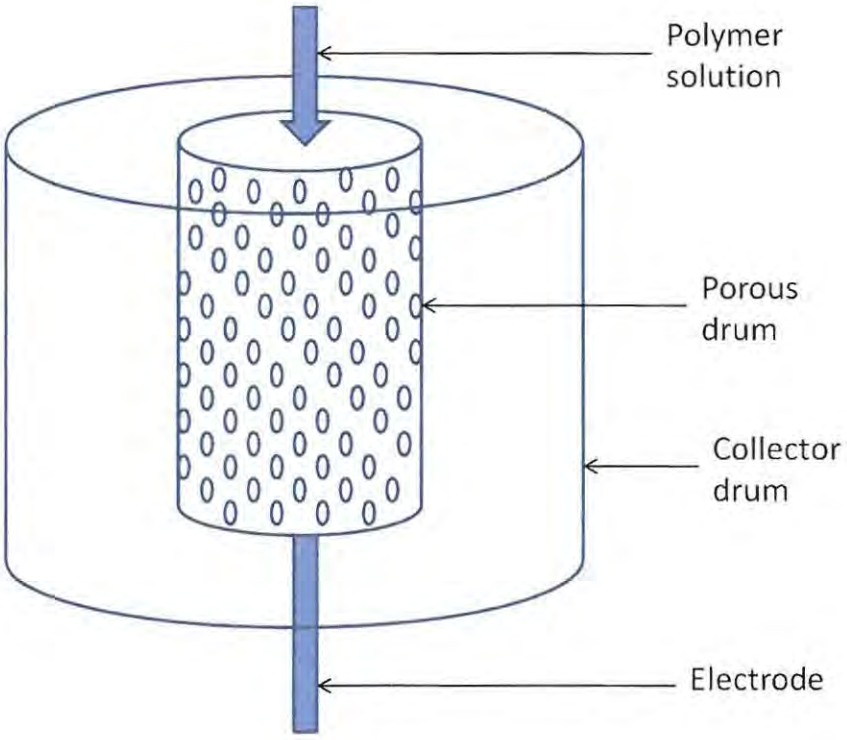

Figure 3.4: Schematic diagram of needleless electrospinning setup

Not much scientific reports are available on multiple needles electrospinning. There exist, however, a good number of patents on multiple needles electrospinning (Table 3.2).

Table 3.2: Trends in the patents filed on multiple nozzle electrospinning (DeVriez 2010)

Year	Numbers filed	Holder(s)
2002	2	Donaldson
2004	10	Donaldson
		State University of New York
2005	6	Donaldson
		Research Triangle Institute
		Raisio Chemicals Korea Inc.
2006	7	Donaldson
		Research Triangle Institute
2007	3	Donaldson
		State University of New York
2008	6	DOW
		Finetex
		BASF
		Teijin
		UGent
2009	3	BASF
		Cook Inc
		Bayer

A large proportion of these patents are owned by companies such Donaldson, which manufacture air filtration products. A few other patents are held by research institutes who developed their own ways of working with multiple needles.

3.6 Electrospinning parameters

A successful electrospinning process is dependent on a myriad of parameters each of which is important in determining quality and yield of the nanofibers. Factors such as the nature and concentration of polymer, characteristics of the solvent, the choice of equipment and its operational conditions as well as the prevailing environmental conditions, all affect the process. These parameters interrelate and a change in one of them affects the entire process (Ramakrishna 2005). For the convenience of description, these parameters are categorized into four as shown in Fig 3.5.

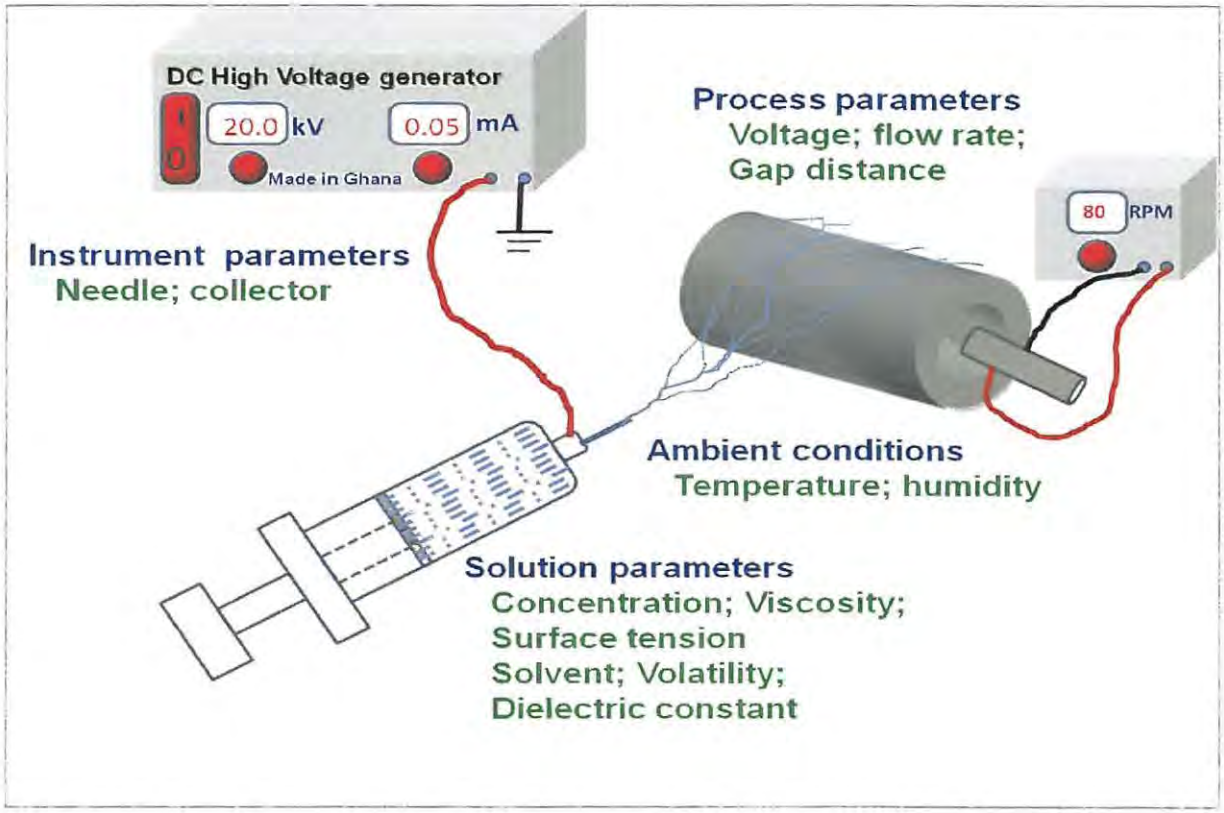

Figure 3.5: A typical electrospinning setup showing the major parameters that affect the process

3.6.1 Solution parameters

The solution parameters cover the properties (such as concentration, conductivity, surface tension) of the polymers solution that determine its electrospinnability.

Concentration: In electrospinning, continuous and uniform nanofibers can only form when the solution concentration is high enough to present a high level of chain entanglement (Deitzel *et al.*, 2001; Pornsopone *et al.*, 2005; Subbiah *et al.*, 2005). The concentration of polymer in solution is the dominant factor that determines whether the fibers will be formed. The polymer concentration in solution determines the morphologies of the fibers (Demir *et al.*, 2002; Zong *et al.*, 2002). It has also been established that the polymer concentration is the main criteria that determines fiber diameter. Higher polymer concentrations generally yield nanofibers of larger average diameter (Gupta *et al.*, 2005; McKee *et al.*, 2004a, 2004b; Demir *et al.*, 2002). Several other researchers have indicated that the fiber diameter increases with polymer concentration (Baumgarten, 1971; Deitzel *et al.*, 2001; Huang *et al.*, 2006; Jun *et al.*, 2003; Mit-uppatham *et al.*, 2004b; Supaphol *et al.*, 2005b). Despite such an agreement, it is reasonable to expect the size of the fibers formed are also affected by other factors such as the nature of solvent used, feed rate (Supaphol *et al.*, 2005a, 2005b), spinning conditions (Kang *et al.*, 2002) and temperature (Mit-uppatham *et al.*, 2004).

Viscosity: Solution viscosity is generally determined by the concentration of the polymer solution, molecular mass of the polymer and the density of the solvents used. Viscosity has effects similar to that of polymer concentration on the electrospinning process (Jun *et al.*, 2003). Although solution viscosity is primarily adjusted by changing polymer concentration, varying the

solvent composition (at a constant concentration of polymer) can also serve the same purpose (Lee *et al.*, 2003a). At the same concentration, poly(*p*-phenylene vinylene) (PPV) in ethanol/DMF solvent system has a higher viscosity than when dissolved in ethanol alone (Xin *et al.*, 2006). Higher concentrations of polymer generally give bead-free fibers. However, concentrations that are too high may lead to tip blockage (Subbiah *et al.*, 2005; Zong, *et al.*, 2002).

Addition of low concentrations of polyelectrolytes as demonstrated by Xin *et al.*, (2006) and vibrating the solution at low frequencies during electrospinning (He *et al.*, 2004; Wan *et al.*, 2006) are the two known methods for changing solution viscosity without an appreciable change in concentration. Vibrations facilitate temporary disentanglement of polymer chains by disrupting the van der Waal's interactions between them and therefore reducing the solution viscosity. By merely vibrating the capillary tip (at 400 kHz) Wan *et al.*, (2007), generated thinner nanofibers of poly(butylene succinate) compared to when vibrations were not used. The vibration technique might also be used in electrospinning gels and coagulated materials that are difficult to electrospin.

Solvent: The nature of solvent used determines the conformation of the dissolved polymer chains, the ease of charging the spinning jet, the strength of cohesion in the solution due to surface tension and the rate of solidification of the jet (Shenoy *et al.*, 2005a). Jarusuwannapoom *et al.*, (2005) demonstrated the effect of solvents by investigating the electrospinnability of polystyrene (PS) using different solvents. Of the 17 solvents that dissolved the polymer, only 4 (DMF, MEK, THF, DCE) yielded electrospinnable solutions. They identified dipole moment and

conductivity of the solutions as the key factors that determined electrospinnability of PS in those solvents (Jarusuwannapoom *et al.*, 2005). Son *et al.*, (2004), studied the electrospinning of PEO at different concentrations in five different solvents. They observed that the average nanofiber diameters varied with the solvent used; thinner fibers were obtained using solvents of higher dielectric constant. Table 3.3 lists the properties of some of the solvents that are commonly used in electrospinning of polymers.

Table 3.3: Physical parameters of some solvents commonly used in electrospinning (Andrady 2008)

	Density (g/cm^3)	Boiling point (°C)	Dielectric constant (25 °C)	Surface tension (mN/m)	Viscosity (mPa.s)
Acetic acid	1.050	118	6.19	26.9	1.1
Acetone	0.790	56	20.7	23.46	0.324
Chloroform	1.483	62	4.81	26.67	0.568
Cyclohexane	0.779	81	2.02	24.65	0.979
DMF	0.944	153	36.7	-	0.92
Ethanol	0.785	78	24.6	22.0	1.1
Formic acid	1.213	101	58.5	37.7	1.8
THF	0.889	66	7.6	23.97	0.468
Toluene	0.867	111	2.38	27.95	0.59
Water	0.998	100	78.5	71.99	1

Four characteristics of solvents (conductivity, dielectric properties, surface tension, volatility) are considered important in electrospinning (Krishnappa *et al.*, 2003; Mit-uppatham *et al.*, 2004; Shawon and Sung 2004; Wannatong *et al.*, 2004; Wu *et al.*, 2005; Yang *et al.*, 2004). Each of these solvent characteristics has a direct influence on electrospinnability of the polymer solution and on the morphology of the nanofiber formed. These parameters generally interrelate and they cannot be independently varied to optimize a solution. For example, addition of a few drops of

alcohol to change the surface tension of a PEO/water system also changed the viscosity and conductivity of the solution (Morota *et al.*, 2004). Selecting an ideal solvent system for a polymer to be electrospun is therefore a complex task (Lu *et al.*, 2006). Solvent is mostly based on trial and error.

Conductivity: Solutions of zero conductivity cannot be electrospun. A minimal electrical conductivity is required in the polymer solution to transfer electric charges from the electrode to the droplet at the tip of the spinneret. Due to the presence of conducting ionic species from the polymer (mostly from impurities or additives), conductivity of a polymer solution is generally expected to be higher than that of the pure solvent. Conductivity may decrease (Jun *et al.*, 2003) or increase (McKee *et al.*, 2006a) with concentration depending on the nature of the polymer. If the polymer has ionic functionality (as in the case of polyelectrolytes), the solution's conductivity will increase with increase in the polymer concentration. Conductivity of polymer solutions can be altered by changing the composition of the solvent system used. Changing solvent composition will also change the surface tension and dielectric constant. The consequent changes in electrospinning behavior cannot be uniquely attributed to changes in conductivity. It is however known that polymer solutions having higher conductivities give nanofibers of smaller diameters (Tan *et al.*, 2005).

A solution may be spiked with an additive if its conductivity is found to be too low to electrospin smooth, continuous fibers. The addition of ionic species to the solution allows a relatively higher surface charge density to be maintained on the jet (Zong *et al.*, 2002). The presence of ionic species in the spinning solution reduces the magnitude of voltage required for electrospinning

and often results in improved fiber morphology. Some of the additives that have been used in electrospinning include inorganic salts such as NaCl (Kim *et al.,* 2005; Lee *et al.,* 2005; Wannatong *et al.,* 2004; You *et al.,* 2006), pyridinium formate (Jun *et al.,* 2003), palladium diacetate (Yu *et al.,* 2004), trialkylbenzyl ammonium chloride (Zeng *et al.,* 2003b).

Dielectric Constant: The dielectric constant (ε) is a measure of how effectively a material placed in electric field can concentrate the electrostatic lines of flux. In a practical sense, it is the solvent's ability to hold electrical charges. Solvents of different dielectric constants will interact differently with the electrostatic field. The dielectric constants of the solvents are therefore important in electrospinning. Solutions with higher dielectric constants tend to disperse the surface charge density on the jet more evenly and this leads to the production of fibers with uniform morphologies and smaller diameters (Wannatong *et al.,* 2004).

The effect of the solvent's dielectric constant on fiber morphology was explicitly demonstrated by Min *et al.,* (2004) by comparing the morphologies of nanofibers electrospun from 15 wt% poly(lactide-co-glycolide) solutions in chloroform and in hexafluoropropylene (HFP). Different fiber morphologies were obtained with the two solvents and the average fiber diameter obtained from HFP (having a higher ε of about 16.7) was lower than those obtained from chloroform (having a lower value ε of about 4.81). This phenomenon also held true when PEO was electrospun in different solvents (Son *et al.,* 2004). Solvents with the higher ε resulted in smaller average diameters. The extent to which solvents affect the nanofiber characteristics have been investigated by several other researchers. For example, Hsu and Shivkumar (2004b) reported that as the volume fraction of DMF in a $CHCl_3$/DMF mixture increased from 0 to 10 wt%, the

average diameter of fibers electrospun from poly(L-caprolactone) (PCL) decreased from 450 nm to 150 nm. The decrease in fiber diameter was attributed to the increase in dielectric constant of the solvent system due to the increase in the proportion of DMF (having ε of 36.7) compared to $CHCl_3$ (having ε of 4.8). A similar effect was also observed in PS dissolved in DMF/THF (Lee *et al.*, 2003a), PCL in DMF/CH_2Cl_2 (Lee *et al.*, 2003b) and PVC in DMF/THF (Lee *et al.*, 2002). The qualitative correlation between ε of solvents and the morphologies of nanofibers they form has also been reported on different polymer solutions such as PMMA (Dong *et al.*, 2004), PCL (Lee *et al.*, 2003b), PLGA (You *et al.*, 2006a), and PVC (Lee *et al.*, 2002).

Surface tension: Surface tension is the main force of attraction that opposes the Coulomb repulsion in electrospinning. The charges induced on the polymer solution must be high enough to overcome the surface tension of the solution before the fibers could form. Surface tension of the solution may cause the solution to breakup into droplets as the solution jet accelerates from the tip of the spinneret towards the collector (Christanti and Walker 2001; Shummer and Tebel 1983). High surface tension is also responsible for a phomonenon called electrospraying (Morozov *et al.*, 1998) where droplets of the polymer rather than fibers are formed on the collector. Surface tension has also been attributed to the formation of beads on the electrospun fibers (Fong *et al.*, 1999; Shawon and Sung 2004). According to Deitzel *et al.*, (2001), surface tension and viscosity of the solution are the main parameters that determine the window within which a specific polymer/solvent system can be electrospun. Surface tension of a polymer solution is dependent on the concentration (Deitzel *et al.*, 2001), the chemical nature of the polymer (Lee *et al.*, 2003b) and temperature (Clark 1938). Surface tension is affected by the

electric field and it is likely to change with time, as the jet moves from the tip of the capillary to the collector (Fong *et al.*, 1999).

All other factors being equal, lower surface tension is a desirable solvent characteristic in electrospinning (Fridrikh *et al.*, 2003). Surface tension of a polymer solution can be controlled by a judicious selection of solvents. However, changing the solvent composition leads to a change in viscosity (Lee *et al.*, 2002). Additives such as surfactants can be employed to reduce the surface tension of a polymer solution to facilitate electrospinning (Jung *et al.*, 2005; Lin *et al.*, 2005a; Zeng *et al.*, 2003b). Lin *et al.*, (2004), electrospun bead-free nanofibers from an otherwise unspinnable 5% PS (w/v) in DMF/THF when 0.03 mmol/L of a cationic surfactant, dodecyl trimethyl ammonium bromide (DTAB), was added to the polymer solution. Some other surfactants that have been used in electrospinning are Triton X-100 (Yao *et al.*, 2003), triethyl benzyl ammonium chloride (TEBAC) and AEO10 (Zeng *et al.*, 2003b).

Volatility: For the best results, all solvents in the polymer solution must dry up before the charged jet hits the collector. Otherwise, the wet fibers may fuse together to form a melded or reticular mat (Hsu and Shivkumar 2004a) or a flat ribbon-like nanofibers (Koombhongse *et al.*, 2001). Using volatile solvents encourages evaporation and removes this challenge. However, the solution may dry up quickly at the needle tip and block the flow when highly volatile solvents are used (Megelski *et al.*, 2002). This may lead to the formation of wrinkled or "raisin-like" nanofibers (Krishnappa *et al.*, 2003). Very rapid drying can also result in the formation of fibers with bigger diameters (Bognitzki *et al.*, 2000; Wannatong *et al.*, 2004; Wei *et al.*, 2006b). At a given gap distance, the rate at which polymer solutions dry during electrospinning is determined

by the environmental temperature, the vapour pressure of the solvents and the degree of whipping instability (Kidoaki *et al.*, 2006; Larsen *et al.*, 2004b).

3.6.2 Spinning parameters

The spinning parameters comprise the nature of the setup (collector material and geometry) as well as the operational variables (magnitude and polarity of the applied voltage, feed rate and gap distance) employed during the spinning process.

Voltage: The applied voltage is needed to induce the necessary charges on the solution and also establish the external electric field to drive the process. While direct current (DC) supply is the most commonly used. It is also possible to use the alternating current (AC) for electrospinning (Ramakrishna *et al.*, 2005). Either positive or negative voltage of more than 6 kV should be able to cause the jet initiation (Taylor 1964).

In general, application of higher voltages brings about greater levels of instability and stretching of the jet (Buchko *et al.*, 1999; Fridrikh *et al.*, 2003; Shin *et al.*, 2001a, 2001b) and results in smaller fiber diameters (Buchko *et al.*, 1999; Jalili *et al.*, 2005; Lee *et al.*, 2004; Megelski *et al.*, 2002; Spasova *et al.*, 2004; Takahashi *et al.*, 2005). Several other researchers (Gu and Ren 2005; Lee *et al.*, 2002; Shukla *et al.*, 2005; Yuan *et al.*, 2004) have however, reported that the applied voltage does not have a significant effect on the average fiber diameter. These discrepancies in observations suggest that the effect of applied voltage on fiber diameter needs to be considered together with other parameters such as feed rate, gap distance (Sukigara *et al.*, 2003) and mass transfer (Baumgarten 1971; Dersch *et al.*, 2003; Khil *et al.*, 2003; Shin *et al.*, 2001a; Theron *et*

al., 2004). The apparent discrepancy in the reported effects of voltage on fiber diameter is likely due to the different polymer concentrations, feed rates and gap distances used in the different studies.

A high voltage may favour the formation of secondary jets resulting in the formation of fibers of smaller average diameters (Demir *et al.*, 2002). Fiber diameter is also affected by the length of the jet's flight time. A longer flight time will allow more time for the fibers to stretch and elongate before they are deposited on the collector plate. At a lower voltage, the reduced acceleration of the jet and the weaker electric field may increase the flight time of the electrospinning jet and results in the formation of fibers with lower average diameters (Zhao *et al.*, (2004).

The polarity of the voltage applied at the capillary tip has an impact on morphology and the average diameter of the fiber formed. A significant difference was observed in the average diameters of nylon-6 nanofibers electrospun separately from positively and negatively charged tips (Mit-uppatham *et al.*, 2004a; Supaphol *et al.*, 2005a). The average diameters of fibers generated from negatively charged capillary tips were found to be significantly larger (Mit-uppatham *et al.*, 2004a; Kalayci *et al.*, 2005). A similar phenomenon was also observed with nanofibers electrospun from PAN in DMF (Kalayci *et al.*, 2005).

Feed rate: Feed rate is the quantity of polymer solution pumped into the tip per unit time. For a steady state and continuous formation of fibers, the feed rate of the solution must match the rate of its removal from the tip. At lower feed rates, the Taylor cone gets depleted and the

electrospinning process may only be intermittent or even stop completely. At higher feed rates however, larger fiber diameters and beads often result (Kidoaki *et al.*, 2006).

The feed rate is itself dependent on the internal diameter of the orifice or needle through which the polymer solution is pumped. An orifice with a smaller internal diameter reduces the incidence of clogging as well as bead formation (Mo *et al.*, 2004) and results in formation of fibers with smaller average diameters (Zhao *et al.*, 2004). The reduction in the incidence of clogging could be due to less exposure of the solution to the atmosphere during electrospinning. In the case of a smaller internal diameter of the orifice, the size of the droplet that forms at the tip of the orifice reduces, and the surface tension of the droplet increases. Surface tension is dependent on the size of the droplet. For the same applied voltage, a greater Coloumbic force is required to cause jet initiation on a smaller sized droplet than a bigger one. As a result, the acceleration on the jet from a smaller droplet decreases and this allows more time for the solution to stretch and elongate before it is collected. This leads to the formation of fibers with smaller average diameters. If the diameter of the orifice is too small, however, it may not be possible to extrude a droplet of solution at the tip of the orifice. The effect of feed rate on fiber formation and morphology has been widely investigated (Buttafoco *et al.*, 2006; Fridrikh *et al.*, 2003; Jeun *et al.*, 2005; Theron *et al.*, 2004; Zhang *et al.*, 2005).

Gap distance: This is the distance extending from the capillary tip to the surface of the collector. The gap determines the electric field strength and the time available for evaporation of the solvent before the jet strikes the collector surface. All factors being equal, an increase in gap distance leads to a decrease in average fiber diameter (Baker *et al.*, 2006; Kidoaki *et al.*, 2006;

Lee *et al.*, 2004) within a limit. Too short a gap distance yields wet fibers that fuse on the collector (Hsu and Shivkumar 2004a; Jalili *et al.*, 2005). The fiber diameter however increases and the fiber morphology deteriorates if the gap distance is too wide (Hong *et al.*, 2006; Yao *et al.*, 2005).

Capillary tip: Conducting materials such as metal needles as well as non-conducting materials such as glass and plastics have been used as the capillary tip in solution electrospinning (Yarin and Zussman, 2004). Although most studies reported the use of a simple and static capillary tip, a number of innovations have explored the use of movable tips. For example, Kidoaki *et al.*, (2005) used a movable tip to obtain an even deposition of nanofibers on a drum collector. Electrospinning with a moving tip help align the fibers. Li (2005), used a tip made of a non-conducting fiber inserted in the lumen of a conducting capillary tip. Accordingly, this modified tip allowed the electric field to be used solely to accelerate the jet and therefore reduced the potential needed to be applied.

Collector: The simplest and the most used collector in laboratory electrospinning is a stationary metal plate or an aluminium foil placed at a fixed distance from the tip. The collector is usually grounded to allow for a rapid discharge of the residual charges on the fibers. The collector may also be held at polarity opposite to that of the tip to increase the strength of the electric field. The material, nature and geometry of the collector play a major role in defining the morphology of the fibers (Teo and Ramakrishna 2006).

The rate of discharge of residual charges of the jet upon contact with the collector is influenced by the dielectric properties of the collector. The collector material is therefore an important factor in determining the morphology of the electrospun fibers (Kessick *et al.*, 2004; Kim and Kim, 2006; Mitchell and Sanders, 2006). It has been demonstrated that some of the common solvents such as water (Khil *et al.*, 2005; Smit *et al.*, 2005), and methanol (Kim *et al.*, 2005) could be better collectors than their solid counterparts. A liquid collector may also be used to precipitate the nanofibers when non-volatile solvents are used. Srinivasan and Reneker (1995) demonstrated this by electrospinning poly(*p*-phenylene terephthalamide) nanofibers from sulfuric acid solution into a grounded water bath to precipitate the polymer.

Several different shapes of collectors such as flat plate (Kidoaki *et al.*, 2005); rotating drum (Wannatong *et al.*, 2004), mandrel (Mo and Weber 2004), rotating disc (Zussman *et al.*, 2003), rectangular, triangular, or wire cylinder frame (Katta *et al.*, 2004), electrode pair arrangements (Li *et al.*, 2003), ring and mesh electrode (Dalton *et al.*, 2005), cones (Bunyan *et al.*, 2006) have been used.

3.6.3 Ambient parameters

The effect of the environmental conditions on electrospinning is not as extensively investigated as the other parameters. Since electrospinning is driven by external electric field, changes in the electrospinning environment will affect the process. Four conditions (humidity, pressure, temperature and type of atmosphere) have been identified to affect the process and consequently, the quality of the fibers formed.

Humidity: Humidity has a pronounced effect on the morphology of the fiber if it is spun from a volatile solvent (Bognitzki *et al.*, 2001; Megelski *et al.*, 2002). Casper *et al.*, (2004) observed that smooth fibers are formed from PSU dissolved in THF only when humidity is less than 50%; circular pores were formed on the fiber surfaces when humidity was higher than 50%. The humidity also affects the rate of evaporation of solvents. At a very low humidity, a volatile solvent may dry very rapidly leading to tip blockage and formation of fibers with bigger average diameters (Baumgarten 1971). As the charged jet interacts with the environment during spinning, the surface charges could be dissipated on contact with the humid air particles (Li and Xia 2004a; Li et. al. 2005a).

Pressure: Electrospinning is not possible at very low pressures due to direct discharge of the electrical charges (Ramakrishna *et al.*, 2005). A stream of air or a gas at a high pressure may be delivered coaxially to the tip to provide an additional drag force for jet extension. When the drag force is dominant over the electrostatic force in driving jet extension, the process is referred to as electroblowing (Um *et al.*, 2004; Wang *et al.*, 2005).

Temperature: Temperature of the electrospinning chamber determines the rate of evaporation of the solvents in the jet and hence controls the final diameter of the nanofibers (Mit-uppatham *et al.*, 2004a). An external heating source such as a heat gun or a high wattage lamp could be used to help dry the fiber rapidly during electrospinning (Subramanian *et al.*, 2005). In electrospinning aqueous solutions of hyalauronic acid (HA), Um *et al.*, (2004) used a jacket of heated air (25-57 ^{o}C) to decrease solution viscosity and increase the rate of drying of the fiber.

Atmosphere: The composition of the atmosphere in the electrospinning setup has an effect on the process because different gases behave differently in an electric field. For example, using a positively charged capillary tip in an electron-rich gaseous environment will impede the process and environment of highly electronegative gases (such as CO_2 or freons) discourages the loss of surface charges and improves nanofiber quality (Ensor and Andrady, 2007).

3.7 Optimization of electrospinning parameters

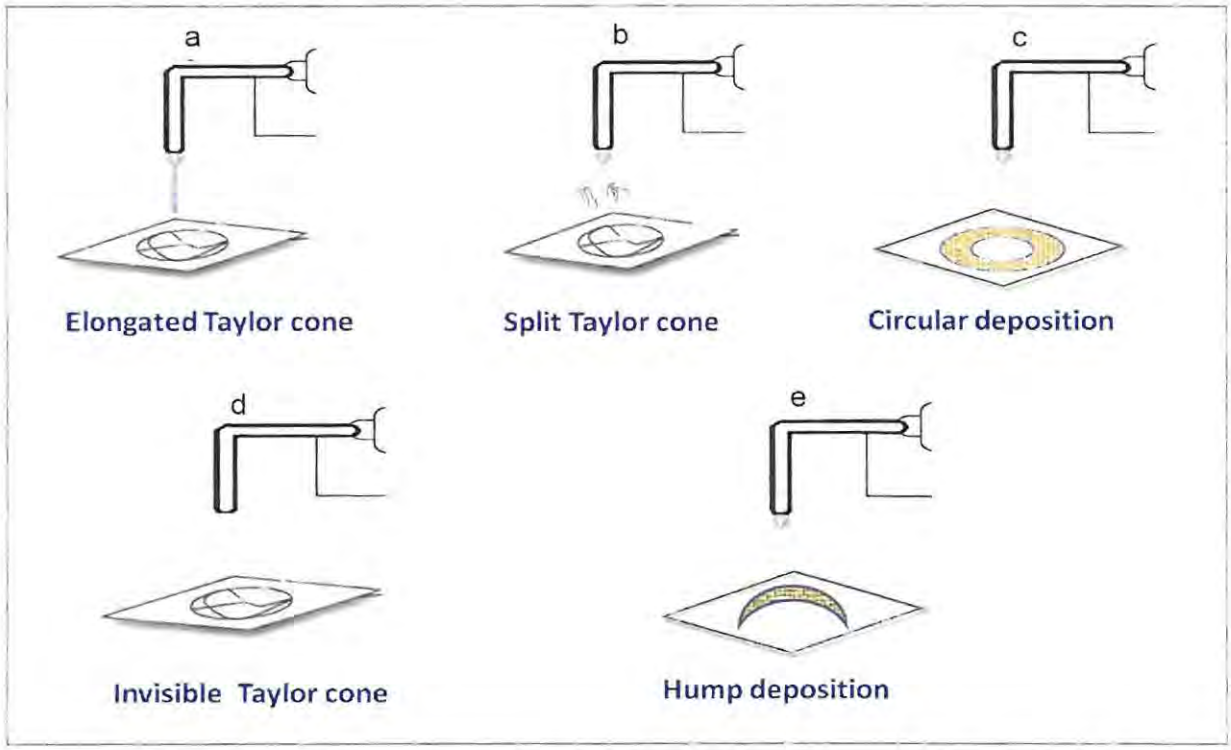

Figure 3.6 Taylor cone and deposition patterns of non-optimized electrospinnning

Uniform and bead-free nanofibers are formed only when all the electrospinning parameters are optimized. However, it is difficult to check case-by-case whether all the parameters are optimized prior to electrospinnning. Optimization of the electrospinning parameters could be checked during electrospinning using the stability and shape of the Taylor cone or the pattern of

nanofiber deposition. Figure 3.6 shows some non-optimized conditions. For example, an elongated Taylor cone (a) depicts high flow rates or too low a voltage. When the voltage is higher than the optimum, the Taylor cone splits into dendrites (b) or a hollow-centre circular deposition is observed. The Taylor cone does not show (d) if the applied voltage is higher than the optimum or the flow rate is low. Otherwise, a hump deposition (e) is observed if the flow rate is higher than the optimum.

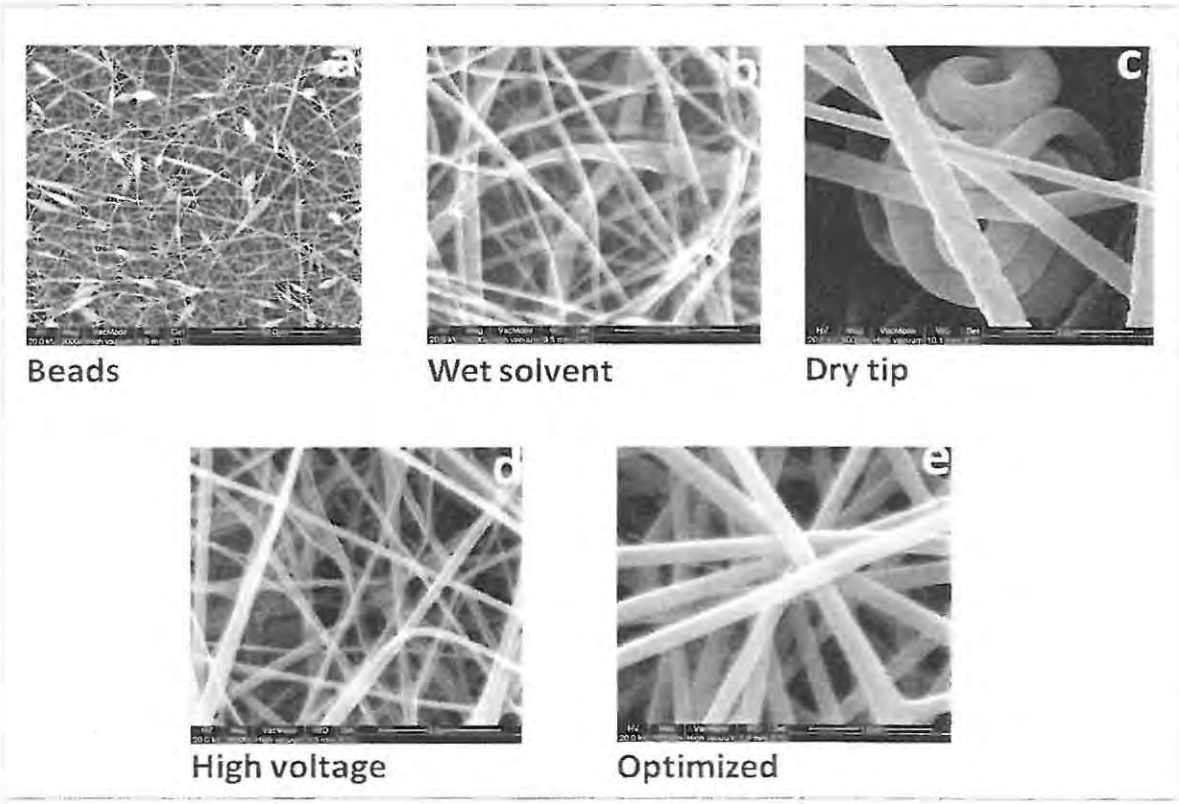

Figure 3.7 Scanning electron microscope images of nanofibers showing different effects of optimization

The SEM images (Fig 3.7) could also give some indication whether the electrospinning parameters were optimized. For example, occurrence of cylindrically shaped beads is an

indication of low polymer concentration. If the solvents do not evaporate during electrospinning, especially when non-volatile solvents like DMF and NMP are used in dissolving the polymer, the nanofibers fused together as shown in (b). Otherwise, if the solvents evaporate too quickly, the capillary tip dries up and forms a knot (c). Figure d is a typical SEM for Taylor cone split where nanofibers of very different diameters are formed.

3.8 Functionalization of electrospun nanofibers

Electrospun polymer nanofibers have a great potential for applications in many fields of science and technology. However, most of polymer nanofibers are chemically inert and do not have reactive functional groups in their structures. For a successful application in fields such as immobilization of chemical/biological agents, the inert nanofibers ought to be functionalized (Ramakrishna 2005) in order to enhance their absorption properties and also extend their life spans. Ikada (1994); Ratner (1995) and Desai et. al. (2004) reviewed the modern trends in functionalization of nanofibers. Some of the common surface modification techniques include treatments by blending, coating, radiation with electromagnetic wave, electron beam, ion beam (Dong and Bell 1999; Brown 2003) or atom beams (Chan *et al.,* 1996), corona or plasmas treatment (Chu *et al.,* 2002; Grace and Gerenser 2003; Liston *et al.,* 1993), chemical vapour deposition, gas oxidation, metallization, chemical modifications use wet-treatment and surface grafting polymerization (Uyama *et al.,* 1998; Kato *et al.,* 2003). The chemical approach has been commonly used. An added advantage of the electrospinning process is that the fibers could be functionalized prior to, during and even after spinning.

Chemical modification involves the introduction of one or more chemical species to a given surface so as to produce a surface which has enhanced chemical and physical properties (Mottola 1992). The chemical modification is a direct and simple approach for functionalizing polymers having functional groups like hydroxyl, carboxyl, amino and ester. Chemical reactions can be carried out at sites that are vulnerable to electrophilic or nucleophilic attack. For example, polyesters like PET, PCL and PLLA can be treated by diamine compounds to introduce amino groups through the aminolysis of the ester groups (Zhu *et al.,* 2002). Through chemical modification, oxygen-containing functional groups (such as carbonyl, hydroxyl, and carboxylic groups) may be introduced at the surface of the polymer. The oxygen-containing functional groups increase the polarity and the ability to hydrogen bond, thus in turn results in the enhancement of wettability and adhesion.

3.9 Applications of electrospun nanofibers

The major advantage of electrospun nanofibers is their nanoscale dimensions as they result in a number of superior properties such as increased surface-to-volume ratio, small pore sizes, high porosity and enhanced mechanical strength. Consequently, electrospun nanofibers are excellent candidates for application in different fields such as tissue engineering, high-performance filtration, chemical-biological protective clothing and polymer composite reinforcement (Ramakrishna *et al.,* 2005). Figure 3.8 adapted from Huang *et al.,* (2003), illustrates the diversity of applications of electrospun nanofibers. The following section provides a comprehensive review of some applications of electrospun nanofibers.

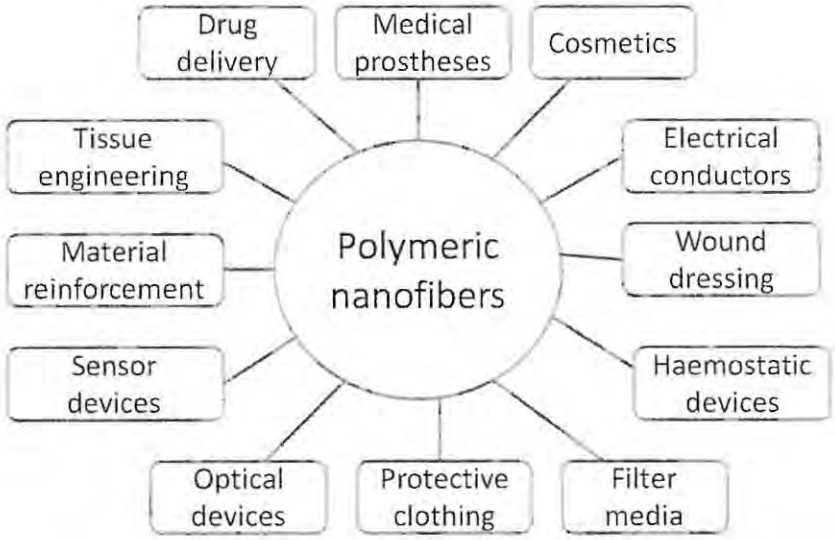

Figure 3.8: Some of the major applications of polymer nanofibers (adapted from Huang et al., 2003)

An affinity membrane is a functionalized membrane that selectively captures target molecules using the ligands on its surface (Ma *et al.*, 2006). Electrospun nanofibers can be surface functionalized with metal adsorbing ligands and be applied as an affinity membrane for the pre-concentration of heavy metals from water. Functionalized electrospun nanofiber membranes permit the purification of water based on chemical properties rather than molecular weight/size (Bhardwaj and Kundu 2010). Their highly porous structures coupled with high surface areas and ease of functionalization make the electrospun nanofibers ideally suited for use as affinity membranes (Zussman *et al.*, 2002). Electrospun nanofibers are increasingly being used for water filtration and purification (Tsai *et al.*, 2002, Wang et al, 2011). Bjorge *et al.*, (2010) evaluated the suitability of electrospun nanofiber for water purification. The study showed that the electrospun membranes could be used for water purification applications, but that further improvements were necessary before these membranes could be practically employed in the

water sector. Bjorge *et al.*, (2010) identified the level of functionality and the properties of irreversible fouling as the major issues requiring further research.

4

Experimental

4.1 Overview

This chapter outlines the materials and methods used in the research. It also describes the experimental procedures that were employed.

4.1 Materials

4.1.1 Chemicals and reagents

All the chemicals were of analytical grade and were used without any further purification. 1-[bis[3-(Dimethylamino)-propyl]amino-2-propanol (98%), 1-methyl-2-pyrrolidinone (99.5%), nitrate salts of Cu(II), Ni(II), Co(II), Cd(II) and Pb(II), all of purity more than 99.0%, were purchased from Aldrich (St Louis, USA). Pyridine (99.9%, anhydrous) was obtained from BDH Chemicals (London, England). Dichloromethane (99%), tetrahydrofuran (98%), N,N-dimethylformamide (99%), nitric acid (65%), hydrochloric acid (32%), 1,1-carbonyldiimidazole, 1,8-diazabicyclo[5,4]undec-1-ene, formic acid (98%) and glacier acetic acid (99%) were purchased from Merck Chemicals (Wadesville, South Africa).

Standard solutions were freshly prepared using ultrapure water generated from MilliQ systems (Massachusetts, USA). All glassware was soaked overnight in 4 M HNO_3 solution prior to use. Working standards of metal solutions were freshly prepared from stock solutions. Solutions used in the potentiometric titrations were prepared using freshly boiled, degassed ultrapure water to ensure the removal of carbon dioxide and oxygen.

4.1.2 Polymers

Polyamide-6 (PA-6: M_W 10000, Sigma 181110), polysulfone (PSU: M_W 22,000, CAS 25135-51-7), polystyrene (PS: M_W 192,000, CAS 9003-53-6), polyethersulfone (PES) and Polyvinylidene fluoride (PVDF) were supplied by Sigma Aldrich (St. Louis, USA). All the polymers were used as received. Polymer solutions were prepared by dissolving known masses of the polymer (pellets or powder) in appropriate volumes of solvents by slowing agitating the solution using Stuart SB-162 magnetic stirrer (Staffordshire, UK). Solutions were prepared in glass bottles with air-tight lids to avoid evaporation of solvents at room temperature.

4.2 Instrumentation

4.2.1 Electrospinning setup

Single nozzle setups (Fig 4.1) consisting of an infusion pump (KD Scientific Syringe Pump Series 100 or New Era Multi-phaser NE-1000) and a high voltage source (Glassman High Voltage Series EH). The collector system was a flat aluminium sheet placed on a support. Electrospinning was carried out at room temperature (293 ± 2 K).

Figure 4.1 Electrospinning setup

4.2.2 Attenuated Total Reflection – Fourier Transform Infrared (ATR-FTIR) spectroscopy

ATR-FTIR spectra (400-4000 cm^{-1}) were recorded with a PerkinElmer FT 100 spectrometer (Massachusetts, USA), equipped with a germanium (Ge) universal ATR sampling accessory. An average of 8 scans with a resolution of 4 cm^{-1} was taken for each spectrum. Scans were taken on 3 different spot for each sample and an average calculated.

4.2.3 Scanning electron microscopy

Morphology of the nanofibers was studied using two scanning electron microscopes (SEM); a low-resolution Tescan TS5136ML (Brno, Czech Republic) and a high-resolution Quanta 200 equipped with a field emission gun (FEG) system from FEI (Eindhoven, The Netherlands). Prior to the SEM analyses, the samples were sputter-coated with a gold or gold-palladium layer using Balzers SCD 030 (Liechtenstein, Germany). Typical magnifications of SEM images taken ranged between 1000 and 150000 and were analyzed through the distance transform approach (Ziabar et al 2009) using either Scandium® or Cell^D Olympus Imaging Software. Average fiber diameters were deduced by finding the diameters of >60 fibers per sample.

4.2.4 Brunauer-Emmet-Teller (BET) analysis

Surface areas and pore characteristics of the nanofibers were determined using the Brunauer-Emmet-Teller (BET) isotherms obtained from nitrogen adsorption on an Accelerated Surface Area and Porosimetry System (ASAP™ 2020), Micromeritics (Bedfordshire, England). Prior to analysis, about 0.3 g portions of samples were degassed overnight at 105 °C (temperature higher than water but lower than the glass transition temperature (t_g) of the polymeric material in N_2 environment using a Micromeritics SmartVac degassing system. Table 3.2 gives the detail operating parameters used for degassing. The pore size distribution and specific surface areas were determined via N_2 adsorption/desorption isotherms obtained at -196 °C. Analyses were repeated, at least twice, for all samples and the measurements were in good agreement.

Table 4.1: Optimal conditions used for BET analysis

Evacuation phase		**Heating phase**	
Target temp (K)	423*	Target temp (K)	423*
Temperature ramp (K/min)	1.0	Ramp rate (K/min)	1.0
Evacuation rate (mbar/s)	6.7	Hold temperature (K)	423*
Vacuum set point (μbar)	13	Hold time (h)	10
Evacuation time (h)	1.0	Hold pressure (mbar)	133

* dependent on the polymeric material.

The BET gas adsorption method is a well-established method for characterizing surface area and pore structure of porous materials (Adamson and Gast 1997). By assuming the Langmuir adsorption model and incorporating the concept of multimolecular layer adsorption, the surface area of the substrate can be calculated the BET equation:

$$\frac{P}{(P_0 - P)} = \frac{1}{V_m C} + \frac{C-1}{V_m C}\left(\frac{P}{P_0}\right) \qquad 4.1$$

where P and P_0 are the gas pressure and the saturated gas pressure at the temperature of experiment, V_a and V_m are the quantity of gas adsorbed under pressure P and the quantity of gas required for a monolayer adsorption on the sample surface, respectively. C is a constant related to the heat of adsorption of the first molecular layer of gas. By plotting $P/V_a(P_0-P)$ against (P/P_0), C and V_m can be calculated from the intercept and the slope of the straight line. Since there is no assumption on cylindrical pore geometry, the specific surface area determined by the BET method is more reliable than capillary flow and mercury porosimetry (Nisbet *et al.*, 2009).

4.2.5 Inductively Coupled Plasma-Optical Emission Spectrometry

Concentrations of metals were determined using an iCAP 6000 series Inductively Coupled Plasma-Optical Emission Spectrometer (ICP-OES) from Thermo Electron Corporation (Cheshire, United Kingdom). Emission lines were selected based on the EPA method of determining trace elements in water (US-EPA 2001). Table 4.2 shows the analytical parameters used for the analyses while Table 4.3 shows the detailed operational conditions of the ICP-OES.

Table 4.2: Analytical parameters used for metal analyses on the ICP-OES

Analyte	Wavelength (nm)	Highest calibration point (mg/L)	Estimated detection limit (µg/L)
As	193.759	10	53
Cd	226.502	2	3.4
Co	228.616	2	7.0
Cu	324.754	2	5.4
Ni	231.640	2	15
Pb	220.353	10	42

Table 4.3: Detailed operational conditions of the ICP-OES

	Analysis preferences				
Sample options	# of repeats:	3			
	Sample flush time:	30 s			
Source	Light source:	ICAP			
	Plasma view:	Axial			
Analysis maximum	Low WL Range	Axial	15	Radial	15
Integration times (s)	High WL Range	Axis	5	Radial	5
Calibration mode	Concentration				
Trailing full flame	Intelli-Flame:	Yes			
Options	Max integration time (s):	30			
	WL Range:	Low			
	View:	Axial			
	Source settings				
Nebulizer pump	Flush pump rate (rpm):	100			
	Analysis pump rate (rpm):	50			
	Pump relaxation time (s):	5			
	Pump tubing type:	Tygon orange/white			
RF Power:	1150 W				
Auxiliary gas:	0.5 L/min				

4.3 Conductivity, temperature and viscosity

Conductivities and temperatures of the solutions were measured using MeterLab CDM 210 conductivity meter (Lyon, France). The pH of the solutions was determined using the Jenway (3510) pH meter (Essex, UK). Solution's viscosity and shear stress were measured using a Brookfield DV-II rotational viscometer (Essex, UK) with variable speed from 0.01 to 200 rpm.

4.4 Potentiometric acid-base titrations

The protonation constants of ligands in aqueous solutions were determined by potentiometric titration at 25.00 ± 1.00 °C in a Metrohm 794 double-walled titration cell (Herisau, Switzerland) in an inert, nitrogen environment. Titrations were performed over a pH range of 2 to 11 using 0.10 M HCl and 0.10 M tetramethylammonium hydroxide. Titrations were controlled using Tiamo software. The glass electrode was calibrated for a strong acid-strong base reaction by the Gran method (Brunelot 1989: Gran 1952) and E° value of the reaction was obtained using the GLEE software (Gans 2000). The pK_w value of 13.83 ± 0.01 in 0.1 M tetramethylammonium chloride (TMACl) as an ionic medium was used for all the computations (Bazzicalupi *et al.*, 2009). The HYPERQUAD program (2008 version) was used for computation of protonation constants in equilibrium state (Gans *et al.*, 1996). About 400 data points emanating from three independent titrations were used in calculating the protonation constants of the ligands. The statistical error (σ) was below 0.03 for both refinements.

4.5 Metal adsorption and desorption studies

Adsorption of metal ions by the functionalized electrospun fibers was investigated in aqueous solutions. The influence of the initial concentrations of the metal ions was investigated for a range (0-10 mg/L) of standard solutions. To vials containing 10 mL aliquots of metal solutions of known concentrations were added optimized sorbent mass of 10 and stirred for 2 h. The nanofibers were filtered off through 0.45 μm sintered filter using suction. The concentration of metal ions left in solution was then determined using the ICP-OES. The concentration of metal adsorbed was taken as the difference between the initial and the final concentrations of the solution. Desorption experiments were carried out on the spent sorbents to confirm the adsorbed

concentrations. For desorption, the loaded fiber was washed three times with 5 mL portions of de-ionized water and was dried on the filter using vacuum suction. The dried fiber was then placed in dilute HNO_3 of pH 2 and stirred with a magnetic stirrer for the stipulated time. The concentration of metal desorbed is taken as the difference in final concentration of the acidic solution and the blank solution. All adsorption studies were carried out at the optimal pH of the respective metals while desorptions were conducted at pH of 2 because no adsorptions were observed at pH values less than 3.

4.6 Sorbent dose

The effect of nanofiber dose on the uptake of metals was investigated for nanofiber mass ranging from 2-20 mg. Portions of the functionalized nanofibers (with masses ranging from 2-20 mg) were stirred, for 2 h, in 10 mL portions of 5 mg/L metal solutions. The loaded sorbent was then filtered off, washed with ultrapure water and was dried on the filter using vacuum suction. The dried fibers were placed in 10 mL aliquot of 0.10 M HNO_3 solution and stirred for 2 min in order to desorb the metal ions enriched on the nanofibers. To investigate the optimal pH for metal ions enrichment, adsorption experiments were carried out in 5 mg L^{-1} standard solutions of the metals buffered to the desired pH values ranging from 2 to 12. The extent to which metal ions were enriched was then determined using the ICP-OES. The effect of contact time on the uptake of metal ions was also investigated in 5 mg/L metal ion solutions in batch experiments. In order to avoid precipitation at higher pH, the solutions were kept at the optimal pH of the metal under study using an ammonia buffer (Sun *et al.*, 2006).

4.7 Effect of fiber size on efficiency of adsorption

Nanofibers of different diameters were electrospun by varying the polymer concentrations and the distance between the needle tip and the collector (gap distance). The effect of the nanofiber diameter on efficiency of adsorption was investigated in 10 mL portions of 100 mg/L standard metal solutions.

4.8 Fiber reusability

To evaluate the reusability of the fibers, 10 mg mass of adsorbent was used repeatedly to adsorb Ni in 20 mL aliquots of 100 mg/L solution. After each adsorption, the adsorbent was desorbed by placing it in HNO_3 solution at a pH of 2 for 5 min (optimized time was > 4 min). The fiber was thoroughly washed in de-ionized water, filtered through 0.45 μm filter using suction. It was then dried and reused to adsorb Ni in another 20 mL aliquot of 100 mg/L solution.

4.9 Acid digestion

The metal ions in the samples were either leached in to solution through acid digestion or were adsorbed onto the polymer nanofiber sorbent and then desorbed into acid solutions for analysis. Three acid digestion procedures were separately employed. For aqua regia digestion, a 100 ml portion of water sample placed in 250 ml pyrex digestion tube was pre-digested at room temperature for 16 h with either 28 ml of 37% HCl:70% HNO_3 (3:1) mixture. Otherwise, 30 ml aliquot of HNO_3+H_2O_2 (v/v) mixture was used for digestion. The suspension was then digested at 130 °C for 2 h in a reflux condenser. It was then filtered through an ashless Whatman 41 filter, diluted to 100 ml with 0.5 M HNO_3, and stored in polyethylene bottles at 4 °C for analyses. Another 100 ml portion was just spiked with with 15 ml of 70% HNO_3 and then filtered through

an ashless Whatman 41 filter and stored in polyethylene bottles at 4 °C for analyses. For metal adsorption, 20-30 mg portion of stamped out nanofiber sorbent was placed in 100 ml portion of water sample and stirred intermittently for 2 h. The fiber was filtered off and dried using vacuum. The loaded fiber was then desorbed in 10 ml portion of 0.01 M HNO_3.

4.10 Analytical quality control procedure

A custom-made certified reference material for groundwater (SEP-3) purchased from Inorganic Ventures (Christiansburg, USA) was used to validate the analytical procedure. Analytical calibrations were carried out in aqueous standard solutions. Adsorption and desorption experiments were carried out using 10 mg of the nanofiber adsorbent in 10 mL portions of the certified reference groundwater. Repeatability of the method was evaluated by comparing the signals obtained from 5 determinations of the reference material. The limits of detection (LOD) and quantification (LOQ) were evaluated as 3 and 10 times the estimated regression standard deviation respectively based on 5 replicate determinations.

5

Steady state electrospinning of polyethersulfone

This chapter is based on:

Darko, G., Zugle, R., Nyokong, T., De Clerck, K., Westbroek, P., Goethals, A., De Schoenmaker, B. Torto, N. (2011). Steady states electrospinning of polyethersulfone (In preparation)

5.1 Overview

Polyethersulfone was electrospun under optimal conditions in DMF-NMP solvent systems. The effects of the processing parameters such as voltage, tip-to-collector distance and flow rate on nanofiber diameter were investigated. The nanofibers were not applied as sorbents for pre-concentrating heavy metals.

5.2 Results and discussions

5.2.1 Dissolution of polymer

Polyethersulfone disolves completely in both DMF and NMP. The surface tension and boiling point of DMF are lower than those of NMP. Also DMF has a higher vapour pressure than NMP. Therefore blending DMF with NMP reduces the rate of solvent evaporation. However, NMP has higer conductivity and a better solvency effect for polymers. Table 5.1 shows the relevant physical characteristics of the solvents used.

Table 5.1: Relevant physical characteristics of the solvents used

	DMF	NMP
Vapour pressure (kPa at 25 °C)	0.30	0.29
Conductivity (mS/cm at 25 °C)	0.000	0.002
Surface tension (nN/m at 20 °C)	37.1	40.7
Boiling point (°C)	153	202
Density (g/cm^3 at 25 °C)	0.944	1.028
Viscosity (cP at 25 °C)	0.92	1.65

Table 5.2: Solubility characteristics of polyethersulfone (23-28 wt%) concentrations in various composition ratios of DMF and NMP

		Percentage composition (DMF:NMP)				
		100:0	95:5	90:10	85:15	80:20
Polymer concentration (wt%)	28					
	27					
	26					
	25					
	24					
	23					

The polymer did not dissolve at concentrations ≥ 28 wt%, regardless of the solvent composition (black zone). Dissolution only occurred when the polymer concentration was less than 28 wt% (grey and brown zones). However, concentrations and solvent combinations indicated in the grey zone formed gels when the solutions were left standing (Table 5.2). The rate and extent of gel formation was found to be dependent on the polymer concentration and the composition of the solvent system. Higher proportions of DMF, for example 100:0, lead to a faster rate of gel formation. For such concentrations and combinations that form gels, the polymer solutions were electrospun before gelation.

5.2.2 Solution characteristics

Table 5.3: Characteristics of the polymer solutions formed

Polymer concentration (wt%)			Percentage composition (DMF:NMP)				
			100:0	95:5	90:10	85:15	80:20
	26	Viscosity (Ns/m^2)	2018	2080	3635	3848	-
		Conductivity (mS/cm)	0.006	0.009	0.009	0.009	0.009
	25	Viscosity (Ns/m^2)	1552	1613	1623	1638	1648
		Conductivity (mS/cm)	0.010	0.010	0.010	0.010	0.010
	24	Viscosity (Ns/m^2)	1486	1542	1559	1576	1583
		Conductivity (mS/cm)	0.011	0.013	0.013	0.013	0.013
	22	Viscosity (Ns/m^2)	1346	1412	1431	1435	1453
		Conductivity (mS/cm)	0.012	0.012	0.013	0.015	0.015

The increase in solution conductivity due to increase in the proportion of NMP was more pronounced in the dilute solutions than in the concentrated ones (Table 5.3). For example, no significant change in conductivity was observed at 26 wt% concentration at different compositions. Similar trends were observed at 25 and 24 wt% concentrations. However, at 22 wt%, conductivity increased gradually with increasing proportion of NMP.

Generally, conductivity of the solutions decreased with increase in polymer concentration. This was not unexpected because the polymer is itself not charged and the solutions derived their conductivities from the solvents. The dilute polymer solutions, containing more solvents will be more conducting than the concentrated solutions containing more of the unconducting polymer. Viscosity of the solutions increased with increase in polymer concentration and proportion of NMP. The density and viscosity of NMP are higher than those of DMF. Increasing the proportion of NMP will therefore increase the viscosity of the solution even at a constant concentration.

5.2.3 Window of eletrospinnability

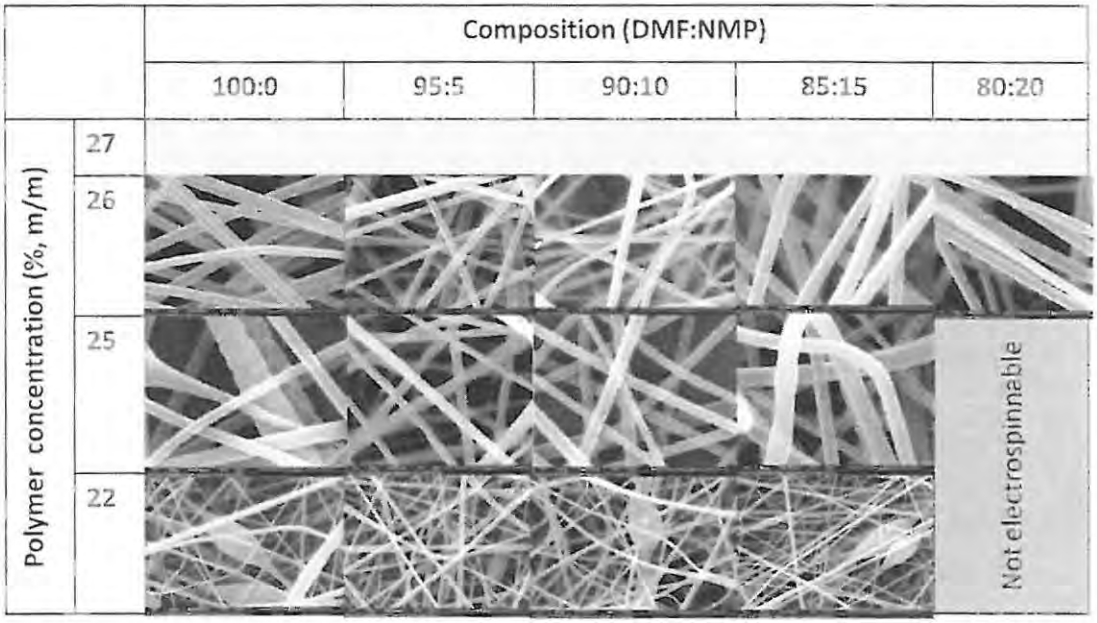

Figure 5.1: Window of electrospinnability of polyethersulfone in different solvent combinations of DMF:NMP

Polymer concentrations up 25 wt% were either not electrospinnable, because of their low viscosity, or gave out beaded nanofibers (Fig 5.1). Solutions of 25 wt% polymer in pure DMF exhibited drying at the spinneret tip and did not give nanofibers of uniform morphologies. Some levels of bead formation were observed in the nanofibers formed from 25 wt concentration at all the solution composition variations. 25 wt% polymer solution containing 20% NMP could not electrospin due to excess of less-volatile NMP in the solution. There was a bit of bead formation in 26 wt% polymer in pure pure DMF, probably due to low conductivity of the solution. Bead-free fibers having uniform morphologies were obtained only from 26 wt% polymer solution (Fig 5.2).

5.2.3 Effect of solvent composition on nanofiber diameter

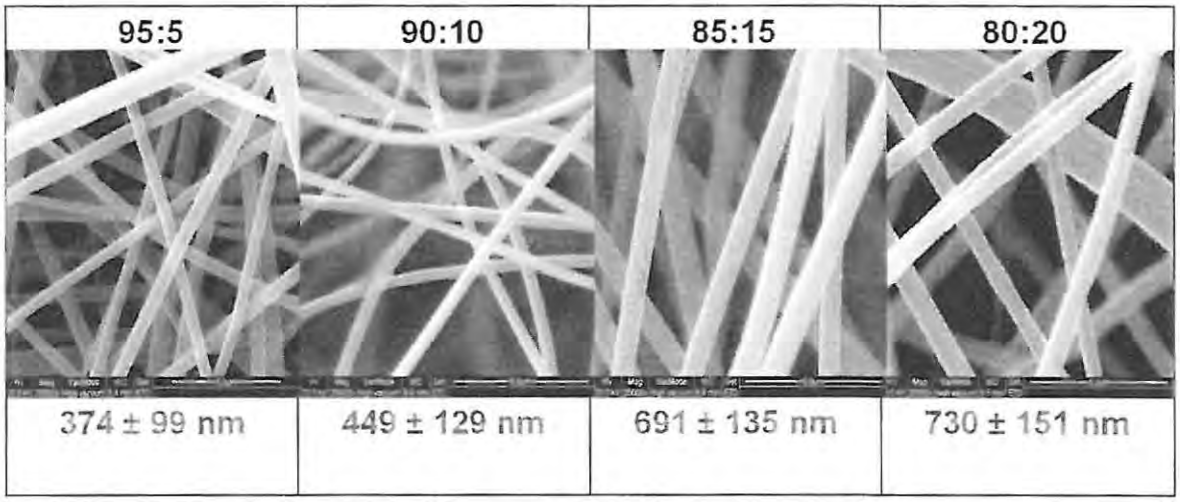

Figure 5.2: SEM images and the corresponding average fiber diameters obtained from 26 wt% polymer in different composition ratios of DMF and NMP

The average fiber diameter increased systematically from 374 ± 99 nm to 730 ± 151 nm when the compostion of NMP was increased from 5 to 20%. The increasing fiber diameter is due to the increase in solution viscosity as proportion of NMP was increased. The size distribution of the nanofibers also increased when the proportion of NMP was increased. This could be due to the differences in the evaporative characteristics of the two solvents used.

5.2.4 Effect of applied voltage on nanofiber diameter

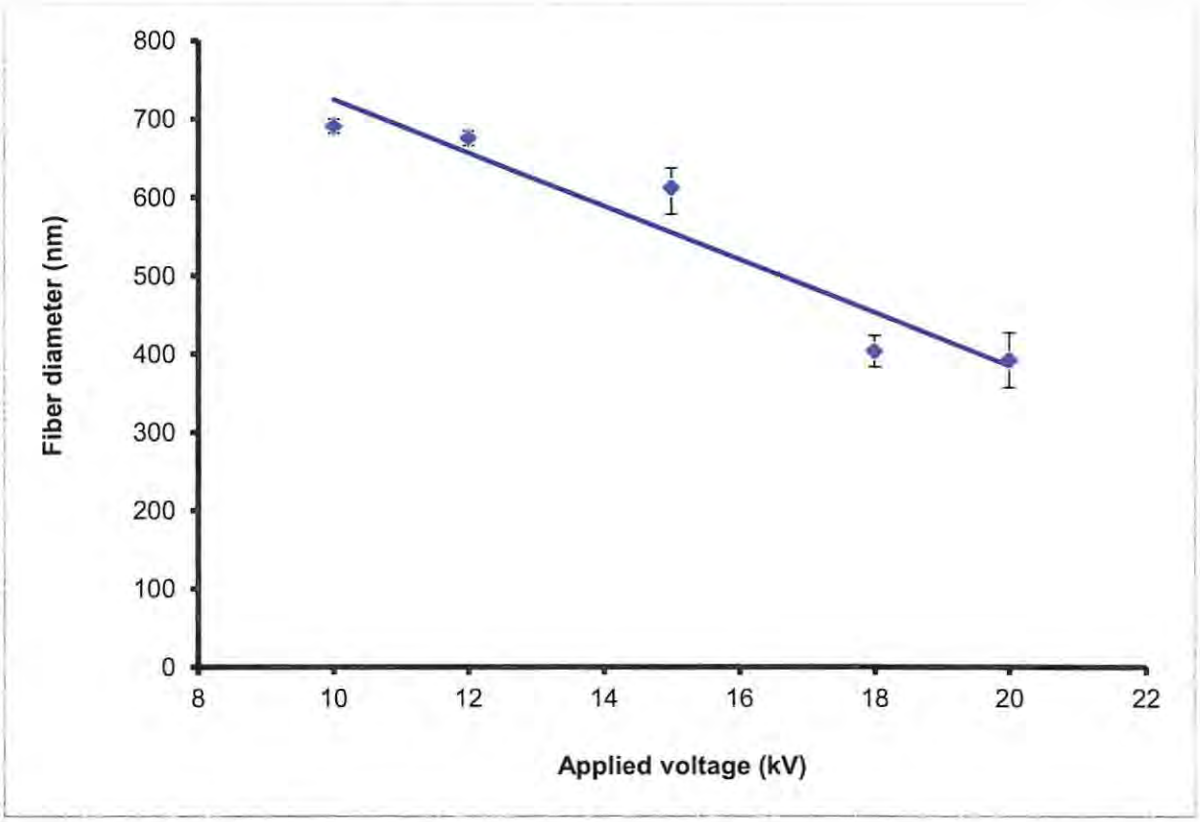

Figure 5.3: The effects of the applied voltage on the average fiber diameter. Polymer concentration, flow rate and and tip-to-collector distance were held at 26 wt% (95 DMF:5 NMP), 1.0 ml/h and 13 cm respectively.

By holding the other processing parameters at constant values, (polymer concentration at 26 wt% (95 DMF:5 NMP), flow rate at 1.0 ml/h and tip-to-collector distance at 13 cm), the effect of the applied voltage on fiber diameter was investigated from 10-20 kV. The average diameter of nanofibers decreased systematically from 690 nm to 392 nm when the applied voltage was increased from 10 kV to 20 kV. There was a wider distribution of nanofiber diameter at the higher voltages (15-20 kV) than they were at lower applied voltages (10-15 kV). The wide distribution of fiber diameter at higher voltages could be due to splitting of the Taylor cone during electrospinning. An increase in the applied voltage leads to increase in the electric field

strength. The resultant increase in the electrostatic repulsive force on the fluid jet favours the formation of thinner fibers. The excess repulsive force could cause a split up of the Taylor cone leading to the generation of fibers of different diameters (broader distribution in fiber diameters). At higher applied voltage, the polymer solution also gets removed from the needle tip more quickly as the jet is ejected from Taylor cone leading to the formation of fibers of lower diameters.

5.2.6 Effect of tip-to-collector distance on nanofiber diameter

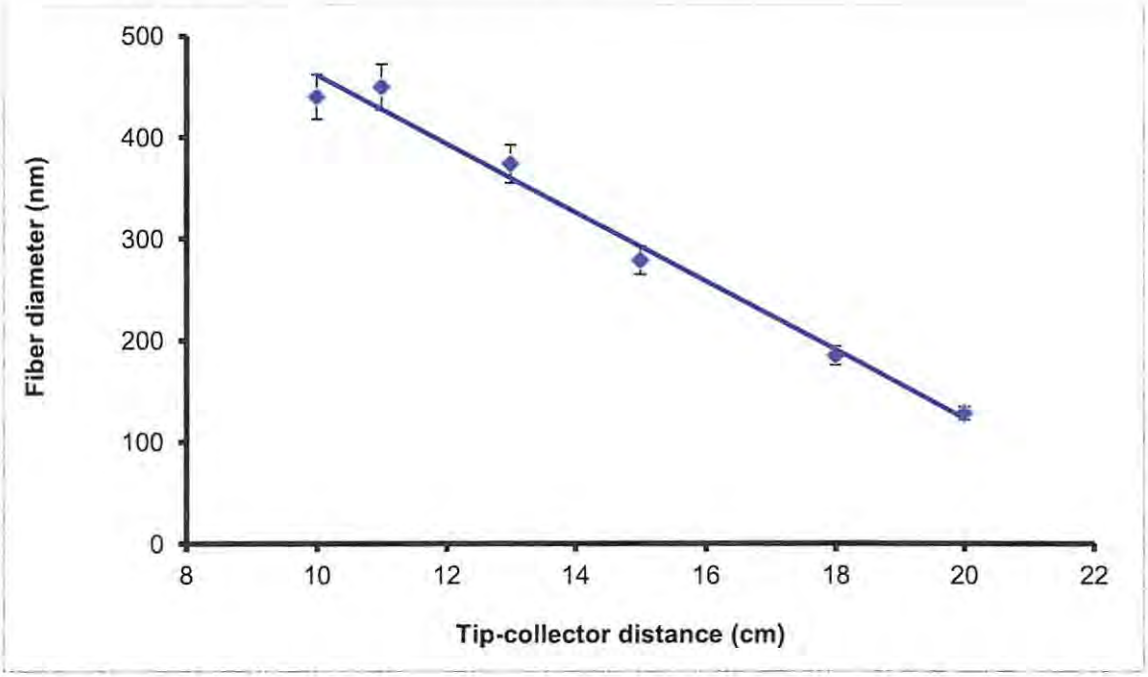

Figure 5.4: The effects of the tip-to-collector distance on the average fiber diameter. Polymer concentration, flow rate and voltage were held at 26 wt% (95 DMF:5 NMP), 1.0 ml/h and 10 kV respectively.

The fiber diameters decreased proportionally with increase in tip-to-collector distance. An optimal tip-to-collector distance is necessary to ensure evaporation of solvents before the jet hits the collector. With an increase in the distance, the electrospinning jet has a longer flight time to

stretch up than when the distance is short. Hence, the increase in tip-to-collector distance was expected to cause a reduction in fiber diameter.

5.3 Conclusion

Polyethersulfone was successfully electrospun at the optimized conditions. A binary mixture consisting of DMF:NMP was found to be an appropriate solvent sytem for dissolving and electrospinning the polymer. The optimal polymer concentration for electrospinning was found to be 26 wt% and the solvent system must contain up to 95% of DMF. Increase in voltage and tip-to-collector distance resulted in decrease in the fiber diameters.

6

Pre-concentration of heavy metals in aqueous environments using diazole-incorporated electrospun polystyrene nanofibers

This chapter is based on:

Darko G., Torto N., Tshentu Z., Darkwa J. (2011). Pre-concentration of heavy metal ions in aqueous environment by electrospun polystyrene nanofibers functionalized with diazole ligands. International Journal of Environmental Analytical Chemistry. (Under review)

6.1 Overview

Electrospun nanofibers that have been functionalized with nitrogen-containing chelating agents have shown excellent adsorption capabilities for metal cations owing to the strong affinity between the nitrogen atom and metal cations (Chang and Chen 2005; Rashchi *et al.*, 2004; Qu *et al.*, 2005; Samal *et al.*, 2000). As bidentate ligands, diazoles (imidazoles and pyrazoles) coordinate strongly with metal ions through their nitrogen atoms (Bogdanovic *et al.*, 2005). When the diazole ring has different donor atoms in position 1-, 3- or 5-, it can also act as bridging polydentate ligand (Köysal *et al.*, 2005; Szécsényi *et al.*, 2005). Electrospun polymer nanofibers functionalized with diazoles are, therefore, being looked up to as a new platform for enrichment of metal ions in aqueous environments prior to their determination. In this study, polystyrene nanofibers functionalized with potassium salts of 1*H*-pyrazole-1-carbodithioate and 1*H*-imidazole-1-carbodithioate were applied as sorbent to the pre-concentrate heavy metal ions from aqueous environments.

6.2 Results and discussions

6.2.1 Nanofiber characterization

A mixture of DMF:THF (4:1 v/v) was found to be a suitable solvent system for dissolving polystyrene into solution. The high conductivity of DMF and volatility of THF both favoured formation of smooth nanofibers (Lee *et al.*, 2003).

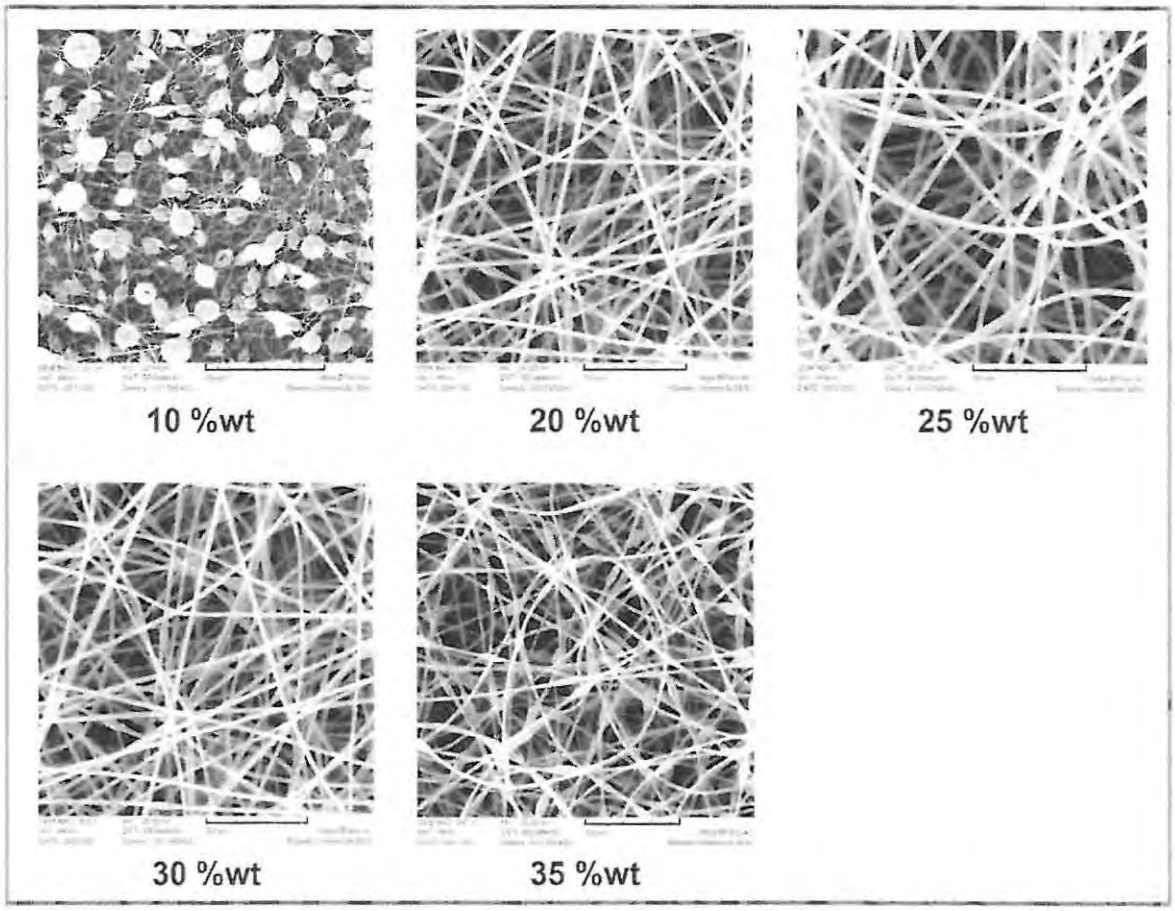

Figure 6.1: Scanning electron microscopy image of different concentrations of polystyrene (10 -35% wt) electrospun at +25 kV, -5 kV and 12 cm gap

Effects of polymer concentration on the formation and morphology of the fiber is illustrated in Fig 6.1. Different concentrations of polystyrene (10-35 wt%) were electrospun at +25 kV, -5 kV, 12 cm gap. Only concentration range of 20-30 wt% could give smooth and bead-free fibers. At low polymer concentrations, the high surface tension due to the solvents leads to formation of beads. At high concentrations, effects such as tip drying and blockages can also result in formation of beads. By optimizing the solution concentration, applied voltage, feed rate and distance between the syringe needle and the collector, it was determined that 25 wt% polystyrene

gives smooth, defect-free nanofibers (Fig 6.2) when it is electrospun at a feed rate of 1.0 mL h^{-1} through an electric field strength of 1.3 kV cm^{-1}. At these conditions, fibers with diameter ranging from about 300 to 800 nm were obtained.

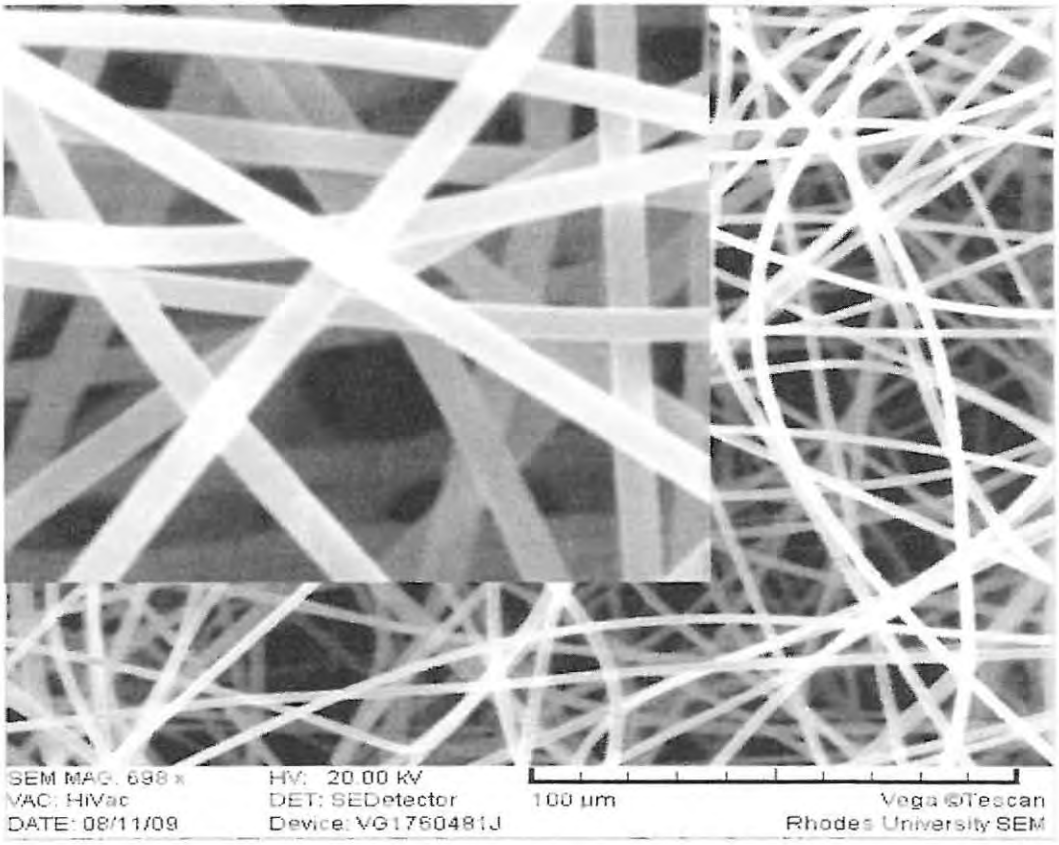

Figure 6.2: SEM image of polystyrene nanofiber formed from 25% polystyrene in DMF:THF (4:1 v/v) electrospun through a field strength of 1.3 kV cm^{-1} at a feed rate of 1 mL h^{-1}. Inset is the SEM image at a higher magnification.

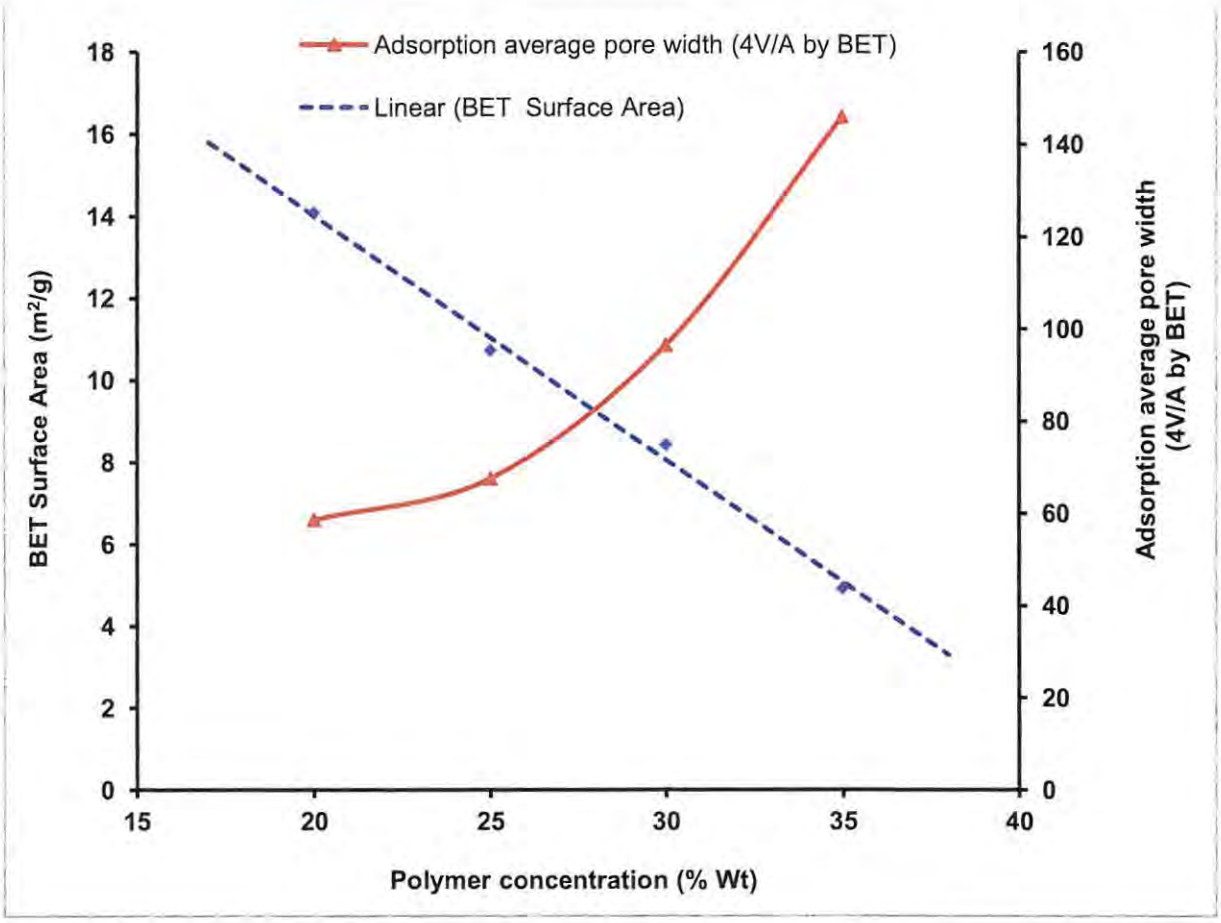

Figure 6.3: The relationship between polymer concentrations, BET surface areas and average pore width of polystyrene nanofibers.

Figure 6.3 shows the relationship between polymer concentrations, BET surface areas and average pore width of polystyrene nanofibers. A linear relationship was observed between the polymer concentration (20-35 %wt) and the BET surface area of the nanofibers formed. The BET surface area decreased linearly from 14.08 m^2/g for nanofibers generated from 20 %wt concentration polymer to 4.95 m^2/g for nanofibers generated from 35 %wt concentration. Increasing the polymer concentration leads to formation of nanofibers of bigger diameters and hence smaller specific surface area (Patanaik *et al.*, 2010). The pore size did not follow the linear

trends observed in BET surface area. The pore sized showed more of a logarithm relationship to the polymer concentration.

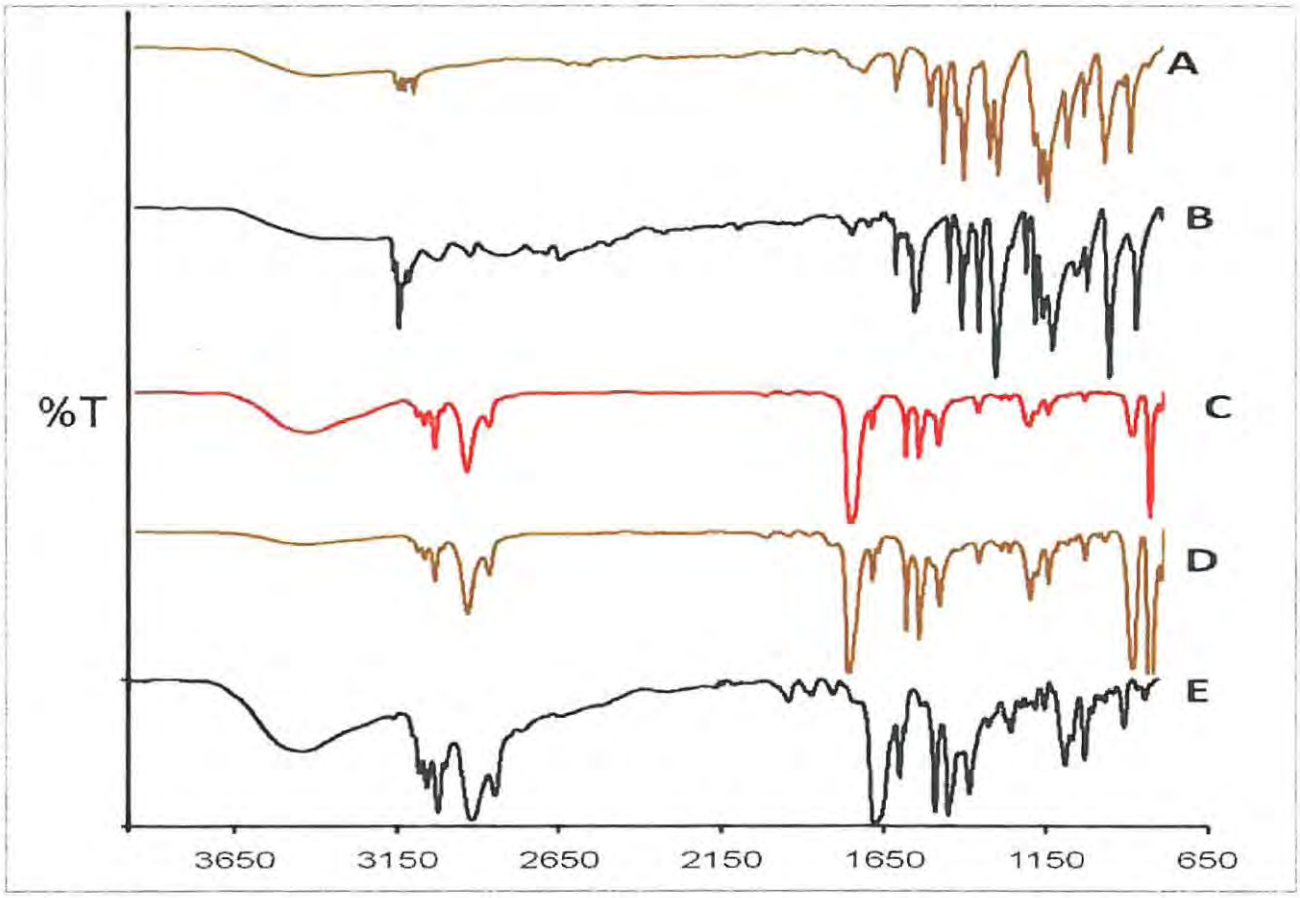

Figure 6.4: ATR-FTIR spectra of (A) potassium 1*H*-pyrazole-1-carbodithioate, (B) potassium 1*H*-imidazole-1-carbodithioate, (C) polystyrene, (D) polystyrene functionalized with potassium 1*H*-pyrazole-1-carbodithioate and (E) polystyrene functionalized with potassium 1*H*-imidazole-1-carbodithioate.

FT-IR spectra of the incorporated and the pristine polystyrene as well as those of the ligands were taken in the range of 4000–650 cm^{-1} (Fig 6.4). The characteristic peaks of the pyrazole (A) 1620 cm^{-1} due to C=S stretching and 850 cm^{-1} assigned to C-N overtones were also found on the functionalized polystyrene (C). The characteristic C=S, C=N and C-N bands of the imidazole

ligand registered at 1200 cm^{-1},1520 cm^{-1} and 850 cm^{-1} respectively on the spectra of both the ligand (B) and the incorporated polystyrene.

6.2.2 pH dependence

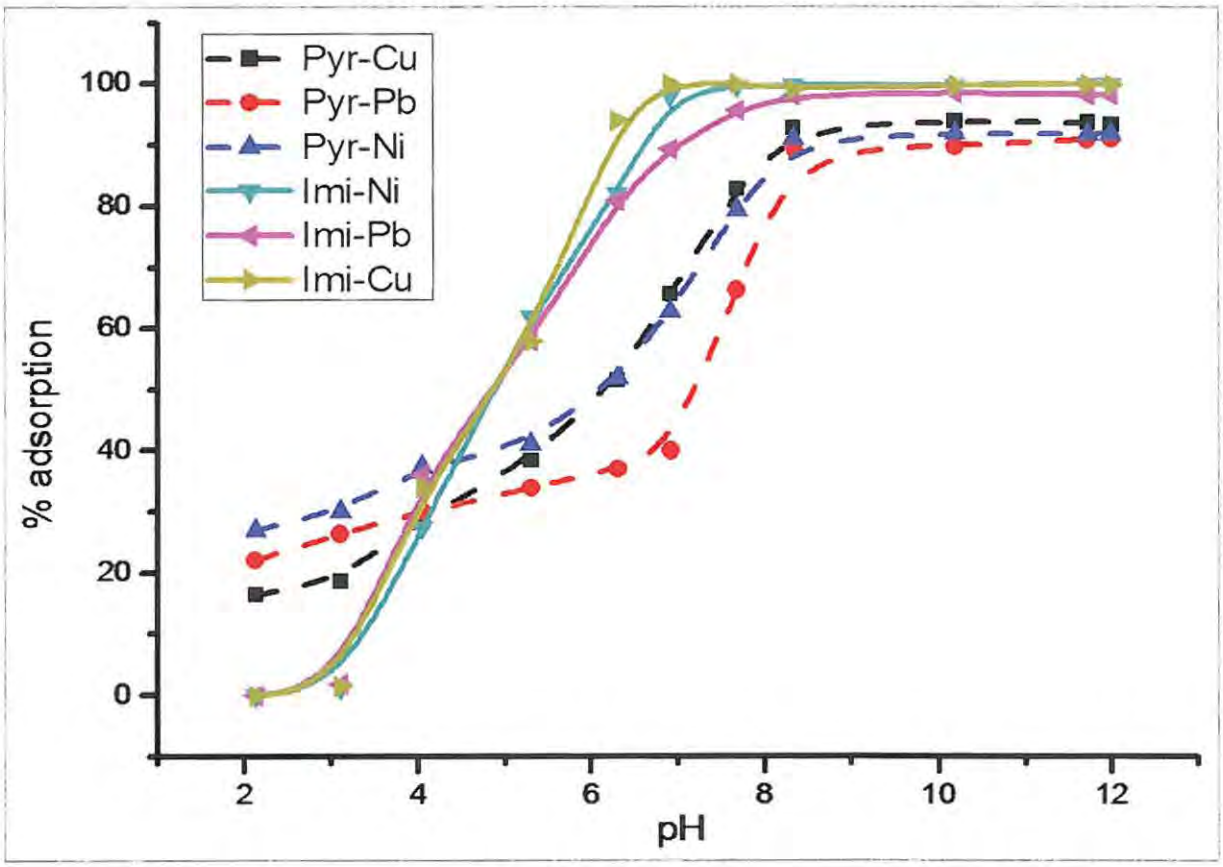

Figure 6.5: Adsorption profile of nanofiber functionalized with potassium 1*H*-pyrazole-1-carbodithioate and potassium 1*H*-imidazole-1-carbodithioate in 0.50 mM standard solutions of metal ions at various pH values; temperature: 25 °C.

Because H^+ ions compete with metal ions ion solution for binding sites on sorbents, pH becomes a very crucial parameter in binding studies. At lower pH, H^+ ion concentration in solution is relatively high and they tend to fill up the binding sites on the adsorbent surface. The presence of H^+ ions on the sorbent surface creates an electrostatic repulsion for the metal cations. Enrichment

of metal ions unto the sorbent is therefore expected to be low at lower pH values. Metal uptake is, however, favoured at higher pH values where H^+ ion concentrations and, consequently, electrostatic repulsions are low.

Figure 6.5 shows the profile of metal ions enrichment on the functionalized nanofiber sorbent at various pH values. No adsorptions were observed on the imidazole-functionalized sorbent at pH values less than 2. The optimal pH for adsorption of Cu, Ni and Pb were 7.0, 7.4, and 11.2 respectively. In an increasing order of their optimal pH for adsorption, these metals could be ranked as Cu<Ni<Pb. This order suggests that pH for metal uptake is determined, somehow, by thermodynamic factors such as electronegativity, acidity and ionic radius of the metal ion. That is, metal ions of higher electronegativity (higher acidity or lower ionic size) are better adsorbed in the acidic range. The optimal pH for enriching the metal ions on the pyrazole-functionalized nanofibers followed the same order (Cu = 6.3; Ni = 7.6 and Pb = 10.3) as with the imidazole. There was, however, a significant uptake at lower pH values. For example at a pH of 2, there were about 16, 22 and 27% adsorptions for Cu(II), Ni(II) and Pb(II) respectively. These relatively high adsorptions at lower pH values may be attributed to the low p*k*a of the pyrazole ligand (Chen *et al.*, 1991; Trofimov 1992). The p*K* indicates pH value at which a ligand is 50% protonated. This means that some binding sites on the pyrazole were available even at the low pH levels.

6.2.3 Protonation and binding constants

Both ligands exhibited two protonation processes in the pH range 2-11. Log K values of the imidazole ligand were higher than those of the pyrazole. The pK of the imidazole was 6.83 (while that of the pyrazole was 3.36). This implies that at pH of 3.36, about 50% of the binding sites on the pyrazole ligand were still free for binding. This gives credence to the relatively high adsorptions that occurred on the pyrazole at lower pH values.

Stability constant (also called formation or binding constant) is the concentration equilibrium for the formation of a complex in solution. Stability constant is a measure of the strength of the interaction between the reagents that come together to form the complex. It also shows the balance between the binding and dissociation processes after an infinite reaction time. The binding constant, β, relates to the Gibbs energy of formation as

$$\Delta G^{\circ} = -2.303\,RT\,\log_{10}\beta \qquad 6.1$$

The magnitude of formation constant is, thus, a direct reflection of the Gibb's free energy of formation (Eqn 6.1). Binding constant is used to quantify the affinity of binding since it is directly related to the molar free enthalpy (Bradbury and Baeyens 2005; Mishustin 2007). The order of the metals stability on the pyrazole was Co<Ni<Pb<Cd<Cu while that of the imidazole was Co<Ni<Cu<Cd<Pb. Based on these trends, it could be speculated that binding of bigger ions with the imidazole was more favourable. Stability of the first row transition metal ions followed the order of their ionic size or electronegativity [Co(II)<Ni(II)<Cu(II)] for both imidazole and pyrazole. The overall stabilities for the pyrazole-metal complex were, in all cases, larger than those for the imidazoles. The divalent metal ions (borderline acids) were better coordinated by

pyrazole (softer base) than the imidazole (harder base) as proposed by Pearson (Pearson 1963). Stability constants obtained for the imidazole complexes of the divalent transition metal ions were in agreement with results previously published (Kapinos *et al.*, 1998). This fast adsorption kinetics of the may be attributed to the morphology (large specific surface area, small fiber size and high porosity) of the fibers (Ramakrishna *et al.*, 2005).

6.2.4 Equilibration time

The rate at which metal ions were enriched on the nanofiber sorbent is profiled in Fig 6.6. The profile showed that the metal ions were, initially, adsorbed rapidly until the sorbent got saturated. Equilibration times for maximum uptake of Cu(II) and for Ni(II) were 10 min and 18 min respectively. These times were roughly the same for both types of functionalized nanofibers. The longest time for equilibrating was 42 min recorded for uptake of Pb(II) on imidazole-functionalized nanofibers. The adsorbents had faster enrichment kinetics than some of the sorbents already reported (Gosset *et al.*, 1986; Sari and Tuzen, 2009; Zhou *et al.*, 2009)

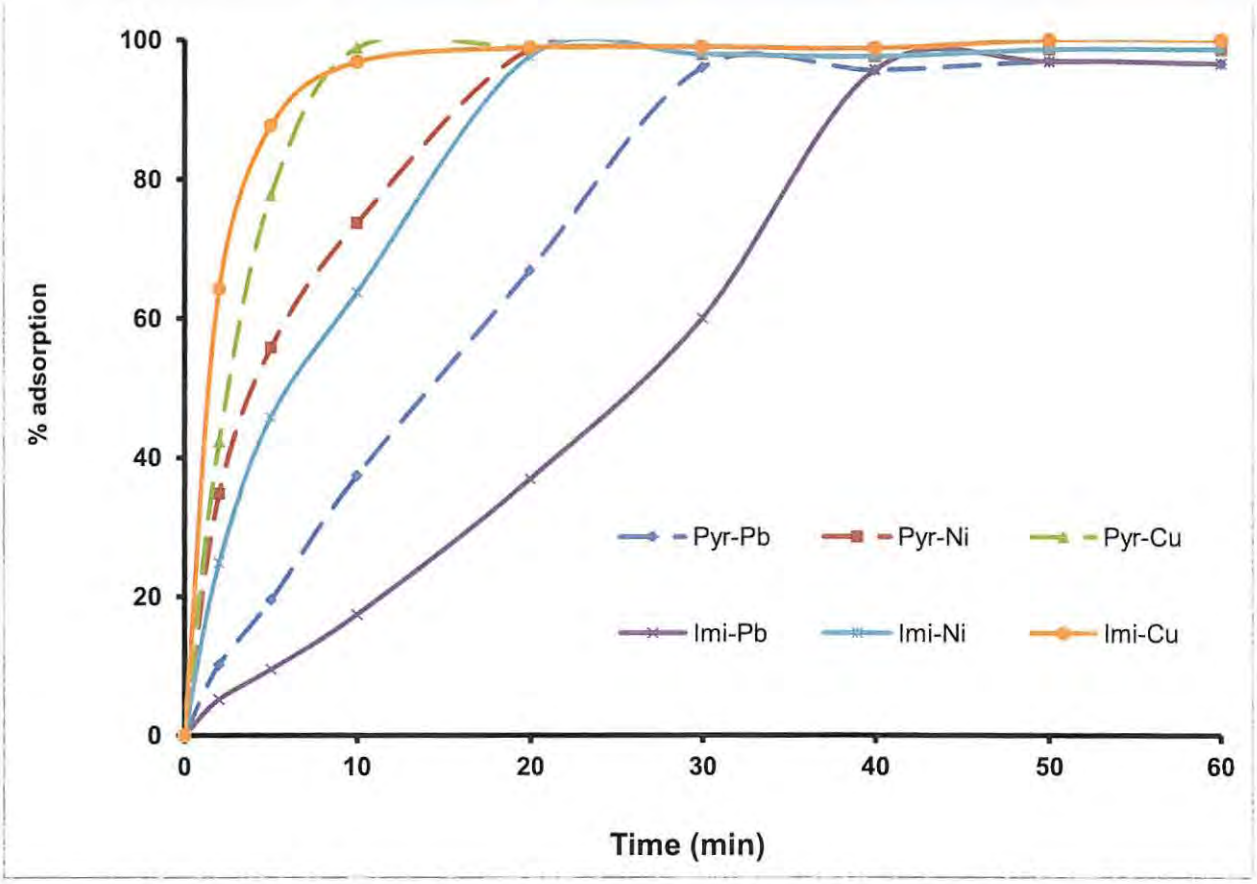

Figure 6.6: Adsorption kinectics of polystyrene nanofibers functionalized with potassium 1*H*-pyrazole-1-carbodithioate and potassium 1*H*-imidazole-1-carbodithioate in 0.50 mM metal solutions

6.2.5 Sorbent dosage

The effect of the mass of nanofibers used on adsorption of metal ions in solution was studied (Fig 6.7). The sorbent dosage is an important parameter because it determines the capacity of the sorbent at a given initial concentration. Adsorption of all metal ions significantly increased with an increase mass of adsorbent to up 8 mg and then leveled off. 10 mg fiber mass was therefore used in all the experiments.

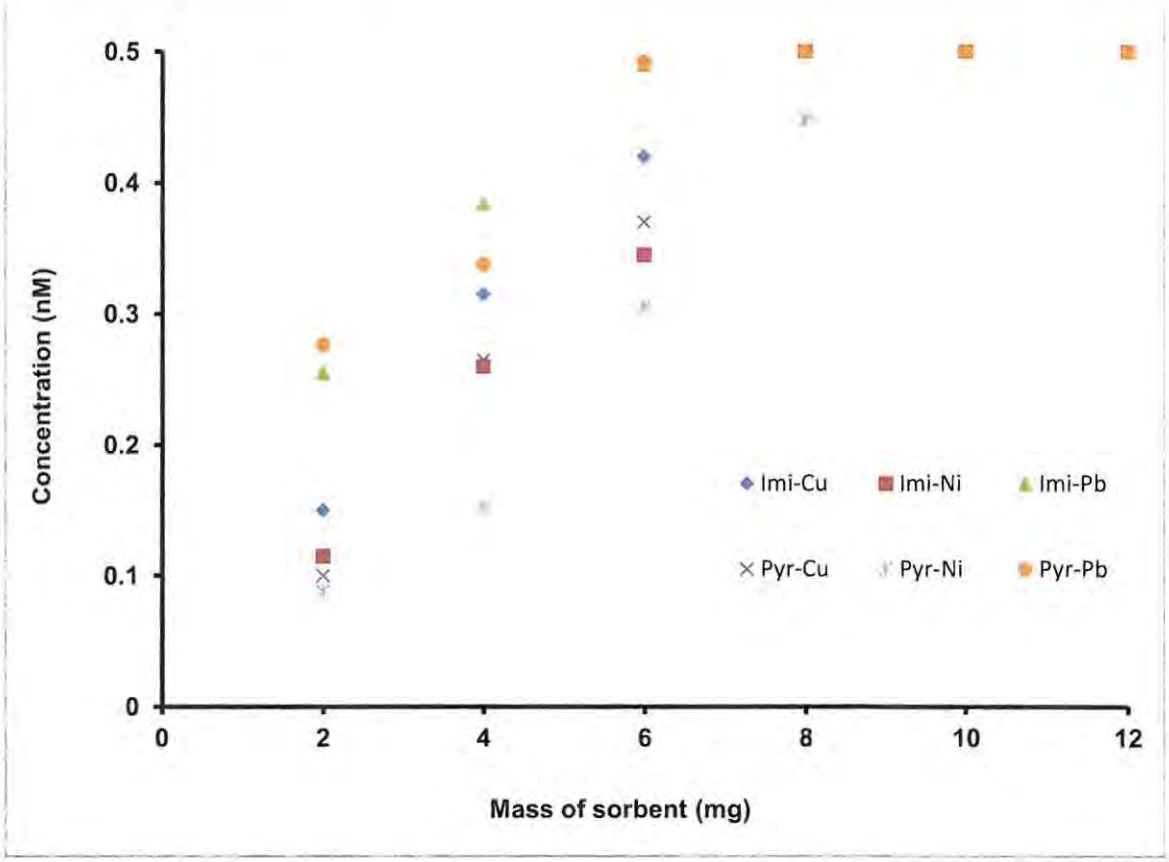

Figure 6.7: Optimization of sorbent mass for adsorption

6.2.6 Desorption of metal ions and sorbent regeneration

Sorbents reusability is largely determined by the efficiencies of their recovery and the extent to which the adsorbed ions are desorbed. The pyrazole-functionalized nanofibers could not desorb in the first instance; they could, therefore, not be regenerated for further usage. The efficiencies of adsorption and desorption of all the metal ions on the imidazole-functionalized nanofibers were nearly constant up to the fourth cycle of usage (Fig 6.8). There was an overall drop of 3.49% in adsorption and 5.07% in desorption up to the fifth cycle of sorbent reuse. This decline in efficiencies could be attributed to losses of trace amounts of the sorbent during usage. The

regeneration of sorbent showed that the adsorption–desorption process was reversible for the imidazole-functionalized nanofibers.

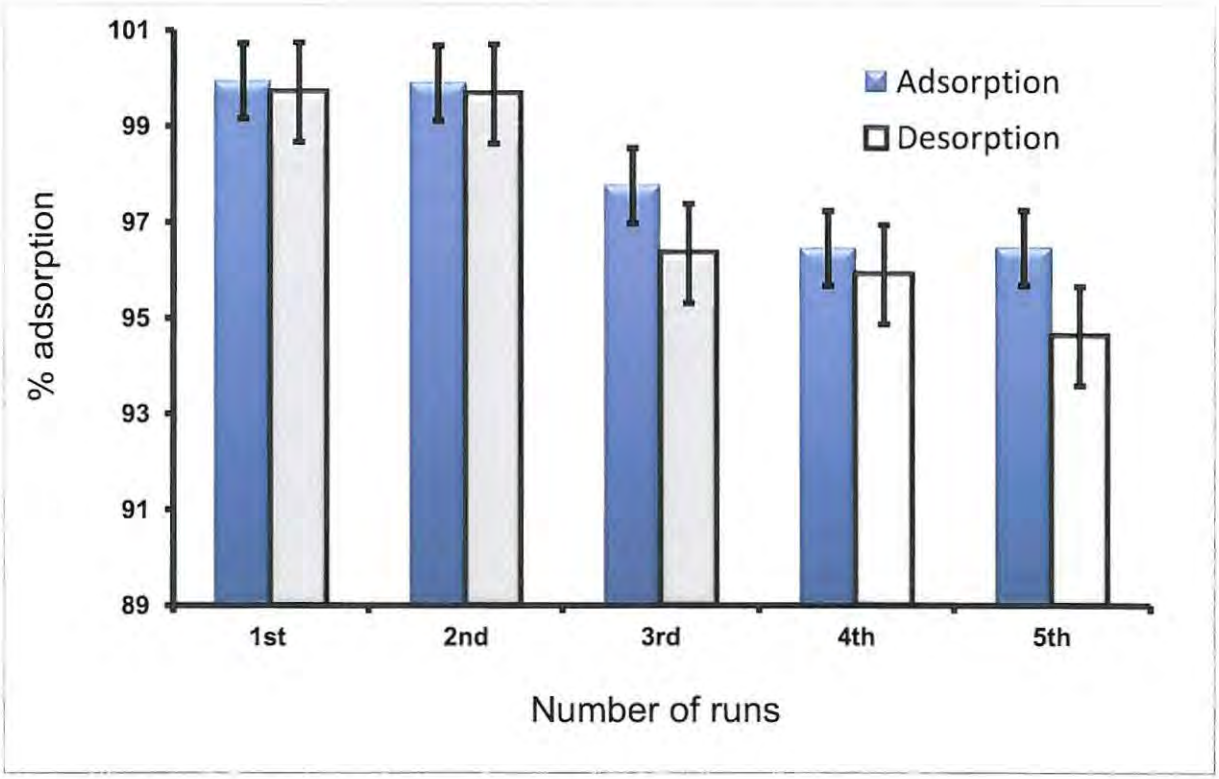

Figure 6.8: Profile of number of times of fiber regeneration

6.2.7 Adsorptions in real aqueous environments

Capacity of the imidazole-functionalized nanofibers to enrich metal ions in the natural aqueous environment was tested in three batches each of three river water, sea water, tap water from three different locations and four batches of treated and untreated sewage from one location. The pH, background concentrations of the metal ions as well as the recovery efficiencies of the functionalized nanofiber sorbent in 100 mg/L spiked natural water samples are recorded in Table 6.1.

Table 6.1: Concentration of heavy metal ions determined in 5 different types of water and the corresponding recovery values from 100 mg/L spiked samples

		Background concentration (mg L^{-1})					Percentage recovery (%)				
	pH	Ni	Cu	Pb	Cd	Co	Ni	Cu	Pb	Cd	Co
River	7.34	0.15	0.09	0.02	0.01	0.08	72.56	95.21	99.00	77.82	70.29
		(0.06)	(0.57)	(0.42)	(0.68)	(0.38)	(3.81)	(0.85)	(7.56)	(1.89)	(0.71)
Sea	7.94	0.02	0.22	0.04	0.03	0.01	78.28	97.59	97.81	78.09	77.48
		(0.01)	(1.29)	(2.24)	(4.48)	(2.73)	(6.22)	(1.04)	(1.42)	(5.44)	(0.20)
Tap	8.13	0.01	0.08	0.01	0.01	ND	72.48	96.65	97.49	98.90	72.07
		(0.37)	(0.37)	(0.77)	(0.18)	-	(0.57)	(1.02)	(1.54)	(4.99)	(0.14)
Untreated	6.51	0.02	0.04	0.02	0.06	0.01	72.12	84.40	82.21	73.68	70.71
sewage		(0.10)	(2.11)	(0.31)	(3.96)	(2.49)	(0.97)	(1.15)	(8.73)	(2.63)	(0.38)
Treated	6.55	0.02	0.04	ND	0.02	ND	71.06	94.16	96.59	84.74	68.54
sewage		(0.17)	(2.79)	-	(1.85)	-	(0.84)	(1.04)	(8.59)	(8.99)	(0.37)

Standard deviations in brackets; ND = below detection

The average pH ranged from 6.51 (in untreated sewage samples) to 8.13 (in tap water). The sorbent was able to quantitatively enrich the trace background concentration of metal ions (0.15 mg L^{-1}) in all the water types. The background concentrations of the metals in water (Ni < 0.15 mg L^{-1}, Cu < 0.22, Pb < 0.04, Cd < 0.06 and Co < 0.08 mg L^{-1}) were ignored during spiking because they were very low, relative to the 100 mg L^{-1} spiking concentration used.

The recoveries (in 100 mg L^{-1} standard solutions) ranged from 71.06-78.28% for Ni(II), 84.40-97.57% for Cu(II), 82.21-99.00% for Pb(II), 73.68-98.90% for Cd(II) and 68.54-77.48% for Co(II). The imidazole-functionalized nanofiber sorbent was found to be more sensitive to Pb(II), Cu(II) and Cd(II) than to Ni(II) and Co(II). Table 6.2 gives the main characteristics (hardness, electronegativity, electron affinity, pK_a) of metal ions that determine their binding to a ligand. The order of adsorption efficiencies, Co<Ni<Cd<Cu<Pb, obtained in this work, does not wholly fit into the order of any of the parameters outline. It could therefore be said that adsorption of the metal ions is not strictly determined by a single factor but, maybe, by a combination of

thermodynamic factors. For the first row metal ions, however, the order of adsorptions followed their order of electron affinity [Co(II)<Ni(II)<Cu(II)] as espoused by Martin (Martin 1998).

Table 6.2: List of some of the properties divalent metal ions that affect their adsorption from aqueous solutions

Metal ion (M^{2+})	Hardness *	Electro negativity	Electron affinity	pK_a
Co	8.22	25.28	17.06	9.65
Ni	8.50	26.67	18.17	9.86
Cu	8.27	28.56	20.29	7.50
Cd	10.29	27.20	16.91	10.08
Pb	8.46	23.49	15.03	7.71

*According to the Pearson's hard-soft acid-base concept, hardness is defined as half the difference between the ionization potential and electron affinity of a metal ion, and electronegativity is defined as half the sum of the ionization potential and electron affinity. Softness is defined as the reciprocal of hardness.

6.2.8 Interference studies

The interfering effect of ions on one another was investigated. Results are presented in Table 6.2. An ion was said to be interfering, if it caused more than 5% reduction in the uptake of another one. Based on the criteria for interference set, it was deduced that the uptake of Ni(II) and Cu(II) are not affected by the presence of any of the metals studied. The uptake of Cd(II) was, however, suppressed somehow by all the metals. Cu(II) and Ni(II) interfered the uptake of each other at higher concentrations of the interfering agents. At higher concentrations of Co(II), it interfered the uptake of both Cu(II) and Ni(II). Uptake of Pb is affected by the presence of Cd.

Table 6.3: Recoveries of metals upon spiking with supposed interfering metal ions

Spiked interfering ions (mgL^{-1})		Concentration of analyte ion adsorbed from a 5 mgL^{-1} solution in the presence of interring ion				
		Pb	Cu	Ni	Co	Cd
Pb	1	-	4.98 (0.06)	4.99 (0.02)	5.00 (0.07)	4.26 (0.09)
	10	-	4.93 (0.69)	4.97 (0.01)	4.96 (0.04)	4.01 (0.10)
Cu	1	4.52 (0.03)	-	4.19 (0.09)	4.81 (0.10)	4.71 (0.06)
	10	5.90 (0.01)	-	4.00 (0.06)	4.28 (0.03)	4.56 (0.09)
Ni	1	4.98 (0.04)	4.73 (0.04)	-	4.71 (0.09)	4.85 (0.12)
	10	4.78 (0.02)	4.04 (0.08)	-	4.67 (0.06)	8.75 (0.08)
Co	1	4.93 (0.12)	4.99 (0.09)	4.91 (0.09)	-	4.99 (0.06)
	10	5.00 (0.06)	4.15 (0.09)	4.09 (0.96)	-	4.12 (0.04)
Cd	1	4.46 (0.08)	4.96 (0.46)	4.94 (0.07)	4.95 (0.08)	-
	10	4.10 (0.05)	4.76 (0.31)	4.92 (0.01)	4.86 (0.01)	-

6.3 Conclusion

Polystyrene solution was successfully functionalized with potassium salts of 1*H*-pyrazole-1-carbodithioate and 1*H*-imidazole-1-carbodithioate and was electrospun into nanofibers. The functionalized nanofibers were found to have optimal adsorption of metal ions around the natural pH of the water types sampled. Bond strengths of the metal-ligand complexes as depicted by their formation constants were high and followed the order of the metals' electronegativity or ionic strength. The functionalized nanofibers exhibited fast adsorption kinetics and high loading capacities for metal ions. These qualities coupled with the high stability of the metal-ligand complexes and tenability for easy desorption of the metal ions from the surface make electrospun polystyrene nanofibers functionalized with diazoles excellent sorbents for the enrichment of heavy metal ions for aqueous environments.

7

Pre-concentration of Cu(II), Ni(II), and Pb(II) in aqueous solutions using electrospun polysulfone nanofibers functionalized with 1-[bis[3-(dimethylamino)-propyl]amino]-2-propanol

This chapter is based on:

Darko, G., Chigome, S., Tshentu, Z., Torto, N. (2011). Enrichment of Cu(II), Ni(II), and Pb(II) in aqueous solutions using electrospun polysulfone nanofibers functionalized with 1-[bis[3-(dimethylamino)-propyl]amino]-2-propanol. Analytical Letters 44(11): 1855- 1867.

7.1 Overview

The diazole-incorporated polystyrene sorbent exhibited sharp decline in efficiencies of adsorptions and desorptions just after the second round of usage. The deterioration in efficiency of use could be as result of either leaching of the ligand or loss of small masses of sorbent upon successive usage. Chemically coupling the ligand (through covalent bonds) with the polymer will halt leaching of the ligand and improve the stability of the sorbent. In this work, polysulfone solution was functionalized with 1-[bis[3-(dimethylamino)-propyl]amino]-2-propanol and electrospun into nanofibers which then employed as sorbents for pre-concentrating heavy metal ions from aqueous environments.

7.2 Results and discussions

7.2.1 FT-IR studies

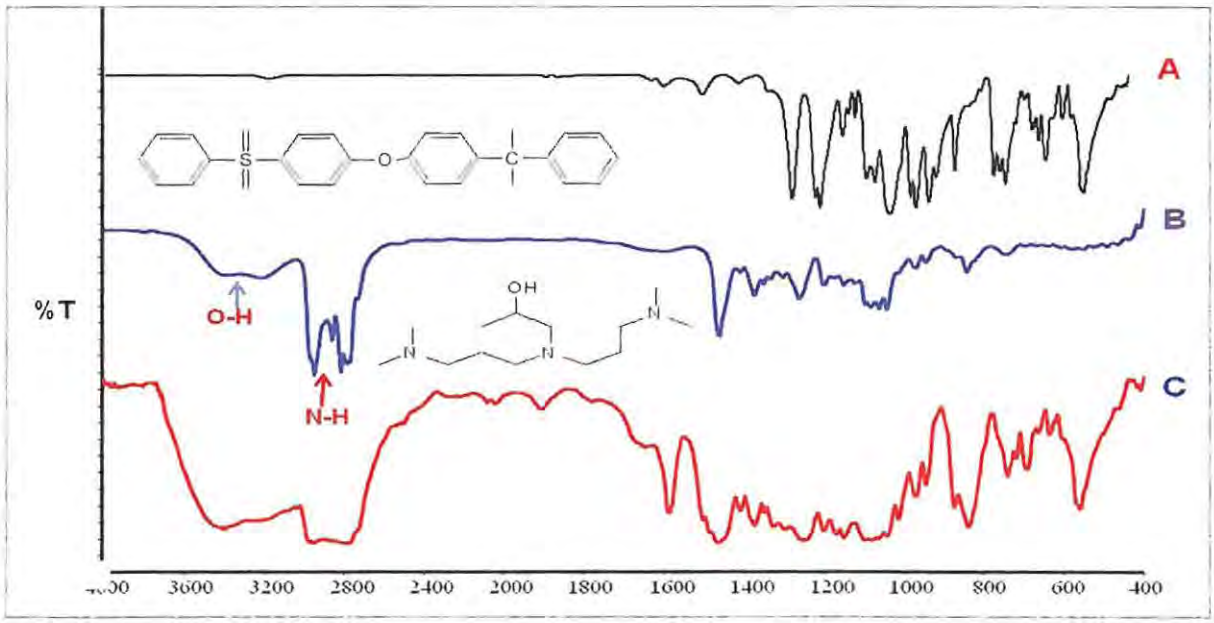

Figure 7.1: FTIR Spectra for unfunctionalized polysulfone nanofiber (A); 1-[bis[3-(dimethylamino)-propyl]amino]-2-propanol (B); and polysulfone nanofiber functionalized with 1-[bis[3-(dimethylamino)-propyl]amino]-2-propanol (C).

Figure 7.1 shows the infra red spectra of the unfunctionalized nanofiber (A), the amine ligand (B) and the functionalized nanofiber (C). The spectrum of the functionalized nanofiber showed the N-H stretch due to an amine group (~ 3000 cm^{-1}, dublet). The N-H adsorption band was, however, absent on the unfunctionalized nanofibers. This indicated that the functionalized nanofiber contained an amine group.

7.2.2 Effect of pH on adsorption and desorption

Figure 7.2 shows the dependence of metal adsorptions on pH. No adsorptions were achieved in the high acidic solutions (pH <3) for all the three metal ions. As the H^+ ions concentration in solution is very high at lower pH, the H^+ ions tend to fill up the binding sites on the adsorbent surface and create electrostatic repulsion for the metal ions. This leads to lower metal enrichment efficiencies at lower pH values. Metal uptake is, however, favoured at higher pH values where H^+ ion concentrations and consequently electrostatic repulsions are lower.

The optimal pH for adsorptions was 5.92, 6.12 and 7.67 for Cu, Ni and Pb respectively. The adsorption profiles of the metal ions showed less variation with pH despite the higher Lewis acidity of Cu compared with Ni and Pb, suggesting that there are other physical parameters at play that overcome this thermodynamic factor.

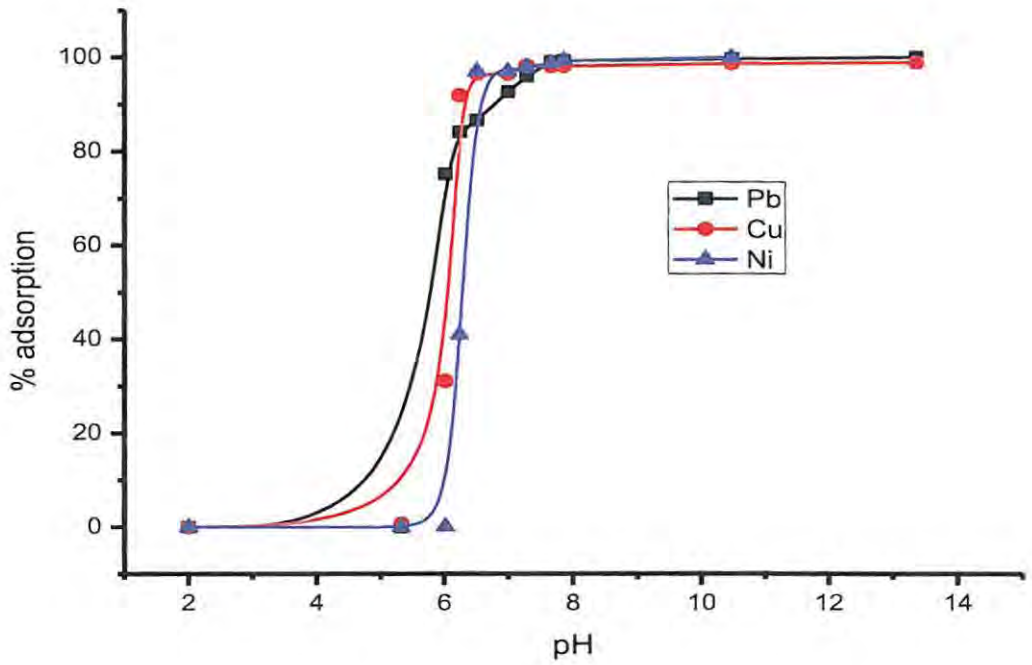

Figure 7.2: Adsorption profiles of Cu, Ni and Pb on functionalized electrospun polysulfone nanofiber

7.2.3 Effect of contact time on adsorption and desorption

Initial rates of adsorption were rapid for all the metal ions in both turbulent and quiescent experiments (Fig 7.3). Equilibrating times were between 20 - 30 min for the three metals (Pb, Cu and Ni) in the turbulent experiments. Equilibrating times for adsorptions were shorter in the quiescent experiments than in the turbulent ones but efficiencies of adsorptions were more than twice better in the turbulent experiments. Adsorptions of the ions were therefore enhanced by stirring. Rates of desorption were very rapid for all the metal ions in both types of experiments. Equilibration times were all less than 5 min (Fig 7.4). The shorter equilibration times offer an advantage of higher sample throughput. The rate of desorption was not affected by stirring. Rate of desorption was affected only by the pH of the solution.

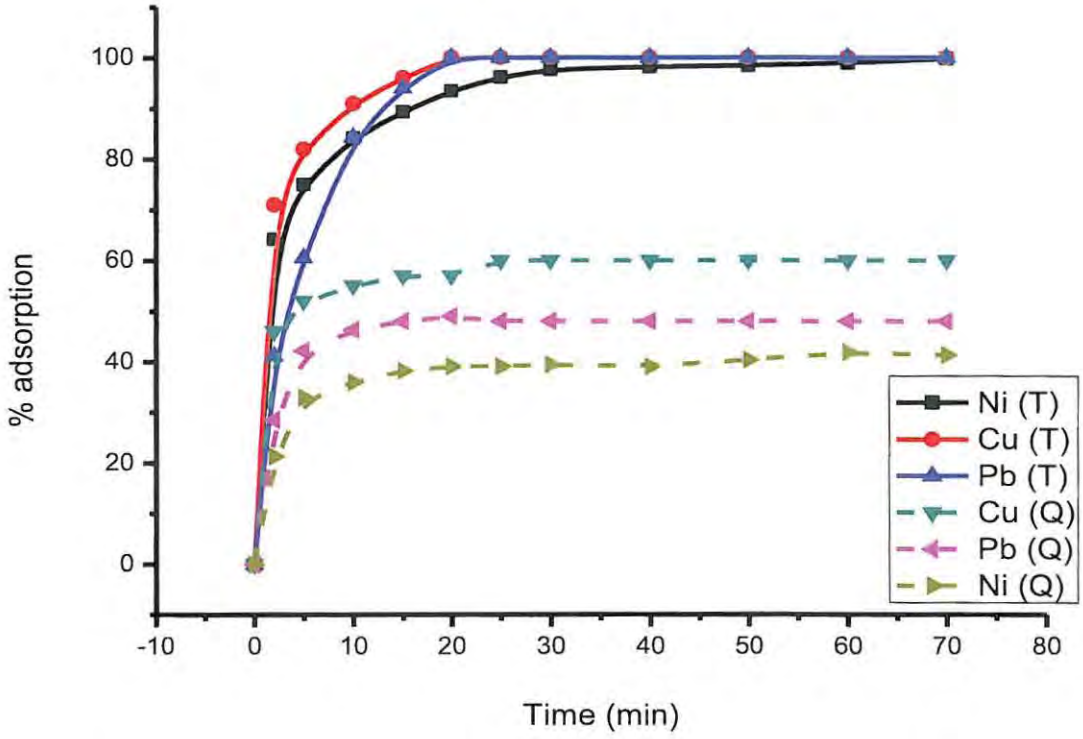

Figure 7.3: Rate at which metal ions were adsorbed from aqueous solutions on the functionalized electrospun polysulfone nanofibers during turbulent (T) and in quiescent (Q) experiments.

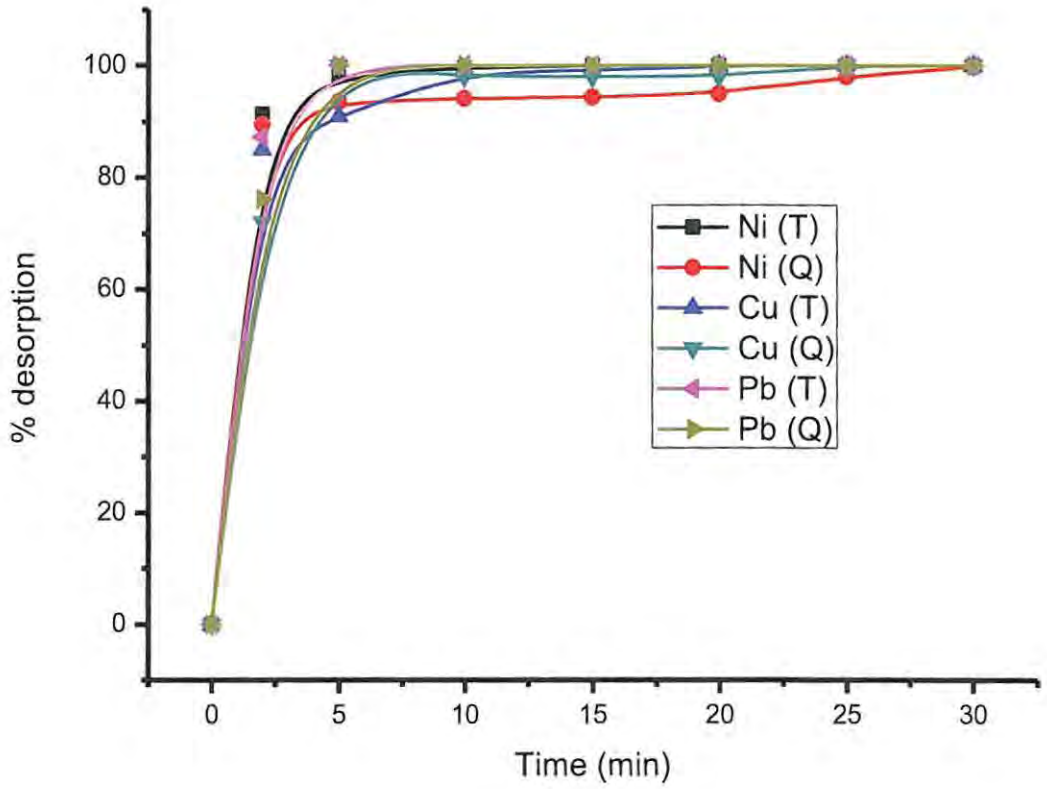

Figure 7.4: Rate at which metal ions were desorbed from the functionalized polysulfone nanofibers using 10 ml of 0.10 M $HNO_{3(aq)}$ in turbulent (T) and in quiescent (Q) experiments.

The fast rates of adsorption and desorption observed is an advantage in that it cuts down significantly on the sample preparation time and increases throughput of sample preparation. An experimenter will have to soak the fiber containing the analyte solution for about 30 min to quantitatively adsorb the metal (Cu, Ni and Pb) ions. The adsorbed ions could be desorbed into acidic solution of pH 2 by soaking for not more than 5 min and the sample is ready for determination. This approach is far more convenient and faster than the conventional acid digestion protocol used for metal ion determination.

7.2.4 Kinetics of adsorptions

Rates of adsorption were assessed using the first order and second order empirical kinetic models and the kinetics best fitted the first order rate law. For first order reactions, the initial concentration of adsorbate (a) relates to the equilibrium concentration (x) and time (t) as:

$$\ln \frac{a}{a - x} = kt \qquad 7.1$$

k is the rate constant (min^{-1}). Equation (1) simplifies into:

$$\ln(a - x) = -kt + \ln a \qquad 7.2$$

Figure 7.5 shows that adsorption of the metal ions on the electrospun fiber follows the first order model as the plots of ln (a - x) versus t gave straight lines. This means for a given mass of the electrospun nanofiber, the rate of adsorption of the metal ions is proportional to the concentration of the ions in solution. First order rate constants were 0.258 min^{-1} for Cu(II), 0.096 min^{-1} for Ni(II) and 0.006 min^{-1} for Pb(II). This trend is consistent with the Lewis acidity of the ions.

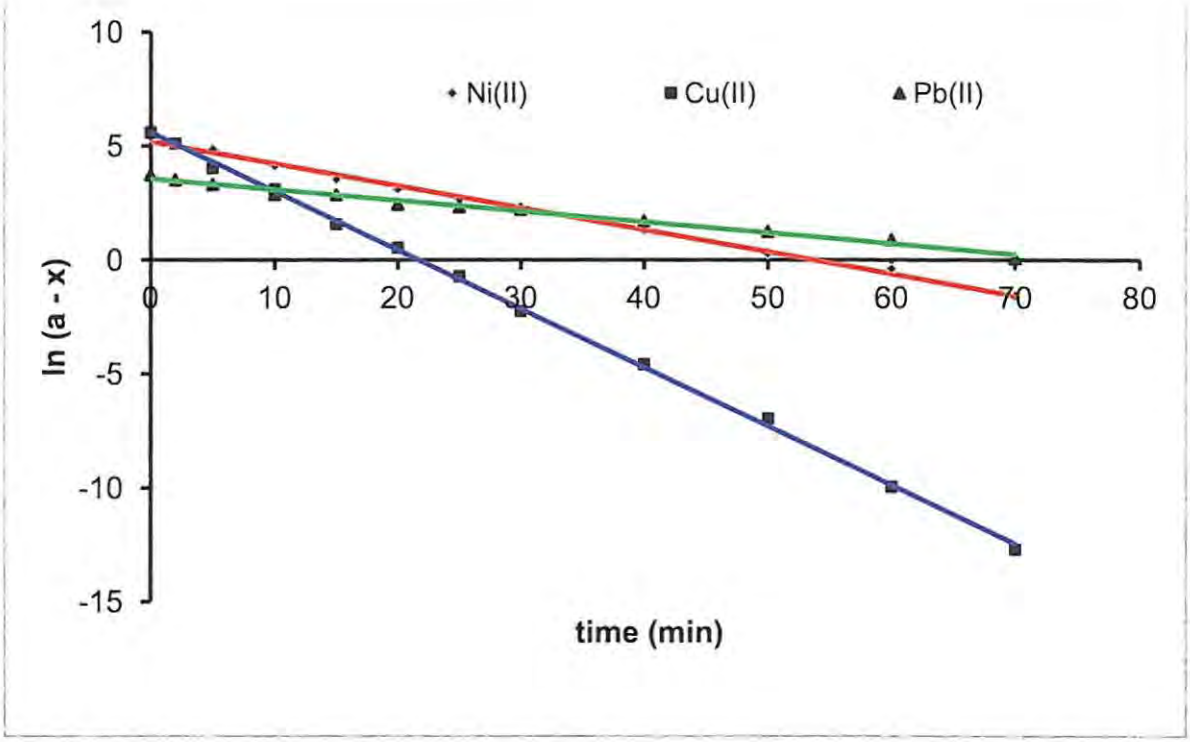

Figure 7.5: First order plots for adsorption of Cu^{2+}, Ni and Pb on the functionalized electrospun polysulfone nanofibers.

7.2.5 Effect of fiber size on efficiency of adsorption

It was found out that efficiency of adsorption was dependent on the fiber size. Fiber of about 900 nm in diameter was the highest fiber size to give quantitative adsorption of the metal ions (Fig 7.6). Adsorption efficiencies declined sharply when the nanofiber diameter increased from 900 to 1000 nm. Small-sized fibers have a higher surface area. An increase in surface area increases the extent of adsorption. Small-sized fibers also generate fiber mat with higher porosity. Adsorption kinetics depends on adsorbent porosity as a porous matrix will allow the adsorbate to reach the binding sites quicker (Beppu *et al.*, 2004).

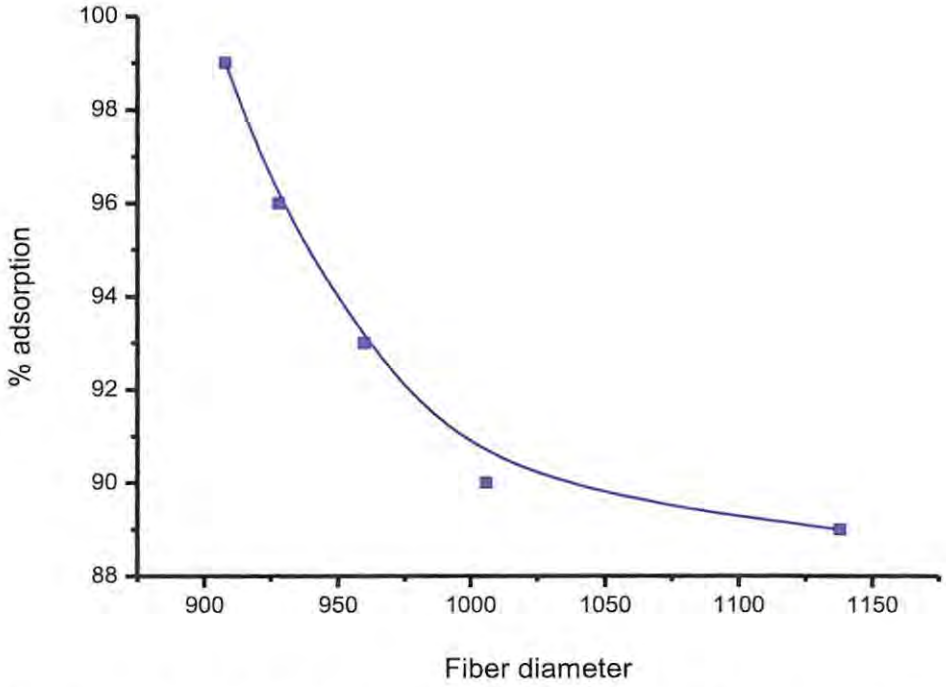

Figure 7.6: Adsorption efficiencies the functionalized polysulfone nanofibers of different diameters

Relation between nanofiber size and their efficiencies of enriching metals in solution was investigated. This was to find out if nanofibers of larger diameters will enrich as efficiently as those with smaller diameters.

7.2.6 Reusability of fiber

Because the adsorbed ions could desorb completely, no significant change in the efficiencies of adsorption and desorption was observed up the 5th time of use (Fig 7.7). Both adsorption and desorption efficiencies were more than 90 ± 2.2% at the fifth time of usage.

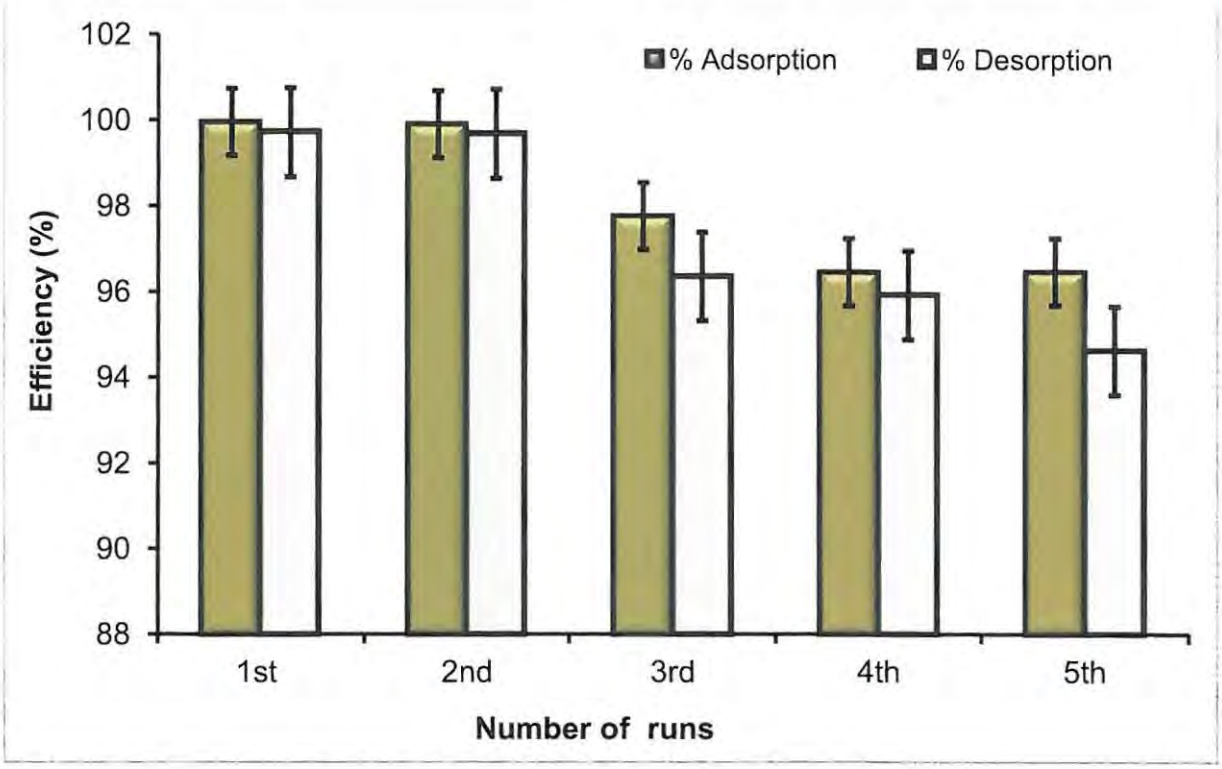

Figure 7.7: Reusability of functionalized electrospun nanofibers

7.2.7 Adsorption isotherms

Adsorption isotherms for the metal ions on functionalized electrospun nanofibers were constructed for a concentration range of 10 - 200 mg L^{-1} at 25 °C, and the data best fitted into the Freundlich model (Fig. 7.8). The isotherm relates the equilibrium concentrations of a solute on the surface of an adsorbent, to the concentration of the solute in the liquid with which it is in contact as

$$\frac{x}{m} = k\, C^{\frac{1}{n}} \qquad 7.3$$

where x = mass of solute adsorbed on a mass m of adsorbent ; C = equilibrium concentration of the solution ; and k and n are constants.

Taking logs of equation 3 yields;

$$\log\left(\frac{x}{m}\right) = \log k + \frac{1}{n}\log C \qquad 7.4$$

Equation 7.4 implies that a plot of log *x/m* against log *C* should be a straight line.

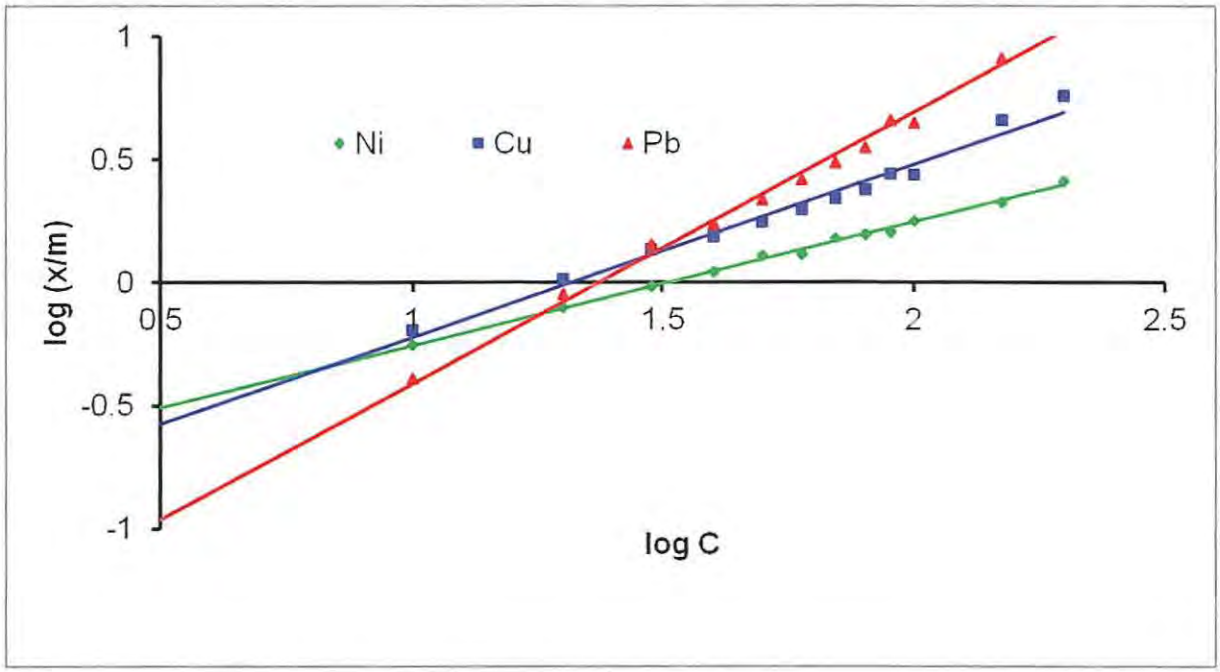

Figure 7.8 Freundlich isotherms for Cu, Ni, and Pb on electrospun nanofiber

Table 7.1: Adsorption parameters obtained from experimental data fitted into Freundlich adsorption model

	Freundlich adsorption constants		
	k	n	R^2
Cu	0.119	1.419	0.998
Ni	0.175	1.992	0.996
Pb	0.031	0.906	0.991

Adsorption parameters obtained by fitting the experimental data are listed in Table 7.1. The Freundlich isotherm is one of the best models that describe adsorptions of metals (Rogers and Sclar 2006). This is partly because the isotherm can be used to calculate the equilibrium concentration as well as the mass of adsorbent necessary to cause a desired change in concentration for the investigation in question.

7.2.8 Application on natural water samples

Applicability of the fibers in real (natural) water environment was evaluated. Table 7.2 shows the adsorption efficiencies (recoveries), minimum metal concentrations that could be detected reproducibly, and standard errors (% RSD) of adsorption. The average pH of all the water types ranged between 6.94 and 7.89. The minimum mean pH of all the water types was higher than the optimal pH for adsorption for all the metal ions. This indicates that the polymer nanofiber will adsorb maximally in all the water types.

Recoveries of Cu ranged from 89.58% (in untreated sewage) to 99.86% in tap water. Recoveries of Ni and Pb ranged from 69.70% (in untreated sewage) to 98.64% (in river water) and 71.46% (in untreated sewage) to 99.01% (for seawater) respectively. Recoveries were higher in less complex water types like tap water than in the more complex water types like sewage. Adsorption of the metal ion by the functionalized nanofiber is therefore affected by the matrix complexity.

Table 7.2: Enrichment efficiencies of functionalized electrospun nanofibers in natural water samples

		Cu(II)				Ni(II)				Pb(II)			
Water type	Avg pH	Back-ground (mg/L)	% ads	LD (mg/L)	% RSD	Back-ground (mg/L)	% ads	LD (mg/L)	% RSD	Back-ground (mg/L)	% ads	LD (mg/L)	% RSD
Sea	7.86	0.38	94.27	0.004	1.28	0.05	97.28	0.001	3.44	0.02	99.01	0.005	2.11
Tap	7.89	0.12	99.86	0.004	1.42	0.01	98.17	0.006	8.62	0.01	98.72	0.006	1.54
River	6.94	0.03	98.63	0.002	0.33	0.07	98.64	0.003	0.19	0.02	96.98	0.002	0.85
Treated sewage	7.25	0.01	98.73	0.009	3.94	0.05	91.60	0.010	1.56	0.01	90.31	0.002	6.55
Untreated sewage	7.25	4.92	89.58	0.008	1.61	0.07	69.70	0.045	1.13	0.02	71.46	0.017	0.97

7.3 Conclusion

Polysulfone has been functionalized with 1-[bis[3-(dimethylamino)-propyl]amino-2-propanol and fabricated into nanofibers through electrospinning techniques. The functionalized electrospun nanofibers exhibited tunable characteristics in the uptake and release of metal ions through pH control. The high enrichment factors observed coupled with the low limits of enrichment and fast adsorption rates of the metal ions in real sample matrices indicate that the functionalized polymer nanofiber is a good adsorbent for fast enrichment and/or removing metal ions from aquatic environments.

8

Pre-concentration of heavy metals using electrospun amino-functionalized nylon-6 nanofiber sorbent

This chapter is based on:

Darko, G., Sobola, A., Chigome, S., Adewuyi, S., Okonkwo, J.O., Torto, N. (2012). Pre-concentration of heavy metals using electrospun amino-functionalized nylon-6 nanofiber sorbent. S. Afr. J. Chem., 65, 14-22.

8.1 Overview

Sorbents derived from electrospun polystyrene and polysulfone functionalized metal-ligands achieved adsorbing capacities higher than those of some of the materials already investigated (Hamissa *et al.*, 2010; Heidari *et al.*, 2009). However, their efficiencies declined sharply with the number of usage (Darko *et al.*, 2011). The decline in efficiency was attributed to the loss of some of the sorbent mass due to the brittle nature of the polymer used or loss of the ligand. It was rationalized that traces of the sorbent might have flaked off during the adsorption-desorption processes leading to sequential decrease in sorbent mass upon successive usage. If these reasons hold, then chemically coupling the ligand with a mechanically stable polymer such as nylon-6 would be the solution.

In this study, nylon-6 was surface-functionalized with a Schiff base ligand, 2-((Z)-(2-aminophenylimino)methyl)-6-methoxyphenol, prior to electrospinning. The nanofiber membranes were stamped out into disks and were employed as sorbent for uptake of heavy metals from water samples. The capacity of the sorbent to pre-concentrate heavy metals (As, Cd, Ni and Pb) was compared with those of conventional acid digestion protocols. The major challenge of sorbent reusability encountered with the sorbents developed earlier on was solved using amino-functionalized nylon-6 electrospun nanofiber sorbents.

8.2 Results and discussions

8.2.1 Functionalization and characterization of nylon-6

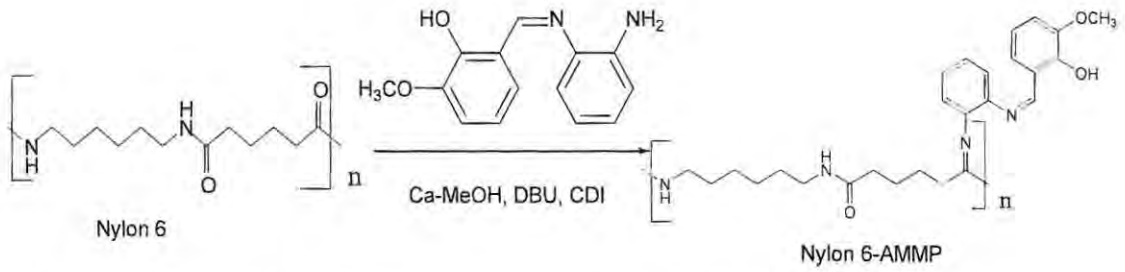

Scheme 8.1: Synthesis of functionalized polymer N-(6-(methylamino)hexyl)-6-oxoheptanamide-2-((Z)-(2-aminophenylimino)methyl)-6-methoxyphenol (Nylon-6-AMMP)

Nylon-6 has a structure in which the N-H groups in the chain are hydrogen bonded to the C=O groups in adjacent chains; thus nylon has good mechanical and chemical stabilities. Consequently, it is difficult to dissolve the polymer before its hydrogen bonds are severed. Although nylon-6 is insoluble in methanol, it was observed to be soluble in hot MeOH/$CaCl_2$ solution (Sun, 1994). Solubility of nylon in MeOH/$CaCl_2$ solution was attributed to an initial complex compound formed by calcium with nylon-6, by breaking the hydrogen bonds, thus forcing the polymer into the solvent molecules. Nylon-6 polymer was functionalized by covalently bonding it with AMMP, a multidentate ligand molecule, in a Schiff base condensation reaction (Scheme 8.1).

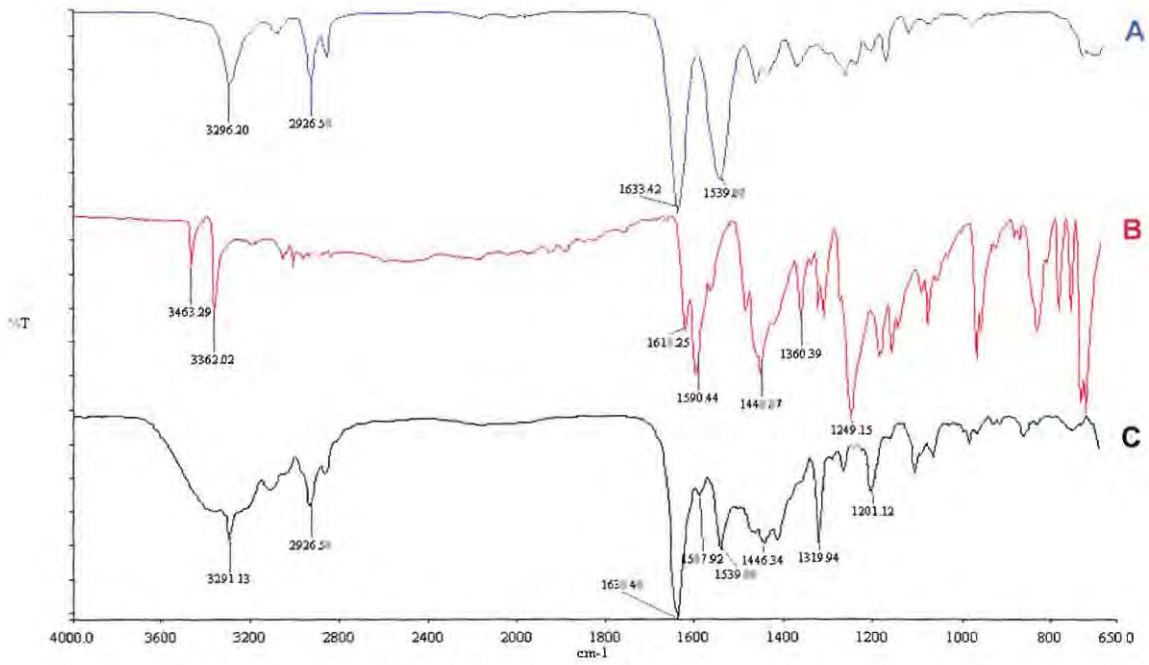

Figure 8.1: FT-IR spectra of AMMP (A), nylon-6 (B) and functionalized nylon-6-AMMP (C) electrospun nanofiber

A comparison of the FT-IR spectra of the AMMP, nylon-6 and functionalized nylon-6-AMMP polymer (Fig 8.1) shows that the changes in the main bond are those anticipated for the covalent functionalization of AMMP with nylon-6. The amide I mode, which is known to be dominated by the C=O absorption band around 1633 cm^{-1}, is shifted and overlaps with the imine stretching frequency initially at 1618 cm^{-1} in the AMMP. This spectral change in nylon-6-AMMP polymer is ascribed to interaction of the C=O bond of nylon-6 with the $-NH_2$ group of the AMMP. Also, the sharp N-H bands in nylon-6 and AMMP (3296 and 3362 cm^{-1} respectively) and AMMP-OH band appeared as broad peak in the new nylon-6-AMMP, suggesting hydrogen bond interaction. In addition, both the symmetrical and asymmetrical $-CH_2$ stretching modes of nylon-6 around 2870 and 2930 cm^{-1} respectively are present in the new nylon-6-AMMP spectrum. The use of ATR is more appropriate in this work because it only scans the surface (up to the depth of 5 μ) of

the nanofiber membrane (Greener *et al.*, 2010). The functional groups identified on the spectra can therefore said to be on the surface of the membrane.

8.2.2 Electrospinning of functionalized nylon-6

The morphologies nanofibers and their formation during electrospinning are dependent on the properties of the polymer solution used (Hussain *et al.*, 2010). Nylon-6 dissolves in formic acid, but not in acetic acid. However, steady states could not be achieved when pure formic acid was used to electrospin nylon-6 (De Vrieze *et al.*, 2011). Therefore, formic acid was blended with acetic acid in order to achieve steady states during the electrospinning of the functionalized nylon-6. Smooth, non-beaded nanofibers of diameter ranging from 80 nm to 95 nm were obtained (Fig 8.2).

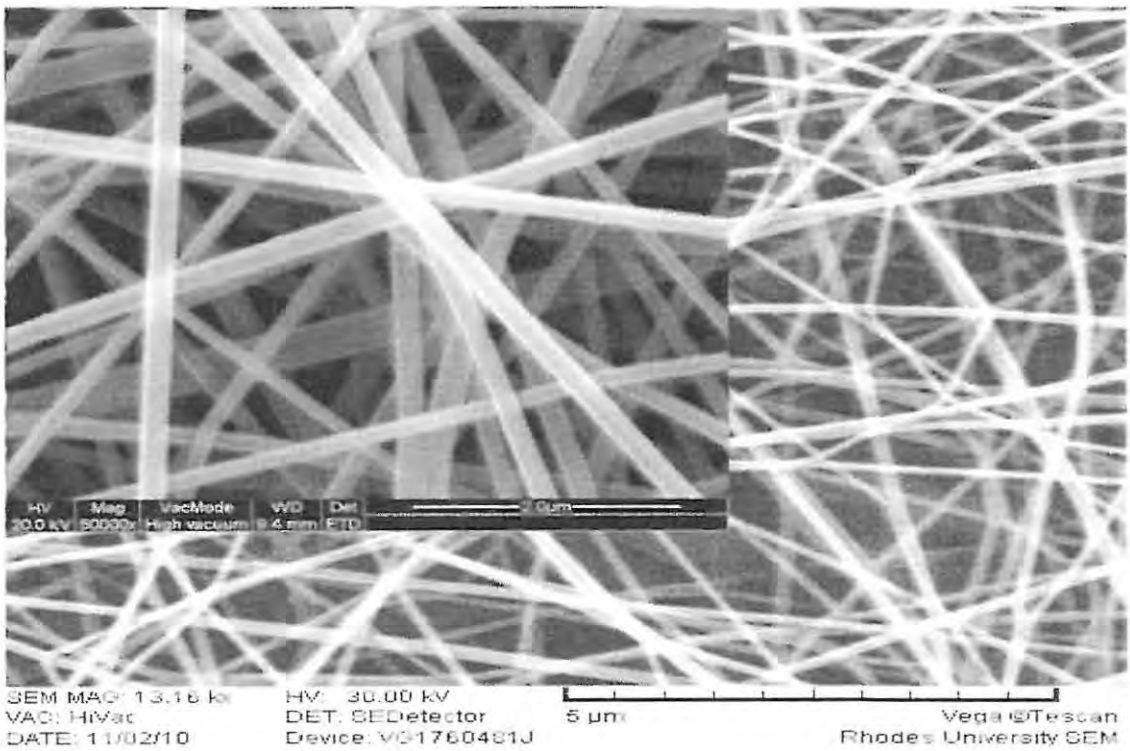

Figure 8.2: Scanning electron microscopy image of nylon-6-AMMP nanofibers

8.2.3 Porosity measurements

The highly porous nature of nanofiber non-woven produced via electrospinning is a key element in their application in many fields (Oh *et al.*, 2008; Shim *et al.*, 2006). For example, the pore sizes of the sorbent material will control the accessibility of the ligand to the metal ions. The specific surface area of the sorbent defines its efficiency of adsorption. Table 8.1 shows the pore characteristics of the amino-functionalized nylon-6 sorbent.

Table 8.1: Pore characteristics of electrospun nylon-6-AMMP nanofiber sorbent

Porosity parameter	Measurement
Average fiber diameter (nm)	80 ± 19
Specific surface area[§] (m^2/g)	58.10 ± 2.25
Average pore size[‡] (Å)	122 ± 1.61
Micropore volume[‡] (cm^2/g)	0.08 ± 0.01

[§] Specific surface area was calculated using the BET method. [‡]Average pore size and micropore volume was calculated using the BJH method.

The specific surface area of the sorbent is determined by the size of the nanofibers it is composed of. Nanofibers of smaller diameters produce sorbents of higher surface areas. The average fiber diameter (80 ± 19 nm) and specific surface area (58.10 ± 2.25 m^2/g) generated from electrospinning 12% nylon-6 in this work, compares favourably with the average diameter of 90 nm and specific surface area of 33 m^2/g recorded on electrospinning 15% nylon-6 (Ryu *et al.*, 2003). Diameter of electrospun nanofibers are directly proportional to the polymer concentration used. Therefore 15 wt% concentration was expected to give nanofibers of bigger diameters (smaller specific surface areas) than those from 12 wt% concentration.

8.2.4 pH dependence

The concentration of H^+ ions in the solution containing the adsorbate is an important criterion in adsorption studies because H^+ ions compete with the metal cations for the binding sites on the sorbent. The concentration of H^+ ion in an acidic solution is relatively high and they tend to fill up the binding sites on the sorbent's surface. The H^+ ions also create a repulsive electrostatic force for the on-coming cations. Adsorption is therefore low in highly acidic solutions (pH less than 4). Adsorption of metals is however favoured in less acidic solutions because such solutions contain less numbers of competing H^+ ions and consequently, electrostatic repulsions are low.

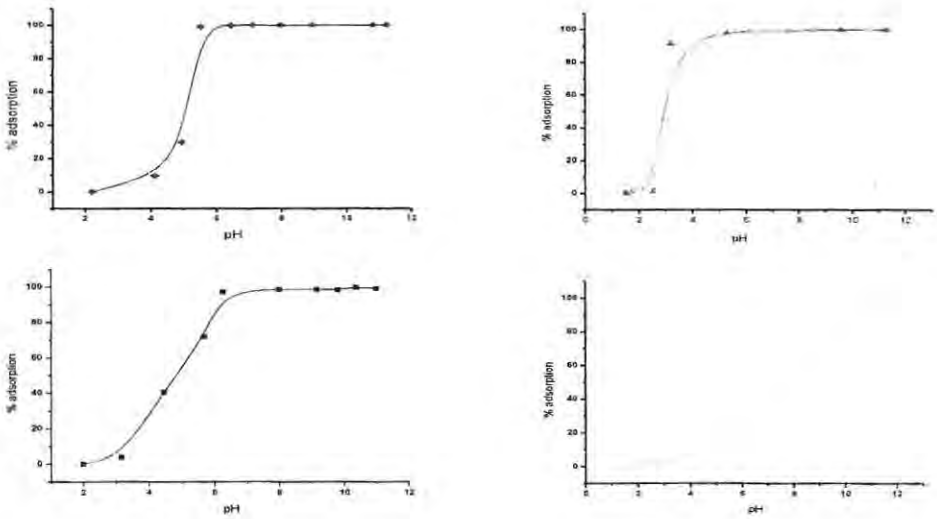

Figure 8.3: Optimal pH for adsorption of heavy metals

Figure 8.3 shows the profile of metal ions pre-concentration on the functionalized nanofiber sorbent for pH values ranging from 2-12. It was observed that adsorption of the metal ions increased rapidly with increase in solution's pH until it reaches equilibrium where no significant

change was observed with a change in pH. These adsorption patterns are typical of cations (Stumm, 1992). The optimal pH for adsorption was found to be 5.5, 6.0, 6.5 and 11 for As, Cd, Ni and Pb respectively. No significant adsorptions were observed when the solution pH was less than 3 in all metals studied. This was the expected trend due to high competition between the H^+ and the metal cations in acidic solutions.

The adsorption curves and the optimal pH values obtained in the work are similar to those observed in the previous studies. For example, Ezoddin et al (2010) found the pH range of 7-8 as the optimal for quantitative recovery (> 95%) of Cd and Pb on a modified nano-ϒ-alumina. Zhou et al (2009) observed that no appreciable uptake of metals occurred on thiourea-modified magnetic chitosan microspheres when the solution pH was less than 2. Because the pH of natural groundwater is often in the range of 5.5-8.5 (Guo and Chen 2007), there will be no need for pH adjustments when the sorbent is used in natural waters. This is of significant importance in applying the sorbent in natural water environments.

8.2.5 Adsorption kinetics

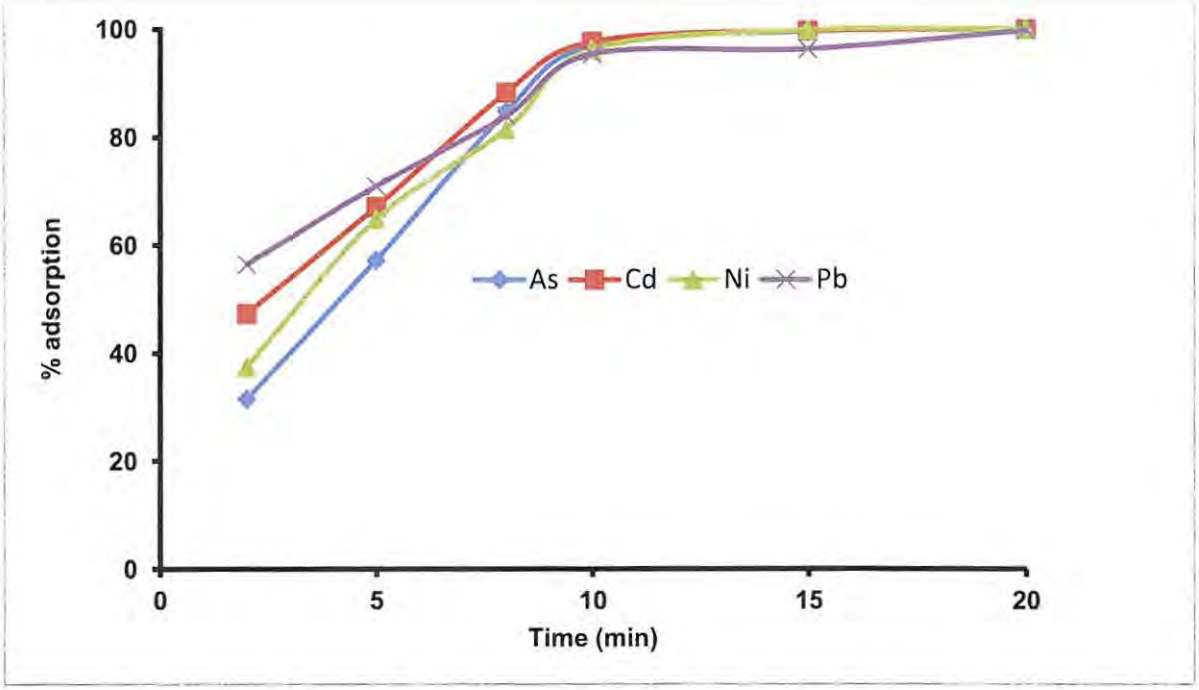

Figure 8.4: Adsorption kinetics of As, Cd, Ni and Pb on nylon-6-AMMP electrospun nanofiber sorbent

Figure 8.4 shows the adsorption profile of metals with respect to time. The process showed considerably fast kinetics at the initial period until equilibrium was attained. For example, by the end of the 10^{th} min after application of the sorbent, 97% of As, 98% of Cd, 96% of Ni and 95% of Pb had already been adsorbed. These equilibration times were shorter than the 3 h recorded for functionalized chitosan sorbents (Justi *et al.,* 2005), 6 h for an ion imprinted composite (Rena *et al.,* 2008) and 8 h for thiourea-modified magnetic chitosan microspheres (Zhou *et al.,* 2009). According to Pierce and Moore (1982), adsorption processes that are purely due to electrostatic attractions are usually very rapid. Hence, the results obtained in this work might indicate a hydrogen bond formation between the metal species and the sorbent. Such fast adsorptions

kinetics is an added advantage of the sorbent as it allows for a high throughput of samples prior to analysis.

8.2.6 Kinetic models

Adsorption data obtained were fitted into kinetic models and the first order kinetics best described the process. For first order reactions, the initial concentration of adsorbate (a) relates to the equilibrium concentration (x) and time (t) as:

$$ln(a - x) = -kt + ln\, a \qquad 8.1$$

k is the rate constant (min^{-1}).

A plot of $ln(a - x)$ vs t (min) will therefore yield a straight line if first order kinetics was obeyed. Figure 8.5 show the first order kinetics for As, Cd, Ni and Pb while Table 8.2 shows their correlation coefficients and the rate constants, k.

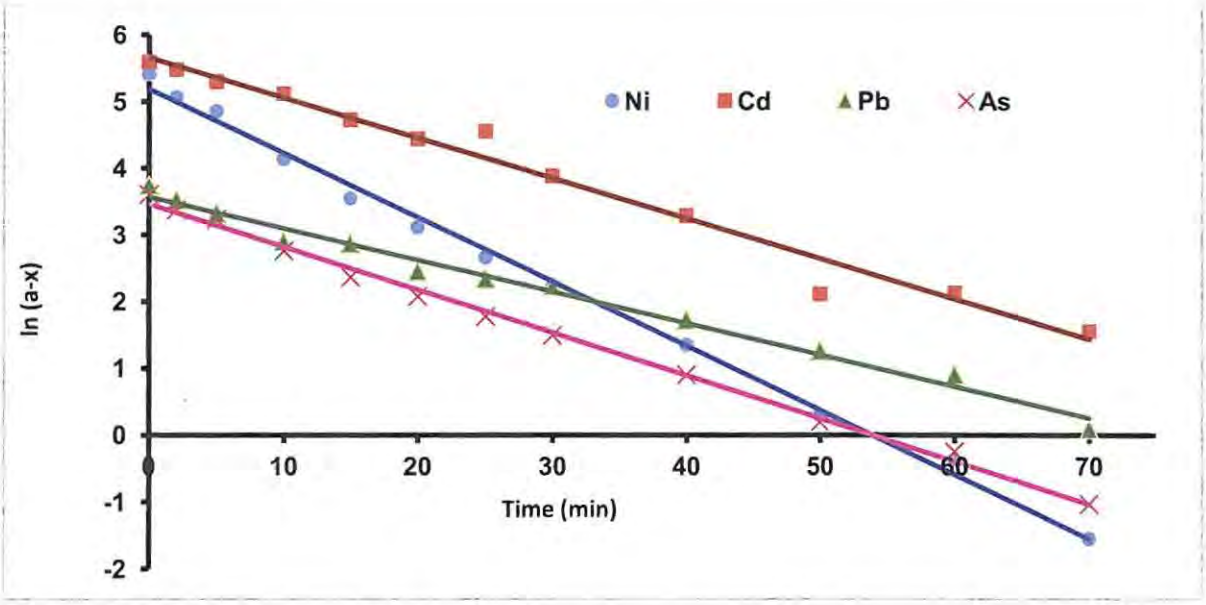

Figure 8.5: First order kinetics of adsorption of As, Cd, Ni and Pb on electrospun nylon-6-AMMP nanofiber sorbent

Table 8.2: Rate constants and the correlation coefficients for first order adsorption of metals on electrospun nylon-6-AMMP nanofiber sorbent

Metal	k (min^{-1})	r^2
Cd	0.0604	0.9781
Ni	0.0963	0.9961
Pb	0.0474	0.9873
As	0.0642	0.9961

8.2.7 Adsorption isotherms

Adsorption data obtained from standard solutions (concentration range of 1.0-10 mg/L) at 25 °C were fitted into known adsorption models and the data best fitted into the Freundlich model. The Freundlich isotherm relates the equilibrium concentrations of a solute on the surface of an sorbent to the concentration of the solute in the liquid with which it is in contact as:

$$\frac{x}{m} = kC^{\frac{1}{n}} \qquad 8.2$$

where x is the mass of solute adsorbed on a fixed mass of sorbent (m) and C is the equilibrium concentration of the solution; and k and n are constants.

Taking logs of equation 3 gives:

$$\log\left(\frac{x}{m}\right) = \log k + \frac{1}{n}\log C \qquad 8.3$$

It could be deduced from Eqn 8.3 that a plot of log(x/m) versus log C should be a straight line if the adsorptions of heavy metals on the electrospun nylon-6 sorbents followed the Freundlich model. Figure 8.6 shows the isotherms obtained for the individual metals.

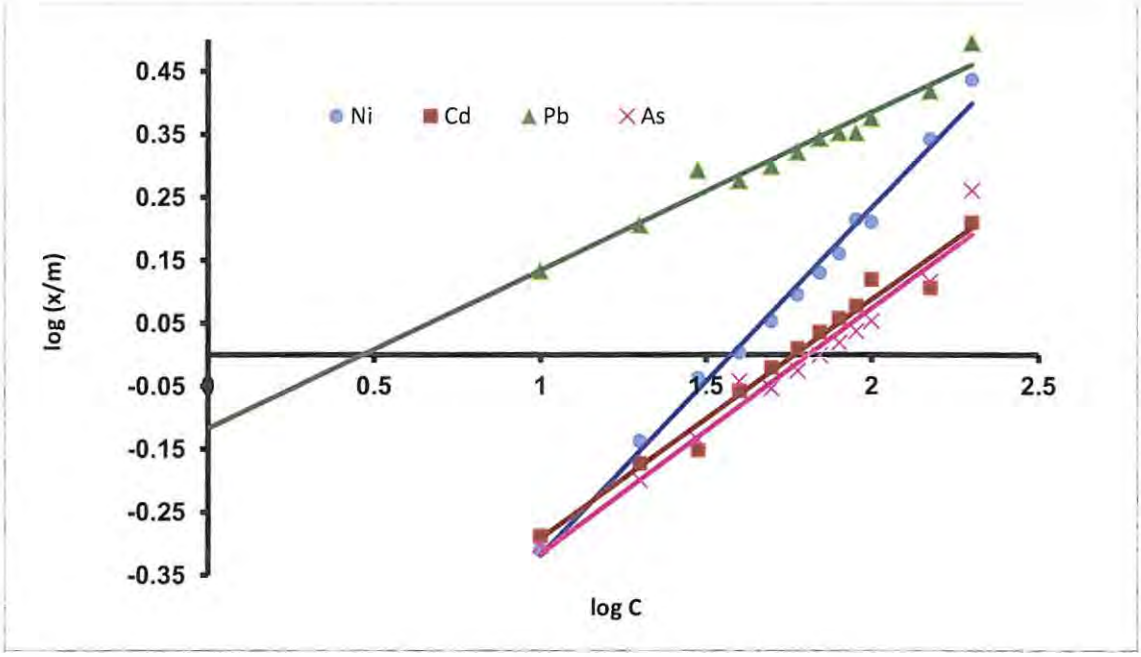

Figure 8.6: Freundlich isotherm depicting the adsorption of As, Cd, Ni and Pb on electrospun nylon-6-AMMP nanofiber sorbent

The Freundlich isotherm best fits a wide range of experimental data (Rogers and Sclar 2006) because it is based on empirical results and not on theoretical assumptions. The benefit of the isotherm is that it could be used to calculate the equilibrium concentration. In any case, adsorptions on the nanofiber sorbent were not expected to obey the Langmuir model due to non-uniformity of the sorbent's surface.

8.2.8 Comparison with digestion protocols

Using the metal concentrations obtained from samples that were only spike with HNO_3 as the bench mark, the capacity of the sorbent to pre-concentrate metals (As, Cd, Ni and Pb) was compared with those of standard digestion protocols, namely aqua regia and HNO_3+H_20_2 digestion methods. The relative pre-concentration factors achieved by the three methods are summarized in Fig 8.7.

The concentrations of As and Cd in all the water samples were generally low compared to those of Ni and Pb. The 3 methods recorded similar levels of pre-concentrating Ni in river water samples; 6.30 for HNO_3+H_2O_2 digestion, 6.69 for aqua regia digestion and 6.55 for adsorptions. That means any of the 3 methods could be used for enriching Ni in river water samples. Pb ions in the river water samples were pre-concentrated slightly better using the two digestion methods (pre-concentration factor ~22) compared to adsorptions (pre-concentration factor ~21). With regards to As and Cd in river water samples, the efficiency of pre-concentration followed the trend: aqua regia digestion > adsorption > HNO_3+H_2O_2 digestion.

The efficiencies of pre-concentrating As in tap and sea water samples were almost the same for all the three methods. Aqua regia digestion was the best pre-concentration procedure for Cd and Ni followed by the adsorption method. The digestion methods recorded higher pre-concentration efficiencies (11.66 for aqua regia digestion and 11.27 for HNO_3+H_2O_2 digestion) compared to the adsorption method (9.87). The sorbent could not pre-concentrate Cd in sea water although the concentrations detected using the digestion methods were higher than the LOD of the adsorption method. This could be due to matrice effect of the sea water. The HNO_3+H_2O_2 and aqua regia digestion methods recorded pre-concentration factors of 0.19 and 0.11 respectively for Cd in sea

water samples. The order of pre-concentration efficiencies for Ni in sea water was HNO_3+H_2O_2 digestion>aqua regia digestion> adsorption. With respect to uptake of Pb in sea water, the sorbent performed better (factor ~10.49) than both HNO_3+H_20_2 (10.45) and aqua regia (9.80).

In the treated waste water samples, the aqua regia digestion method achieved higher pre-concentration levels than the other two methods. The adsorption process was also slightly more efficient than the HNO_3+H_2O_2 digestion with respect to Cd and Ni. However, the efficiency of HNO_3+H_2O_2 digestion superseded that of the adsorption process in terms of Ni and Pb in the treated water samples. The pre-concentration efficiencies of the two acid digestion protocols in untreated waste water samples were slightly higher than that of the adsorption process, for all the metals investigated. Ideally, one expects fouling on the sorbent when it is applied in complex matrices like untreated waste water. The high performance of the nanofiber sorbent, relative to other membrane sorbents, is attributable to the highly porous nature of the nanofibers.

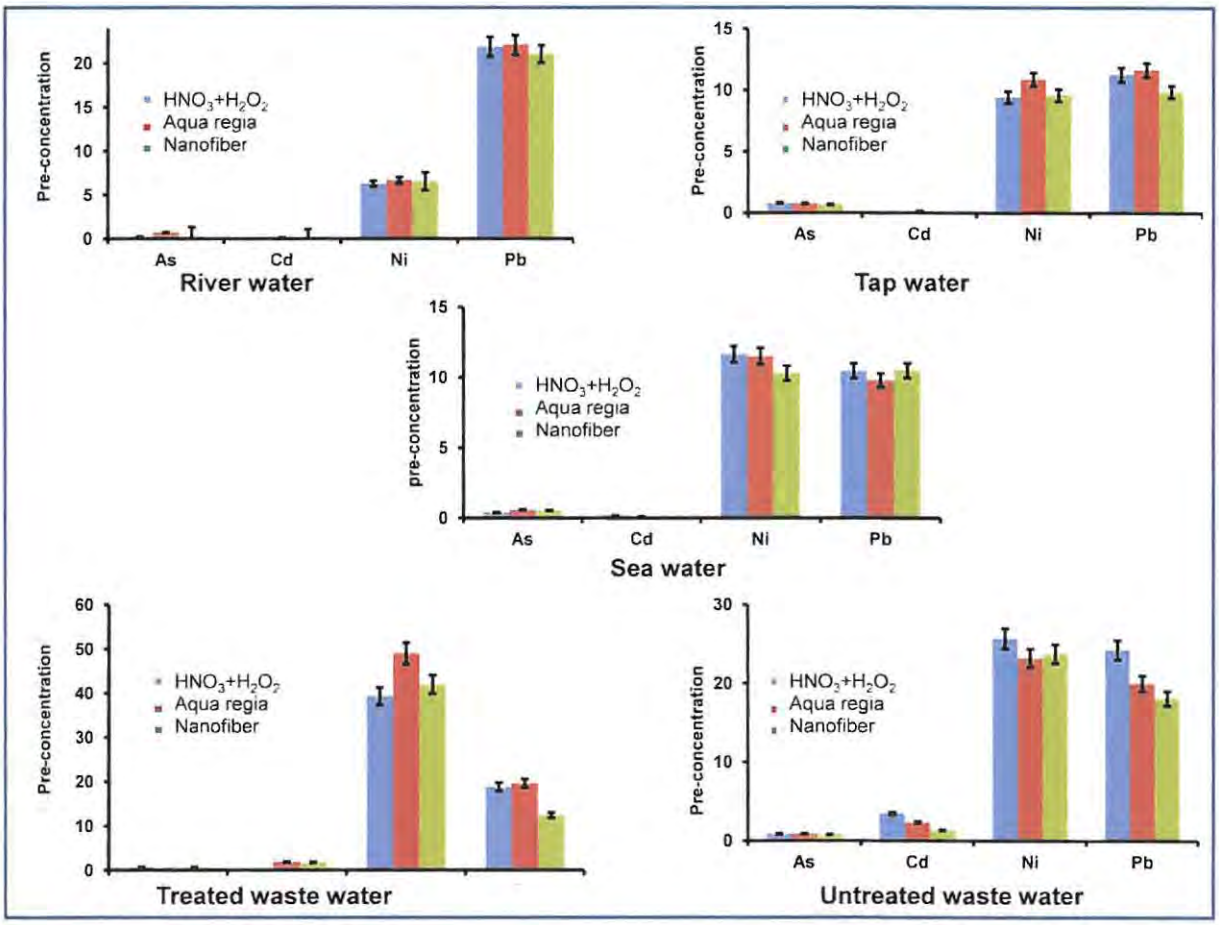

Figure 8.7: Comparison of pre-concentration of As, Cd, Ni and Pb achieved using HNO_3+H_2O_2 digestion, aqua regia digestion or adsorption in river, tap, sea, treated and untreated waste water samples

8.2.9 Reusability of nanofiber sorbent

The sorbent showed a remarkable stability in reusability. Sorbent reusability which used to be a challenge with some of the electrospun nanofiber sorbents we prepared early was not encountered in this work. This is because the ligand was covalently bonded to a mechanically stable nylon-6 backbone. Leaching of the ligand and loss of traces of the sorbent during use was therefore restricted. Just about 0.1% reduction in adsorption/desorption efficiencies was observed at the 10th round of usage (Fig 8.8).

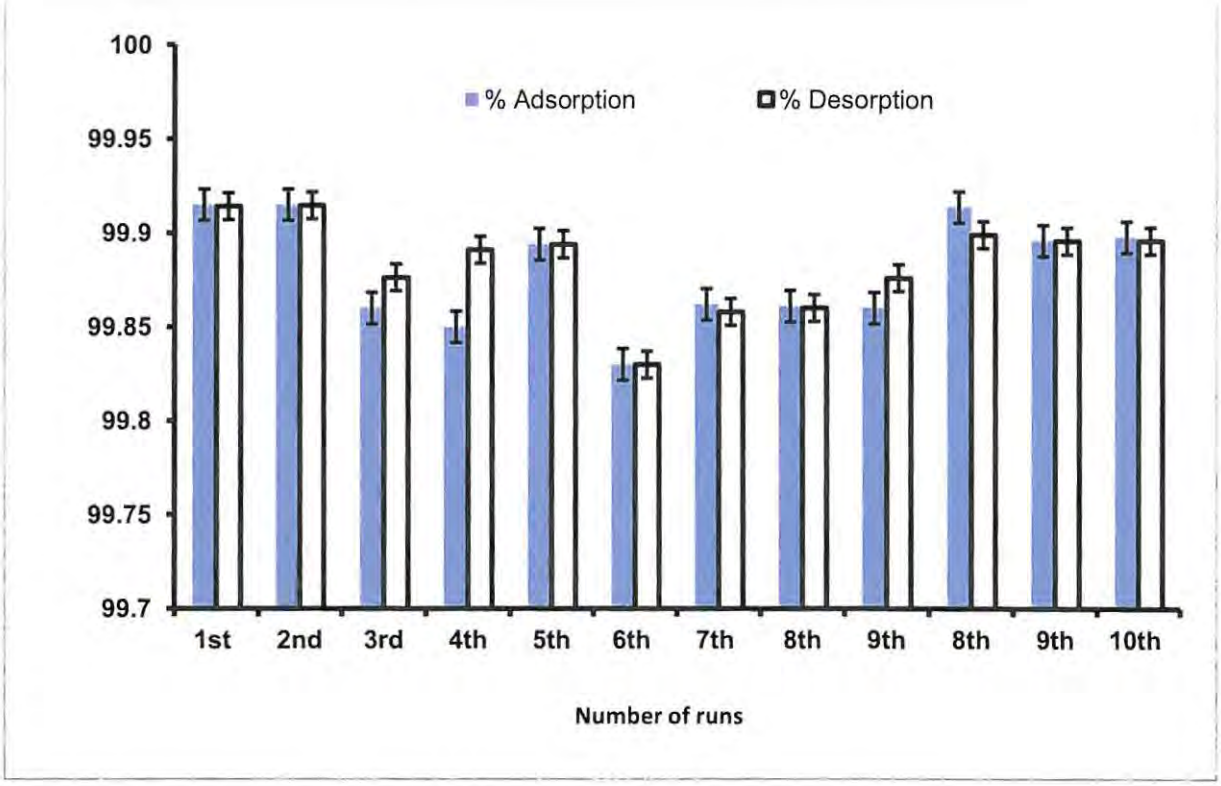

Figure 8.8: Reusability of the sorbent

8.3 Conclusion

Nylon-6 was successfully functionalized with a Schiff base ligand that has a high affinity for heavy metal ions. The functionalized polymer was electrospun to get nanofibers which was them stamped out into sorbents for uptake of heavy metal ions from different aqueous environments. The sorbent tuned as a function pH, for both uptake and release of the metals. The sorbent exhibited high pre-concentration capacity comparable to acid digestion protocols currently in use. It also presents the advantage of good reusability and high chemical stability. Electrospun functionalized nylon-6 nanofiber sorbent has been successfully applied to pre-concentrate heavy metals from different aqueous environments.

9

Conclusions

9 Conclusions

This thesis presented an evaluation on the applicability of electrospun nanofiber sorbents in pre-concentration of heavy metals from different aqueous environments. The optimal conditions for electrospinning polyamide-6, polyethersulfone, polysulfone and polystyrene were established and their nanofibers fully characterized in terms of their morphologies and porosities. The electrospun nanofibers had mesoporous structures, smaller diameters and large surface areas. The sorbents were characterized regarding their tunability for uptake and release of heavy metals, reusability and loading capacities. They exhited fast adsorption kinetics, high loading capacities, good stability for reuse and high recovery levels for heavy metals in water.

Parameters affecting adsorption such as fiber diameter, contact time, and pH were investigated. The adsorption characteristics of the sorbents best fitted the Freundlich isotherm and followed the first order kinetics. The maximum equilibration time for pre-concentrating Cu, Ni and Pb in different water sources using polysulfone functionalized with 1-[bis[3-(dimethylamino)-propyl]amino]-2-propanol was up to 30 min. The optimal pH for pre-concentrating heavy metals using diazole-incorporated polystyrene nanofibers was found to be dependent on the basicity of the ligands. The functionalized polystyrene and polysulfone nanofibers sorbents could be regenerated and re-used up to five times without a significant deterioration in adsorption and desorption efficiencies.

Sorbent reusability improved dramatically (up to 10 runs of usage) when mechanically stable amino-functionalized nylon-6 electrospun nanofibers were used. The capacity of the amino-functionalized nylon-6 sorbent to pre-concentrate heavy metals compared favourably with those

of aqua regia and HNO_3+H_2O_2 digestions especially in less complex matrixes. Due to their highly porous nature, the electrospun nanofibers exhibited high adsorption capacities (up to 50 mg/g) for heavy metal ions. The loading capacities of the electrospun nanofiber sorbents exceeded those of chitosan microparticles, ion imprinted composites and amino-functionalized mesoporous materials.

This thesis has demonstrated the potential of electrospun nanofiber as novel sorbents for efficient and cost effective alternative for pre-concentrating heavy metals in aqueous environments.

References

Abbas, M.A., Latham, J. (1967). The instability of evaporating charged drops. J. Fluid. Mech. 30(4): 663-670.

Abo-Farha, S.A., Abdel-Aal, A.Y., Ashourb, I.A., Garamon, S.E. (2009). Removal of some heavy metal cations by synthetic resin purolite C100. J. Hazard. Mater. 169: 190-194.

Acar, F.N., Malkoc, E. (2004). The removal of chromium(VI) from aqueous solutions by Fagus orientalis L. Biores. Technol. 94(1) 13–15.

Adamson, A.W., Gast, A.P. (1997). Physical Chemistry of Surfaces, 6th ed., Wiley-International, New York.

Aguado, J., Arsuaga, J.M., Arencibia, A., Lindo, M., Gascón, V. (2009). Aqueous heavy metals removal by adsorption on amine-functionalized mesoporous silica. J. Haz. Mater. 163: 213–221.

Ahmet, D., Fevzi, Y., Tuna, A.L., Nedim, O. (2006). Heavy metals in water, sediment and tissues of Leuciscus cephalus from a stream in southwestern Turkey, Chemosphere 63: 1451-1458.

Al-Jlil, S.A., Alsewailem, F.D. (2009). Saudi Arabian clays for lead removal in wastewater. Appl. Clay Sci. 42: 671-674.

Alluri, H.K., Ronda, S.R., Settalluri, V.J., Bondili, J.S., Suryanarayana, V., Venkateshwar, P. (2007). Biosorption: an eco-friendly alternative for heavy metal removal, African J. Biotechnol. 6: 2924-2931.

Al-Rub, F.A.A. (2006). Biosorption of zinc on palm tree leaves: equilibrium, kinetics, and thermodynamics studies, Sep. Purif. Technol. 41: 3499-3515.

Alyüz, B., Veli, S (2009). Kinetics and equilibrium studies for the removal of nickel and zinc from aqueous solutions by ion exchange resins. J. Hazard. Mater. 167 (1–3) 482–488.

Aman, T., Kazi, A.A., Sabri, M.U., Bano, Q. (2008). Potato peels as solid waste for the removal of heavy metal copper(II) from waste water/industrial effluent. Colloid Surf. 63: 116-121.

Amarasinghe, B.M.W.P.K., Williams, R.A. (2007). Tea waste as a low cost adsorbent for the removal of Cu and Pb from wastewater. Chem. Eng. J. 32: 299-309.

Amudaa, O.S., Adelowoa, F.E., Ologunde, M.O. (2009). Kinetics and equilibrium studies of adsorption of chromium(VI) ion from industrial wastewater using *Chrysophyllum albidum* (Sapotaceae) seed shells. Colloid Surf. 68: 184-192.

Andrady A.L. (2008). Science and technology of polymer nanofibers. John Wiley & Sons, Inc., Hoboken, New Jersey.

Apiratikul, R., Pavasant, P. (2008). Batch and column studies of biosorption of heavy metals by Caulerpa lentillifera. Bioresour. Technol. 99: 2766-2777.

Aussawasathien, D., Sahasithiwat, S., Menbangpung, L. (2008). Electrospun camphorsulfonic acid doped poly(o-toluidine)-polystyrene composite fibers: Chemical vapor sensing. Synthetic Met. 158(7), 259-263.

Axtell, N.R., Sternberg, S.P.K., Claussen, K. (2003). Lead and nickel removal using microspora and lemna minor. Bioresour. Technol. 89: 41-48.

Baker, S.C., Atkin, N., Gunning, P.A., Granville, N., Wilson, K., Wilson, D., Southgate, J. (2006). Characterisation of electrospun polystyrene scaffolds for three dimensional in vitro biological studies. Biomaterials 27(16): 3136-3146.

Baumgarten, P.K. (1971). Electrostatic spinning of acrylic microfibers. J. Colloid Interf. Sci. 36(1): 71-79.

Bazzicalupi, C., Bencini, A., Bianchi, A., Danesi, A., Giorgi, C., Valtancoli, B. (2009). Anion Binding by Protonated Forms of the Tripodal Ligand Tren. Inorg. Chem. 48: 2391-2398.

Beppu, M.M., Arruda, E.J., Vieira, R.S., Santos, N.N. (2004). Adsorption of Cu(II) on porous chitosan membranes functionalized with histidine. J. Memb. Sci. 240: 227-235.

Bhardwaj, N., Kundu, S.C. (2010). Electrospinning: A fascinating fiber fabrication technique. Biotechnol. Adv. 28: 325-347.

Bjorge, D., Deels, N., De Vrieze, S., Dejans, P., Van Camp, T., Audenaert, W., Westbroek, P., De Clerck, K., Boeckaert, C. And Van Hulle, S.W.H. (2010). Initial testing of electrospun nanofibre filters in water filtration applications. Water SA 36: 151-155.

Bogdanovic, G.A., Jacimovic, Z.K., Leovac, V.M. (2005). Transition metal complexes with pyrazole-based ligands. XXII. Di-μ-thiocyanato-bis[(3,5-dimethyl-1*H*-pyrazole-1-carboxamidine-$_k^2$N,N')(thiocyanato-$_k$N)copper(II)] and a redetermination of bis(3,5-dimethyl-1H-pyrazole-1-carboxamidine-$_k^2$N,N')bis(nitrato-$_k$O)copper(II). Acta. Cryst. 61: 376-379.

Bojic, A.L., Bojic, D., Andjelkovic, T. (2009). Removal of Cu^{2+} and Zn^{2+} from model wastewaters by spontaneous reduction-coagulation process in flow conditions. J. Hazard. Mater. 168: 813-819.

Boran, M., Altınok, I. (2010). A Review of Heavy Metals in Water, Sediment and Living Organisms in the Black Sea. Turk. J. Fish. Aquat. Sci. 10: 565-572

Borba, C.E., Guirardello, R., Silva, E.A., Veit, M.T., Tavares, C.R.G. (2006). Removal of nickel(II) ions from aqueous solution by biosorption in a fixed bed column: experimental and theoretical breakthrough curves. Biochem. Eng. J. 30: 184-191.

Bradbury, M.H., Baeyens, B. (2005). Modelling the sorption of Mn(II), Co(II), Ni(II), Zn(II), Cd(II), Eu(III), Am(III), Sn(IV),Th(IV), Np(V) and U(VI) on montmorillonite: Linear free energy relationships and estimates of surface binding constants for some selected heavy metals and actinides. Geochim. Cosmochim. Acta. 69: 875-892.

Bresee, R.R. (2004). Influence of processing conditions on melt blown web structure: Part 1 – DCD. INJ Spring, 49-55.

Brown, I.G. (1993). Metal-ion implantation for large-scale surface modification. J. Vac. Sci. Technol. A. 11: 1480-1485.

Brunelot, G., Adrian, P., Rouiller, J., Guillet, B., Andreux, F. (1989). Determination of dissociable acid groups of organic compounds extracted from soils, using automated potentiometric titration. Chemosphere. 19(8-9): 1413-1419.

Buchko, C.J., Chen, L.C., Shen, Y., Martin, D.C. (1999). Processing and microstructural characterization of porous biocompatible protein polymer thin films. Polymer. 40(26): 7397-7407.

Buer, A., Ugbolue, S.C., Warner, S.B. (2001). Electrospinning and properties of some nanofibers. Text. Res. J. 71(4): 323-328.

Bunyan, N.N., Chen, J., Chen, I., Farboodmanesh, S. (2006). Electrostatic effects of electrospun fiber deposition and alignment. In: Polymeric Nanofibers. ACS Symposium Series 918. Edited by D. H. Reneker and H. Fong. Oxford University Press (USA), p.106.

Burger, C., Hsiao, B.S., Chu, B. (2006). Nanofibrous materials and their applications. Ann. Rev. Mater. Res. 36: 333-368.

Buttafoco, L., Kolkman, N.G., Engbers-Buijtenhuijs, P., Poot, A.A., Dijkstra, P.J., Vermes, I., Feijen, J. (2006). Electrospinning of collagen and elastin for tissue engineering applications. Biomater. 27(5): 724-734.

Celik, A., Demirbas, A. (2005). Removal of heavy metal ions from aqueous solutions via adsorption onto modified lignin from pulping wastes. Energy Sour. 27: 1167-1177.

Chan, C.M., Ko, T.M., Hiraoka, H. (1996). Polymer surface modification by plasmas and photons. Surf. Sci. Rep. 24: 3-54.

Chang, Q., Wang, G. (2007). Study on the macromolecular coagulant PEX which traps heavy metals. Chem. Eng. Sci. 62: 4636-4643.

Chang, Y.C., Chen, D.H. (2005). Preparation and adsorption properties of monodisperse chitosan-bound Fe_3O_4 magnetic nanoparticles for removal of Cu(II) ions. J. Colloid Interf. Sci. 283: 446-451.

Chanpiwat, P., Sthiannopkao, S., Kim, K.W. (2010). Metal content variation in wastewater and biosludge from Bangkok's central wastewater treatment plants. Microchem. J. 95: 326-332.

Chen, L.Z., Flammang, R., Maquestiau, A., Taft, R.W., Catalan, J., Cabildo, P., Claramunt, R.M., Elguero, J.T. (1991). Hermodynamic basicity vs. kinetic basicity of diazoles (imidazoles and pyrazoles). J. Org. Chem. 56: 179-183.

Chen, T., Li, L., Huang, X. (2005). Fiber diameter of polybutylene terephthalate melt-blown nonwovens. J. Appl. Polym. Sci. 97: 1750-1752.

Chigome, S., Darko, G., Buttner, U., Torto, N. (2010). Semi-micro solid phase extraction with electrospun polystyrene fiber disks. Anal. Methods. 2: 623-626.

Christanti, Y. and Walker, L. M. (2001). Surface tension driven jet break up of strain hardening polymer solutions. J. Non-Newton. Fluid. 100: 9-26.

Chu, P.K., Chen, J.Y., Wang, L.P., Huang, N. (2002). Plasma-surface modification of biomaterials. Mater. Sci. Eng. 36: 143-206.

Clark, A.L. (1938). The critical state of pure fluids. Chem. Rev. 23: 1-15.

Clarke, A.R., Eberhardt, C.N. (2002). Microscopy techniques for materials science. Woodhead Publishing Electronic ISBN: 978-1-59124-613-8. Available at: http://www.knovel.com/web/portal/browse/display?_ext_knovel_display_bookid=46&verticalid=0

Dalton, P. D., Klee, D. and Moller, M. (2005). Electrospinning with dual collection rings. Polymer 46(3):611-614.

Darko, G., Chigome, S., Tshentu, Z., Torto, N. (2011). Enrichment of Cu(II), Ni(II) and Pb(II) in aqueous solutions using electrospun polysulfone nanofibers functionalized with 1-[Bis[3-(dimethylamino)-propyl]amino]- 2-propanol. Anal. Lett. 44: 1855-1867.

De Moel, K., van Ekenstein, G.O.R.A., Nijland, H., Polushkin, E., ten Brinke, G., Maki Ontto, R., Ikkala, O. (2001). Polymeric nanofibers prepared from self organized supramolecules. Chem. Mater. 13(12): 4580-4583.

De Vrieze, S, De Schoenmaker, B., Ceylan, Ö., Depuydt, J., Landuyt, L.V., Rahier, H., Guy Van Assche, G.V., De Clerck, K. (2011). Morphologic study of steady state electrospun polyamide 6 nanofibres. J. Appl. Polym. Sci. 119(5): 2984-2990.

Deitzel, J.M., Kleinmeyer, J., Harris, D., Tan, N.C.B. (2001). The effect of processing variables on the morphology of electrospun nanofibers and textiles. Polymer 42(1): 261-272.

Deitzel, J.M., Krauthauser, C., Harris, D., Perganis, C., Kleinmeyer, J. (2006). Key parameters influencing the onset and maintenance of electrospinning jet. In: Polymeric Nanofibers. ACS Symposium Series 918. Oxford University Press (USA), p. 56.

Demir, M.M., Yilgor, I., Yilgor, E., Erman, B. (2002). Electrospinning of polyurethane fibers. Polymer. 43(11): 3303-3309.

Demirbas, A. (2008). Heavy metal adsorption onto agro-based waste materials: A review. J Hazard. Mater. 157: 220-229

Demirbas, A. Pehlivan, E. Gode, F. Altun, T. Arslan, G. (2005). Adsorption behavior of Cu(II), Zn(II), Ni(II), Pb(II), and Cd(II) from aqueous solution on Amberlite IR-120 synthetic resin. J. Colloid Interface Sci. Surf. 282: 16-21.

Demirbas, A., Sari, A., Isildak, O. (2006). Adsorption thermodynamics of stearic acid onto bentonite. J. Hazard. Mater. 135: 226-231.

Demirbas, A. (2008). Heavy metal adsorption onto agro-based waste materials: A review. J. Hazard. Mater. 157: 220-229

Deng, L., Su, Y., Su, H., Wang, X., Zhu, X. (2006). Biosorption of copper(II) and lead(II) from aqueous solutions by nonliving green algae *Cladophora f ascicularis*: equilibrium, kinetics and environmental effects. Adsorption. 2: 267-277.

Dersch, R., Graeser, M., Greiner, A., Wendorff, J.H. (2007). Electrospinning of nanofibres: Towards new techniques, functions, and applications. Australian Journal of Chemistry, 60(10): 719-728.

Dersch, R., Liu, T.Q., Schaper, A.K., Greiner, A., Wendorff, J.H. (2003). Electrospun nanofibers: internal structure and intrinsic orientation. J. Polym. Sci. Part A: 41(4): 545-553.

Desai, S.M., Singh, R.P. (2004). Surface modification of polyethylene: long-term properties of polyolefins. Adv. Polym. Sci. 169: 231-293.

Ding, B., Kim, J., Miyazaki, Y., Shiratori, S. (2004b). Electrospun nanofibrous membranes coated quartz crystal microbalance as gas sensor for NH_3 detection. Sensors Actuator. B: 101(3): 373-380.

Ding, B., Kimura, E., Sato, T., Fujita, S., Shiratori, S. (2004). Fabrication of blend biodegradable nanofibrous nonwoven mats via multi-jet electrospinning. Polymer. 45(6): 1895-1902.

Ding, B., Wang, M., Yu, J., Sun, G. (2009). Gas sensors based on electrospun nanofibers. Sensors. 9(3): 1609-1624.

Ding, B., Yamazaki, M., Shiratori, S. (2005). Electrospun fibrous polyacrylic acid membrane-based gas sensors. Sensors Actuator. B: 106 (1): 477-483.

Diniz, M.C.T., Filho, O.F., Rohwedder, J.J.R. (2004). An automated system for liquid–liquid extraction based on a new micro-batch extraction chamber with on-line detection: preconcentration and determination of copper(II). Anal. Chim. Acta. 525: 281-287.

Dizge, N., Keskinler, B., Barlas, H. (2009). Sorption of Ni(II) ions from aqueous solution by Lewatit cation-exchange resin. J. Haz. Mat. doi:10.1016/j.jhazmat.2009.01.073.

Dong, H., Bell, T. (1999). State-of-the-art overview: ion beam surface modification of polymers towards improving tribological properties. Surf. Coat. Technol. 111 (1): 29-40.

Dong, H., Nyame, V., MacDiarmid, A.G., Jones, W.E. Jr. (2004). Polyaniline/ poly(methyl methacrylate) coaxial fibers: the fabrication and effects of the solution properties on the morphology of electrospun core fibers. J. Polym. Sci. Part B: 42(21): 3934-3942.

Dong, L.F., Cui, Z.L., Zhang, Z.K. (1997). Gas sensing properties of nano-ZnO prepared by arc plasma method. ACS Sym. Ser. 8(7): 815-823.

Doshi, J. and D. H. Reneker (1995). Electrospinning process and applications of electrospun fibers. J.Electrostat. 35(2-3): 151-160.

Doshi, J. Reneker, D.H. 1995. Electrospinning Process and Application of Electrospun Fibers. J. Electrostat. 35: 151-160.

Duffus, J.H. (2002). "Heavy metals"- a meaningless term? Pure and Applied Chemistry. 74: 793-807.

Dzenis, Y.A. (2004). Spinning continuous fibers for nanotechnology. Science. 304(5679): 1917-1919.

Ellison, J.C., Phatak, A., Giles, D.W., Macosko, C.W., Bates, F.S. (2007). Melt blown nanofibers: Fiber diameter distributions and onset of fiber breakup. Polymer. 48: 3306-3316.

Ensor, D.S., Andrady, A.L. (2007). Electrospinning in a controlled gaseous environment. U.S. Patent 7,297,305.

Ezoddin, M., Shemirani, F., Abdi, Kh., Khosravi Saghezchi, M., Jamali. M.R. (2010). Application of modified nano-alumina as a solid phase extraction sorbent for the preconcentration of Cd and Pb in water and herbal samples prior to flame atomic absorption spectrometry determination. J. Hazard. Mater. 178: 900-905.

Feng, L., Li, S.H., Li, H.I., Zhai, J., Song, Y.L., Jiang, L., Zhu, D.B. (2002). Super-hydrophobic surface of aligned polyacrylonitrile nanoflbers. Angew. Chem. Int. Ed., 41(7): 1221-1223.

Fong, H., Chun, I., Reneker, D.H. (1999). Beaded nanofibers formed during electrospinning. Polymer. 40(16): 4585-4592.

Fridrikh, S.V., Yu, J.H., Brenner, M.P., Rutledge, G.C. (2003). Controlling the fiber diameter during electrospinning. Phys. Rev. Lett. 90(14): 144-502.

Fu, F., Wang, Q. (2011). Removal of heavy metal ions from wastewaters: A review. J. Environ. Manage. 92: 407-418.

Gans, P., O'Sullivan, B. (2000). Glee, a new computer program for glass electrode calibration. Talanta. 51: 33-37.

Gans, P., Sabatini, A., Vacca, A. (1996). Investigation of equilibria in solution. Determination of equilibrium constants with the HYPERQUAD suite of programs. Talanta. 43: 1739-1753.

Garbarino, J.R., Hayes, H.C., Roth, D.A., Antweiler, R.C., Brinton, T.I., Taylor, H.E. (1995). Heavy Metals in the Mississippi River. U.S. Geological Survey Circular 1133, Reston, Virginia.

Gode, F., Pehlivan, E. (2006). Removal of chromium (III) from aqueous solutions using Lewatit S 100: the effect of pH, time, metal concentration and temperature. J. Hazard. Mater. 136: 330-337.

Godt, F.S.J., Grosse-Siestrup, C., Esche, V., Brandenburg, P., Reich, A., Groneberg, D.A. (2006). The toxicity of cadmium and resulting hazards for human health. J. Occup. Med. Toxicol. 1: 1-6.

Göpel, W. (1995). Supramolecular and polymeric structures for gas sensors. Sensor Actuator: B. Chemical, 24(1-3): 17-32.

Göpel, W., Schierbaum, K.D. (1995). SnO_2 sensors: current status and future prospects. Sensor Actuator: B. Chemical. 26(1-3): 1-12.

Gosset, T., Trancart, J., Thevenot, D.R. (1986). Batch metal removal by peat: kinetics and thermodynamics. Wat. Res. 20: 21-26.

Grace, J.M., Gerenser, L.J. (2003). Plasma treatment of polymers. J. Dispersion Sci. Technol. 24(3-4): 305-341.

Gran, G. (1952). Determination of the equivalence point in potentiometric titrations. Part II. Analyst. 77: 661-671.

Greener, J., Abbasi, B., Kumacheva, E. (2010). Attenuated total reflection Fourier transform infrared spectroscopy for on-chip monitoring of solute concentrations. LabChip. 10: 1561-1566.

Greiner, A., Wendorff, J.H. (2007). Electrospinning: A fascinating method for the preparation of ultrathin fibers. Angewandte Chemie - International Edition. 46(30): 5670-5703.

Gu, S.Y., Ren, J. (2005). Process optimization and empirical modeling for electrospun poly(D,L-lactide) fibers using response surface methodology. Macromol. Mater. Eng. 290(11): 1097-1105.

Gu, X.Y., Evans, L.J. (2008). Surface complexation modelling of Cd(II), Cu(II), Ni(II), Pb(II) and Zn(II) adsorption onto kaolinite. Geochim. Cosmochim. Acta. 72: 267-276.

Gundacker, C. (2000). Comparison of heavy metal bioaccumulation in freshwater molluscs of urban river habitats in Vienna. Environ. Pollut. 110(1): 61-71.

Gundogdu, A., Ozdes, D., Duran, C., Bulut, V.N., Soylak, M., Senturk, H.B. (2009). Biosorption of Pb(II) ions from aqueous solution by pine bark (*Pinus brutia Ten.*). Chem. Eng. J.153: 62-69.

Guo, M.X., Qiu, G.N., Song, W.P. (2010). Poultry litter-based activated carbon for removing heavy metal ions in water. Waste Manage. 30: 308-315.

Guo, X., Du, Y., Chen, F., Park, H.S., Xie, Y. (2007). Mechanism of removal of arsenic by bead cellulose loaded with iron oxyhydroxide (b–FeOOH): EXAFS study. J. Colloid Interf. Sci. 314: 427-433.

Gupta, P., Elkins, C., Long, T.E., Wilkes, G.L. (2005). Electrospinning of linear homopolymers of poly(methyl methacrylate): exploring relationships between fiber formation, viscosity, molecular weight and concentration in a good solvent. Polymer. 46(13): 4799-4810.

Haghi, A.K., Akbari, M. (2007). Trends in Electrospinning of Natural Nanofibers. Physica Status Solidi A. 204: 1830-1834.

Hamissa, A.M.B., Lodi, A., Seffen, M., Finocchio, E., Botter, R., Converti, A. (2010). Sorption of Cd(II) and Pb(II) from aqueous solutions onto Agave americana fibers Chem. Eng. J. 159: 67-74.

Hartgerink, J.D., Beniash, E., Stupp, S.I. (2001). Self-assembly and mineralization of peptide-amphiphile nanofibers. Science. 294(5547): 1684-1688.

Hayati, I., Bailey, A.I., Tadros T.F. (1987). Investigations into the mechanisms of electrohydrodynamic spraying of liquids: I. Effect of electric field and the environment on pendant drops and factors affecting the formation of stable jets and atomization. J. Colloid. Interf. Sci. 117(1): 205-221.

He, J.-H., Wan, Y.-Q., Yu, J.-Y. (2004). Application of vibration technology to polymer electrospinning. Int. J. Nonlin. Sci. Num. 5(3): 253-262.

He, W., Z. W. Ma, T. Yong, W. E. Teo, and S. Ramakrishna (2005a). "Fabrication of collagen-coated biodegradable polymer nanofiber mesh and its potential for endothelial cells growth." Biomaterials 26(36):7606–7615.

He, W., T. Yong, W. E. Teo, Z. Ma, and S. Ramakrishna (2005b). "Fabrication and endothelialization of collagen-blended biodegradable polymer nanofibers: potential vascular graft for blood vessel tissue engineering." Tissue Engineering 11(9–10):1574–1588.

Hegde, R.R., Dahiya, A., Kamath, M.G., Nanofiber nonwovens. http://www.engr.utk.edu/mse/Textiles/Nanofiber%20Nonwovens.htm Updated: June 13, 2005

Heidari, A., Younesi, H., Mehraban, Z. (2009). Removal of Ni(II), Cd(II), and Pb(II) from a ternary aqueous solution by amino functionalized mesoporous and nano mesoporous silica. Chem. Eng. J. 153(1-3): 70-79.

Hendricks, C.D.Jr., Carson, R.S., Hogan, J.J., Schneider, J.M. (1964). Photomicrography of electrically sprayed heavy particles. AIAA Journal 2(4): 733-737.

Hillie, T., Hlophe, M. (2007). Nanotechnology and the challenge of clean water. Nature Nanotechnol. 2 (11): 663-664.

Hohman, M.M., Shin, M. Rutledge, G., Brenner, M.P. (2001a). Electrospinning and electrically forced jets. I. Stability theory. Physic Fluid. 13(8): 2201-2220.

Hohman, M.M., Shin, M., Rutledge, G. and Brenner, M.P. (2001b). Electrospinning and electrically forced jets. II. Applications. Physic Fluid. 13(8): 2221-2236.

Hong, K.H., Park, J.L., Sul, I.H., Youk, J.H., Kang, T.J. (2006). Preparation of antimicrobial poly(vinyl alcohol) nanofibers containing silver nanoparticles. J. Polym. Sci. Part B: 44(17): 2468-2474.

Hsu, C.M., Shivkumar, S. (2004a). Nano-sized beads and porous fiber constructs of poly(1-caprolactone) produced by electrospinning. J. Mater. Sci. 39(9): 3003-3013.

Hsu, C.M., Shivkumar, S. (2004b). N,N-dimethylformamide additions to the solution for the electrospinning of poly(1-caprolactone) nanofibers. Macromol. Mater. Eng. 289(4): 334-340.

Huang, C.B., Chen, S.L. Reneker, D.H. Lai, C.L., Hou, H. (2006b). High strength mats from electrospun poly(p-phenylene biphenyltetracarboximide) nanofibers. Adv. Mater. 18(5): 668-671.

Huang, C.B., Chen, S.L., Lai, C.L., Reneker, D.H., Qiu, H.Y., Ye, Y., Hou, H.Q. (2006a). Electrospun polymer nanofibres with small diameters. Nanotechnol. 17(6): 1558-1563.

Huang, Z.M. Zhang, Y.Z. Kotaki, M. Ramakrishna, S. (2003). A review on polymer nanofibers by electrospinning and their applications in nanocomposites. Compos. Sci. Technol. 63: 2223-2253.

Huber, W. (2003). Basic calculations about the limit of detection and its optimal determination. Accred. Qual. Assur. 7: 256-257.

Huisman, J.L., Schouten, G., Schultz, C. (2006). Biologically produced sulphide for purification of process streams, effluent treatment and recovery of metals in the metal and mining industry. Hydrometallurgy 83: 106-113.

Hussain, D. Loyal, F. Greiner, A. Wendorff, J.H. (2010). Structure property correlations for electrospun nanofiber nonwovens. Polymer. 51: 3989-3997.

Ignatious, F. and Baldoni, J.M. (2003). Electrospun pharmaceutical compositions, United States Patent PCT/UDS01/02399.

Ikada, Y. (1994). Surface modification of polymers for medical applications. Biomaterials 15: 725-736.

Jaeger, C.R., Bergshoef, M.M., Batlle, C.M., Schoenherr, H., Vancso, G.J. (1998). Electrospinning of ultra-thin polymer fibers. Macromol. Sy. 127: 141-150.

Jai, P.H., Wook, J.S., Kyu, Y.J., Gil, K.B., Mok, L.S. (2007). Removal of heavy metals using waste eggshell. J. Environ. Sci. 19: 1436-1441.

Jalili, R., Hosseini, S.A., Morshed, M. (2005). The effects of operating parameters on the morphology of electrospun polyacrilonitrile nanofibres. Iranian Polymer Journal 14(12): 1074-1081.

Jamshidi, M., Ghaedi, M., Mortazavi, K. Nejati Biareh, M., Soylak, M. (2011). Determination of some metal ions by flame-AAS after their preconcentration using sodium dodecyl sulfate coated alumina modified with 2-hydroxy-(3-((1-H-indol 3-yle)phenyl) methyl) 1-H-indol (2-HIYPMI). Food Chem. Toxicol. 49: 1229-1234.

Jarusuwannapoom, T., Hongrojjanawiwat, W., Jitjaicham, S., Wannatong, L., Nithitanakul, M., Pattamaprom, C., Koombhongse, P., Rangkupan, R., Supaphol, P. (2005). Effect of solvents on electro-spinnability of polystyrene solutions and morphological appearance of resulting electrospun polystyrene fibers. Eur. Polym. J. 41(3): 409-421.

Jeun, J.P., Lim, Y.M., Nho, Y.C. (2005). Study on morphology of electrospun poly(caprolactone) nanofiber. J. Ind. Eng. Chem. 11(4): 573-578.

Ji, S., Li, Y., Yang, M. (2008). Gas sensing properties of a composite composed of electrospun poly(methyl methacrylate) nanofibers and in situ polymerized polyaniline. Sensor Actuator. 133(2): 644-649.

Jiang, H., Fang, D., Hsiao, B., Chu, B., Chen, W. (2004). Preparation and characterization of ibuprofen-loaded poly(lactide-co-glycolide)/poly(ethylene glycol)-g-chitosan electrospun membranes. J. Biomat. Sci-Polym. E. 15(3): 279-296.

Jin, Z., Zhou, H., Jin, Z., Savinell, R.F., Liu, C. (1998). Application of nano-crystalline porous tin oxide thin film for CO sensing. Sensor Actuator. B: Chemical, 52(1-2): 188-194.

Jun, Z., Hou, H.Q., Schaper, A., Wendorff, J.H., Greiner, A. (2003). Poly-L-lactide nanofibers by electrospinning-influence of solution viscosity and electrical conductivity on fiber diameter and fiber morphology. e-Polymers: 009:1-9.

Jung, Y.H., Kim, H.Y., Lee, D.R., Park, S.Y., Khil, M.S. (2005). Characterization of PVOH nonwoven mats prepared from surfactant-polymer system via electrospinning. Macromol. Res. 13(5): 385-390.

Kabbashi, N.A., Atieh, M.A., Al-Mamun, A., Mirghami, M.E.S., Alam, M.D.Z., Yahya, N. (2009). Kinetic adsorption of application of carbon nanotubes for Pb(II) removal from aqueous solution. J. Environ. Sci. 21: 539-544.

Kaczala, F., Marques, M., Hogland,W. (2009). Lead and vanadium removal from a real industrial wastewater by gravitational settling/sedimentation and sorption onto *Pinus sylvestris* sawdust. Bioresour. Technol. 100: 235-243.

Kalayci, V.E., Patra, P.K., Kim, Y.K., Ugbolue, S.C., Warner, S.B. (2005). Charge consequences in electrospun polyacrylonitrile (PAN) nanofibers. Polymer. 46(18): 7191-7200.

Kandah, M.I., Meunier, J.L. (2007). Removal of nickel ions from water by multi-walled carbon nanotubes. J. Hazard. Mater. 146: 283-288.

Kang, S., Lee, J., Kima, K. (2007). Biosorption of Cr(III) and Cr(VI) onto the cell surface of pseudomonas aeruginosa, Biochem. Eng. J. 36: 54-58.

Kang, X., Pan, C., Xu, Q., Yao, Y., Wang, Y., Qi, D., Gu, Z. (2007). The investigation of electrospun polymer nanofibers as a solid-phase extraction sorbent for the determination of trazodone in human plasma. Anal. Chim. Acta. 587: 75-81.

Kang, Y.S., Kim, H.Y., Ryu, Y.J., Lee, D.R., Park, S.J. (2002). The effect of processing parameters on the diameter of electrospun polyacrylonitrile (PAN) nano fibers. Polymer (Korea) 26(3): 360.

Kapinos, L.E., Song, B., Sige, H. (1998). Metal ion-coordinating properties of imidazole and derivatives in aqueous solution: interrelation between complex stability and ligand basicity. Inorg. Chim. Acta. 280: 50-56.

Karlsson, H.L., Cronholm, P., Gustafsson, J., Möller, L. (2008). Copper Oxide Nanoparticles Are Highly Toxic: A Comparison between Metal Oxide Nanoparticles and Carbon Nanotubes. Chem. Res. Toxicol., 21 (9): 1726–1732.

Kato, K., Uchida, E., Kang, E.T., Uyama, Y., Ikada, Y. (2003). Polymer surface with graft chains, Prog. Polym. Sci. 28(2): 209-259.

Katta, P., Alessandro, M., Ramsier, R.D., Chase, G.G. (2004). Continuous electrospinning of aligned polymer nanofibers onto a wire drum collector. Nano Letters 4(11): 2215-2218.

Katti, D.S., Robinson, K.W., Ko, F.K., Laurencin, C.T. (2004). Bioresorbable nanofiber-based systems for wound healing and drug delivery: Optimization of fabrication parameters. J. Biomed. Mater. Res. - Part B: 70(2): 286-296.

Kemp, P.C., Neumeister-Kemp, H.G., Lysek, G., Murray, F. (2001). Survival and growth of micro-organisms on air filtration media during initial loading. Atmosp. Environ. 35(28): 4739-4749.

Kenawy, E., Bowlin, G.L., Mansfield, K., Layman, J., Simpson, D.G., Sanders, E.H. and Wnek, G.E. (2002). Release of tetracycline hydrochloride from electrospun poly(ethylene-co-vinylacetate), poly(lactic acid), and a blend. J. Control. Release. 81(1-2): 57-64.

Kessick, R., Fenn, J., Tepper, G. (2004). The use of AC potentials in electrospraying and electrospinning processes. Polymer. 45(9): 2981-2984.

Khademhosseini, A., Langer, R. (2007). Microengineered hydrogels for tissue engineering. Biomaterials. 28(34): 5087-5092.

Khezami, L., Capart, R. (2005). Removal of chromium(VI) from aqueous solution by activated carbons: kinetic and equilibrium studies. J. Hazard. Mater. 123: 223-231.

Khil, M., Bhattarai, S.R., Kim, H., Kim, S., Lee, K. (2005). Novel fabricated matrix via electrospinning for tissue engineering. J. Biomed. Mater. Res. Part B 72(1): 117-124.

Khil, M., Cha, D., Kim, H., Kim, I., Bhattarai, N. (2003). Electrospun nanofibrous polyurethane membrane as wound dressing. J. Biomed. Mater. Res. - Part B: 67(2): 675-679.

Khil, M.S., Bhattarai, S. R. Kim, H.Y. Kim, S.Z., Lee K.H. (2005). Novel fabricated matrix via electrospinning for tissue engineering. J. Biomed. Mater. Res. Part B: 72B:117-124.

Kidoaki, S., Kwon, I.K., Matsuda, T. (2005). Mesoscopic spatial designs of nano- and microfiber meshes for tissue-engineering matrix and scaffold based on newly devised multilayering and mixing electrospinning techniques. Biomaterials. 26(1): 37-46.

Kidoaki, S., Kwon, K., Matsuda, T. (2006). Structural features and mechanical properties of in situ-bonded meshes of segmented polyurethane electrospun from mixed solvents. J. Biomed. Mater. Res. Part B: 76B(1): 219-229.

Kim, G.H., Kim W.D. (2006). Nanofiber spraying method using a supplementary electrode. Appl. Phys. Lett. 89(1):013111.

Kim, H.Y., Lee, B.M., Kim, I.S., Jin, T.H., Ko, K.H., Ryu, Y.J. (2004). Fabrication of triblock copolymer of poly(ρ-dioxanone-co-L-lactide)-block-poly(ethylene glycol) nonwoven mats by electrospinning and applications for wound dressing. PMSE Preprints. 91: 712-713.

Kim, J.H., Kim, S.H., Shiratori, S. (2004). Fabrication of nanoporous and hetero structure thin film via a layer-by-layer self assembly method for a gas sensor. Sensor Actuator. B. 102(2): 241-247.

Kim, K., Chang, C., Zong, X., Fang, D., Hsiao, B.S., Chu, B., Hadjiargyrou, M. (2004). Incorporation of an antibiotic drug in electrospun poly(lactide-co-glycolide) non-woven nanofiber scaffolds. J. Control. Release. 98(1): 47-56.

Kim, S.H., Kim, S.H., Nair, S., Moore, E. (2005). Reactive electrospinning of cross-linked poly(2-hydroxyethyl methacrylate) nanofibers and elastic properties of individual hydrogel nanofibers in aqueous solutions. Macromol. 38(9): 3719-3723.

Kim, S.J., Lee, C.K., Kim, S.I. (2005). Effect of ionic salts on the processing of poly(2-acrylamido-2-methyl-1-propane sulfonic acid) nanofibers. J. Appl. Polym. Sci. 96(4): 1388-1393.

Ko, F.K., Macdiarmid A.G., Norris, I.D., Shaker, M., Lec, R.M., PCT/US01/00327, 2001.

Koh, C.J., Atala, A. (2004). Tissue Engineering, Stem Cells, and Cloning: Opportunities for Regenerative Medicine. J. Am. Soc. Nephrol. 15(5): 1113-1125.

Kolachi, N.F., Kazi, T.G., Afridi, H.I., Khan, S., Wadhwa, S.K., Shah, A.Q., Shah, F., Baig, J.A., Sirajuddin (2010). Determination of selenium content in aqueous extract of medicinal plants used as herbal supplement for cancer patients. Food Chem.Toxicol. 48: 3327-3332.

Kong, J., Franklin, N.R., Zhou, C., Chapline, M.G., Peng, S., Cho, K., Dai, H. (2000). Nanotube molecular wires as chemical sensors. Science. 287(5453): 622-625.

Koombhongse, S., Liu, W.X., Reneker, D.H. (2001). Flat polymer ribbons and other shapes by electrospinning. J. Polym. Sci. Part B: 39(21): 2598-2606.

Köysal, Y., Isik, S., Sahin, G., Palaska. E. (2005). Two N-substituted 3,5-diphenyl-2 pyrazoline-1-thiocarboxamides. Acta Cryst. 61: 542-544.

Krishnappa, R.V.N., Desai, K., Sung, C. (2003). Morphological study of electrospun polycarbonates as a function of the solvent and processing voltage. J. Mater. Sci. 38(11): 2357-2365.

Ku, Y., Jung, I.L. (2001). Photocatalytic reduction of Cr(VI) in aqueous solutions by UV irradiation with the presence of titanium dioxide. Water Res. 35: 135-142.

Kuo, C.Y., Lin, H.Y. (2009). Adsorption of aqueous cadmium (II) onto modified multiwalled carbon nanotubes following microwave/chemical treatment. Desalination. 249: 792-796.

Kurniawan, T.A., Chan, G.Y.S., Lo, W.H., Babel, S. (2006). Physicoechemical treatment techniques for wastewater laden with heavy metals. Chem. Eng. J. 118: 83-98.

Lala, N.L., Ramaseshan. R., Li. B.J., Sundarrajan, S., Barhate. R.S., Liu, Y.J., Ramakrishna, S. (2007). Fabrication of nanofibers with antimicrobial functionality used as filters: protection against bacterial contaminants. Biotechnol. Bioeng. 97(6): 1357.

Landaburu-Aguirre, J., García, V., Pongrácz, E., Keiski, R.L. (2009). The removal of zinc from synthetic wastewaters by micellar-enhanced ultrafiltration: statistical design of experiments. Desalination. 240: 262-269.

Larsen, G., Noriega, S., Spretz, R., Velarde-Ortiz R. (2004a). Electrohydrodynamics and hierarchical structure control: submicron-thick silica ribbons with an ordered hexagonal mesoporous structure. J. Mater. Chem. 14(15): 2372-2373.

Larsen, G., Spretz, R., Velarde-Ortiz, R. (2004b). Use of coaxial gas jackets to stabilize Taylor cones of volatile solutions and to induce particle-to-fiber transitions. Adv. Mater. 16(2): 166-169.

Lee, C. K., Kim, S.I., Kim, S.J. (2005). The influence of added ionic salt on nanofiber uniformity for electrospinning of electrolyte polymer. Synthetic Met. 154(1-3): 209-212.

Lee, D., Han, S., Huh, J., Lee, D. (1999). Nitrogen oxides-sensing characteristics of WO_3-based nanocrystalline thick film gas sensor. Sensor Actuator. B: 60(1): 57-63.

Lee, E. R. (2003). Microdrop Generation. CRC Press, Boca Raton, FL.

Lee, J.S., Choi, K.H., Ghim, H.D., Kim, S.S., Chun, D.H., Kim, H. Y., Lyoo, W.S. (2004). Role of molecular weight of atactic poly(vinyl alcohol) (PVA) in the structure and properties of PVA nanofabric prepared by electrospinning. J. Appl. Polym. Sci. 93(4): 1638-1646.

Lee, K.H., Kim, H.Y., Bang, H.J., Jung, Y.H., Lee, S.G. (2003a). The change of bead morphology formed on electrospun polystyrene fibers. Polymer. 44(14): 4029-4034.

Lee, K.H., Kim, H.Y., Khil, M.S., Ra, Y.M., Lee D.R. (2003b). Characterization of nano-structured poly(1-caprolactone) nonwoven mats via electrospinning. Polymer. 44(4): 1287-1294.

Lee, K.H., Kim, H.Y., Ra, Y.M., Lee, D.R. (2003). Characterization of nanostructured poly(e caprolactone) nonwoven mats via electrospinning. Polymer. 44: 1287-1294.

Lee, S.G., Choi, S.S., Joo, C.W. (2002). Nanofiber formation of poly(ether imide) under various electrospinning conditions. J. Korean Fiber Soc. 39(1): 1-13.

Lemos, V.A., de Carvalho, A.L. (2010). Determination of cadmium and lead in human biological samples by spectrometric techniques: A review. Environ. Monit. Assess. 171: 255-265.

Letterman, R.D. (1999). Water Quality and Treatment. 5th Ed. (New York: American Water Works Association and McGraw-Hill.) ISBN 0070016593.

Lewis, L. N. (1993). Chemical catalysis by colloids and clusters. Chem. Rev. 93(8): 2693-2730.

Li, C.M., Jin, H.J., Botsaris, G.D., Kaplan D.L. (2005). Silk apatite composites from electrospun fibers. J. Mater. Res. 20(12): 3374-3384.

Li, D., Wang, Y.L., Xia Y.N. (2003b). Electrospinning of polymeric and ceramic nanofibers as uniaxially aligned arrays. Nano Lett. 3(8): 1167-1171.

Li, H., Wu, C., Tepper, F., Lee, J., Lee, C.N. (2009). Removal and retention of viral aerosols by a novel alumina nanofiber filter. J. Aerosol. Sci. 40(1): 65-71.

Li, Y.H., Liu, F.Q., Xia, B., Du, Q.J., Zhang, P., Wang, D.C., Wang, Z.H., Xia, Y.Z. (2010). Removal of copper from aqueous solution by carbon nanotube/calcium alginate composites. J. Hazard. Mater. 177: 876-880.

Liang, D., Hsiao, B.S., Chu, B., (2007). Functional electrospun nanofibrous scaffolds for biomedical applications. Adv. Drug. Deliver. Rev. 59(14): 1392-1412.

Lin, T., Wang, H. X., Wang, H. M., Wang X.G. (2004). The charge effect of cationic surfactants on the elimination of fibre beads in the electrospinning of polystyrene. Nanotechnol. 15(9): 1375-1381.

Lin, T., Wang, H.X., Wang, H.M., Wang, X.G. (2005). Effects of polymer concentration and cationic surfactant on the morphology of electrospun polyacrylonitrile nanofibres. J. Mater. Sci. Technol. 21: 9-12.

Liston, E.M., Martinu, L., Wertheimer, M.R. (1993). Plasma surface modification of polymers for improved adhesion - a critical-review. J. Adhes. Sci. Technol. 7: 1091-1127.

Liu, G. (1997) Diblock copolymer nanostructures. Macromolecular Symposia. 113(1): 233-248.

Lu, C., Chen, P., Li, J.F., Zhang Y.J. (2006). Computer simulation of electrospinning. Part I. Effect of solvent in electrospinning. Polymer. 47(3): 915-921.

Luoh, R., Hahn, H.T. (2006). Electrospun nanocomposite fiber mats as gas sensors. Compos. Sci. Technol. 66(14): 2436-2441.

Luu, Y.K., Kim, K., Hsiao, B.S., Chu, B., Hadjiargyrou, M. (2003). Development of a nanostructured DNA delivery scaffold via electrospinning of PLGA and PLA-PEG block copolymers. J. Control. Release. 89(2): 341-353.

Ma, P.X., Zhang, R. (1999). Synthetic nano-scale fibrous extracellular matrix. J. Biomed. Mater. Res., 46(1): 60-72.

Ma, Z., Kotaki, M., Ramakrishna, S. (2006). Surface modified nonwoven polysulphone (PSU) fiber mesh by electrospinning: A novel affinity membrane. J. Membr. Sci. 272: 179-187.

Macdiarmid A. G., JonesW. E., Norris I. D., Gao J., Johnson A. T., Pinto N. J., Hone J., Han B., Ko F.K., Okuzaki H., Llaguno M., (2001). Synthetic Met. 119 27.

Madhugiri, S., Dalton, A., Gutierrez, J., Ferraris, J.P. and Balkus Jr., K.J. (2003). Electrospun MEH-PPV/SBA-15 composite nanofibers using a dual syringe method. J. Am. Chem. Soc. 125(47): 14531-14538.

Madrakian, T., Afkhami, A., Zolfigol, M.A., Solgi, M. (2006). Separation, pre-concentration and determination of silver ion from water samples using silica gel modified with 2,4,6-trimorpholino-1,3,5-triazin. J. Hazard. Mater. 128: 67-72.

Mapolelo, M., Torto, N., Prior, B. (2005). Evaluation of yeast strains as possible agents for trace enrichment of metal ions in aquatic environments. Talanta. 65: 930-937.

Martin, R.B. (1998). Metal ion stabilities correlate with electron affinity rather than hardness or softness. Inorg. Chim. Acta. 283: 30-36.

Mata, Y.N., Blázquez, M.L., Ballester, A., González, F., Muñoz, J.A. (2009). Sugar-beet pulp pectin gels as biosorbent for heavy metals: preparation and determination of biosorption and desorption characteristics. Chem. Eng. J. 150: 289-301.

Matlock, M.M., Henke, K.R., Atwood, D.A. (2002). Effectiveness of commercial reagents for heavy metal removal from water with new insights for future chelate designs. J. Hazard. Mater. 92: 129-142.

Matsumiya, M., Shin, W., Izu, N., Murayama, N. (2003). Nano-structured thin-film Pt catalyst for thermoelectric hydrogen gas sensor. Sensor Actuator. 93(1-3): 309-315.

Maus, R., Goppelsröder, A., Umhauer, H. (1997). Viability of bacteria in unused air filter media. Atmos. Environ. 31(15): 2305-2310.

McKee, M.G., Elkins, C. L., Long, T.E. (2004a). Influence of self-complementary hydrogen bonding on solution rheology/electrospinning relationships. Polymer. 45(26): 8705-8715.

McKee, M.G., Wilkes, G.L. Colby, R.H., Long, T.E. (2004b). Correlations of solution rheology with electrospun fiber formation of linear and branched polyesters. Macromolecules. 37(5): 1760-1767.

McKee, M.G., Hunley, M.T., Layman, J.M., Long T.E. (2006a). Solution rheological behavior and electrospinning of cationic polyelectrolytes. Macromolecules 39(2):575.

Megelski, S., Stephens, J.S., Chase, D.B., Rabolt J.F. (2002). Micro- and nanostructured surface morphology on electrospun polymer fibers. Macromol. 35(22): 8456-8466.

Mermet, J.M. (2005). Is it still possible, necessary and beneficial to perform research in ICP-atomic emission spectrometry? J. Anal. At. Spectrom. 20: 11-16.

Min, B., Lee, S.W., Lim, J.N., You, Y., Lee, T.S., Kang, P.H., Park, W.H. (2004a). Chitin and chitosan nanofibers: Electrospinning of chitin and deacetylation of chitin nanofibers. Polymer, 45(21): 7137-7142.

Min, B.M., You, Y., Kim, J.M., Lee, S.J., Park, W.H. (2004b). Formation of nanostructured poly(lactic-co-glycolic acid)/chitin matrix and its cellular response to normal human keratinocytes and fibroblasts. Carbohyd. Polym. 57(3): 285.

Miretzky, P., Muñoz, C., Carrillo-Chavez, A. (2010). Cd (II) removal from aqueous solution by *Eleocharis acicularis* biomass, equilibrium and kinetic studies. Biores. Technol.101: 2637-2642.

Mishra, P.C., Patel, R.K. (2009). Removal of lead and zinc ions from water by low cost adsorbents. J. Hazard. Mater. 168: 319-325.

Mishustin, A.I. (2007). Formation Constants for Complexes of Transition-Metal Cations with O- and N-Donor Ligands in Aqueous Solutions, Russ. J. Inorg. Chem. 52: 283-288.
Mitchell, S.B., Sanders, J.E. (2006). A unique device for controlled electrospinning. J. Biomed. Materials Res. Part A. 78A(1): 110-120.
Mit-uppatham, C., Nithitanakul, M., Supaphol, P. (2004a). Effects of solution concentration, emitting electrode polarity, solvent type, and salt addition on electrospun polyamide-6 fibers: a preliminary report. Macromol. Sy. 216(1): 293-300.
Mit-uppatham, C., Nithitanakul, M., Supaphol, P. (2004b). Ultrafine electrospun polyamide-6 fibers: effect of solution conditions on morphology and average fiber diameter. Macromol. Chem. Physic. 205(17): 2327-2338.
Mo, X.M., Weber H.J. (2004). Electrospinning P(LLA-CL) nanofiber: a tubular scaffold fabrication with circumferential alignment. Macromol. Sy. 217(1): 413-416.
Mo, X.M., Xu, C.Y., Kotaki, M., Ramakrishna, S. (2004a). Electrospun P(LLA-CL) nanofiber: a biomimetic extracellular matrix for smooth muscle cell and endothelial cell proliferation. Biomater. 25: 1883-1890.
Morota, K., Matsumoto, H., Mizukoshi, T., Konosu, Y., Minagawa, M., Tanioka, A., Yamagata, Y., Inoue K. (2004). Poly(ethylene oxide) thin films produced by electrospray deposition: morphology control and additive effects of alcohols on nanostructure. J. Colloid Interf. Sci. 279(2): 484-492.
Morozov, V. N., Morozova, T. Y. and Kallenbach N. R. (1998). Atomic force microscopy of structures produced by electrospraying polymer solutions. Int. J. Mass. Spectrom. 178: 143-159.
Mottola, H.A. (1992). Chemical immobilization in chemistry. In: Chemically modified surfaces, ed by Mottola, H.A., Steinmetz, J.R., Elsevier, New York, pp. 1-14.
Muhammad, S., Shah, M.T., Khan, S. (2010). Arsenic health risk assessment in drinking water and source apportionment using multivariate statistical techniques in Kohistan region, Northern Pakistan. Food Chem. Toxicol. 48: 2855-2864.
Muhammad, S., Shah, M.T., Khan, S. (2011). Health risk assessment of heavy metals and their source apportionment in drinking water of Kohistan region, Northern Pakistan. Microchem. J. 98: 334-343.
Murthy, Z.V.P., Chaudhari L.B. (2008). Application of nanofiltration for the rejection of nickel ions from aqueous solutions and estimation of membrane transport parameters. J. Hazard. Mater. 160(1): 70–77.
Muthukrishnan, M., Guha, B.K. (2008). Effect of pH on rejection of hexavalent chromium by nanofiltration. Desalination 219 (1–3): 171–178.
Namasivayam, C., Kadirvelu, K. (1999). Uptake of mercury (II) from wastewater by activated carbon from unwanted agricultural solid by-product: coirpith. Carbon 37: 79-84.
Naseem, R., Tahir, S.S. (2001). Removal of Pb(II) from aqueous solution by using bentonite as an adsorbent. Water Res. 35: 3982-3986.
Nisbet, D.R., Rodda, A.E., Finkelstein, D.I., Horne, M.K., Forsythe, J.S., Shen, W. (2009). Surface and bulk characterisation of electrospun membranes: Problems and improvements. Colloid Surface B: Biointerfaces 71: 1-12.
Norris I. D., Shaker M. M., Ko F. K. and Macdiarmid A. G. (2000). Synthetic Met. 114: 109.
Oh, G.-Y., Ju, Y.-W., Kim, M.-Y., Jung, H.-R., Kim, H.J., Lee, W.-J. (2008). Adsorption of toluene on carbon nanofibers prepared by electrospinning. Sci. Total Environ. 393: 341-347.

Oh, S., Kwak, M.Y., Shin, W.S. (2009). Competitive sorption of lead and cadmium onto sediments. Chem. Eng. J. 152: 376-388.

Ohno, K., Ishikawa, K., Kurosawa, Y., Matsui, Y., Matsushita, T., Magara, Y. (2010). Exposure assessment of metal intakes from drinking water relative to those from total diet in Japan. Water Sci Technol. 62(11): 2694-2701.

Oliveira, L., Franca, A.S., Alves, T.M., Rocha, S.D.F. (2008). Evaluation of untreated coffee husks as potential biosorbents for treatment of dye contaminated waters. J. Hazard. Mater. 155: 507-512.

Ondarçuhu, T., Joachim. C. (1998). Drawing a single nanofibre over hundreds of microns. Europhys. Lett. 42(2): 215-220.

Oyaro, N., Juddy, O., Murago, E.N.M., Gitonga, E. (2007). The contents of Pb, Cu, Zn and Cd in meat in Nairobi, Kenya. Int. J. Food Agric. Environ. 5: 119-121.

Palanivelu, K.V., Velan, M. (2006). Biosorption of copper(II) and cobalt(II) from aqueous solutions by crab shell particles, Bioresource Technol. 97: 1411-1419.

Pastircakova, K. (2004). Determination of trace metal concentrations in ashes from various biomass, Mater. Energy Edu. Sci. Technol. 13: 97-104.

Patanaik, A., Jacobs V., Anandjiwala R.D., (2010). J. Membr. Sci. 352: 136-142.

Paulino, A.T., Minasse, F.A.S., Guilherme, M.R., Reis, A.V., Muniz, E.C., Nozaki, J. (2006). Novel adsorbent based on silkworm chrysalides for removal of heavy metals from wastewaters. J. Colloid Interf. Sci. 301: 479-487.

Pearson, R.G. (1963). Hard and Soft Acids and Bases, J. Am. Chem. Soc. 85: 3533-3539.

Pierce, M.L., Moore, C.B. (1982). Adsorption of arsenite and arsenate on amorphous iron hydroxide. Water Res. 16: 1247-1253.

Pillay, K., Cukrowska, E.M., Coville, N.J. (2009). Multi-walled carbon nanotubes as adsorbents for the removal of parts per billion levels of hexavalent chromium from aqueous solution. J. Hazard. Mater. 166: 1067-1075.

Pinto, N.J., Ramos, I., Rojas, R., Wang, P., Johnson, A.T.Jr. (2008). Electric response of isolated electrospun polyaniline nanofibers to vapours of aliphatic alcohols. Sensor Actuator. B: 129(2): 621-627.

Plattes, M., Bertrand, A., Schmitt, B., Sinner, J., Verstraeten, F., Welfring, J. (2007). Removal of tungsten oxyanions from industrial wastewater by precipitation, coagulation and flocculation processes. J. Hazard. Mater. 148: 613-615.

Pornsopone, V., Supaphol, P., Rangkupan, R., Tantayanon, S. (2005). Electrospinning of methacrylate-based copolymers: effects of solution concentration and applied electrical potential on morphological appearance of as-spun fibers. Polym. Eng. Sci. 45(8): 1073-1080.

Pourang, N. (1995). Heavy metal bioaccumulation in different tissue of two fish species with regards to their feeding habits and trophic levels. Environ. Monit. Asses. 35: 207-219.

Qu, R., Wang, C., Ji, C., Sun, C., Sun, X., Cheng, G. (2005). Preparation, characterization, and metal binding behavior of novel chelating resins containing sulfur and polyamine, J. Appl. Polym. Sci. 95: 1558-1656.

Ramakrishna, S., Fujihara, K., Teo, W., Lim, T., Ma, Z. (2005). An Introduction to Electrospinning and Nanofibers. World Scientific Publishing Co. Singapore.

Ramakrishna, S., Fujihara, K., Teo, W-E., Yong, T., Ma, Z., Ramaseshan, R. (2006). Electrospun nanofibers: solving global issues. Materials Today. 9(3): 40-50.

Ramírez, S.A., Gordillo, G.J. (2009). Adsorption and reduction of palladium–dimethylglyoxime complex. J. Electroanal. Chem. 629: 147-151.

Rao, G.P., Lu, C., Su, F. (2007). Sorption of divalent metal ions from aqueous solution by carbon nanotubes: a review. Sep. Purif. Technol. 58: 224-231.

Rashchi, F., Finch, J.A., Sui, C. (2004). Action of DETA, dextrin and carbonate on lead contaminated sphalerite, Colloids Surf. A: Physicochem. Eng. Aspects 245: 21-27.

Ratner, B.D. (1995). Surface modification of polymers - chemical, biological and surface analytical challenges. Biosens. Bioelectron. 10: 797-804.

Rayleigh, J.W.S. (1882). On the equilibrium of liquid conducting mass charged with electricity. Philosophical Magazine 14(5th Series): 184-186.

Reneker D.H., Chun I., (1996). Nanometre diameter fibres of polymer, produced by electrospinning. Nanotechnology. 7: 216-223.

Reneker, D.H., Fong, H. (2006). Polymeric nanofibers: Introduction. In: Polymeric Nanofibers. ACS Symposium Series 918. Edited by D. H. Reneker and H. Fong. Oxford University Press (USA). p. 430.

Reneker, D.H., Yarin, A.L. (2008). Electrospinning jets and polymer nanofibers. Polymer. 49: 2387-2425.

Reneker, D.H., Kataphinan, W., Theron, A., Zussman, E., Yarin, A.L. (2002). Nanofiber garlands of polycaprolactone by electrospinning. Polymer. 43(25): 6785-6794.

Reneker, D.H., Yarin, A. L., Fong, H., Koombhongse, S. (2000). Bending instability of electrically charged liquid jets of polymer solutions in electrospinning. J. Appl. Physic. 87(9): 4531-4547.

Rezaei, B., Sadeghi, E., Meghdadi, S. (2009). Nano-level determination of copper with atomic absorption spectrometry after pre-concentration on N,N-(4-methyl-1,2-phenylene)diquinoline-2-carboxamide-naphthalene. J. Hazard. Mater. 168: 787-792.

Rho, K.S., Jeong, L., Lee, G., Seo, B., Park, Y.J., Hong, S., Roh, S., Cho, J.J., Park, W.H., Min, B. (2006). Electrospinning of collagen nanofibers: Effects on the behavior of normal human keratinocytes and early-stage wound healing. Biomaterials. 27(8): 1452-1461.

Riboldi, S.A., Sampaolesi, M., Neuenschwander, P., Cossu, G., Mantero, S. (2005). Electrospun degradable polyesterurethane membranes: Potential scaffolds for skeletal muscle tissue engineering. Biomaterials. 26(22): 4606-4615.

Rogers Jr., W. Sclar, M. The Journal of Physical Chemistry B, doi: 10.1021/j150338a014. ACS Legacy Archive

Ryu, Y.J., Kim, H.Y., Lee, K.H., Park, H.C., Lee, D.R. (2003). Transport properties of electrospun nylon-6 nonwoven mats. Eur. Polym. J. 39: 1883-1889.

Saeed, A., Iqbal, M., Akhtar, M.W. (2005). Removal and recovery of lead(II) from single and multimetal (Cd, Cu, Ni, Zn) solutions by crop milling waste (black gram husk). J. Hazard. Mater. 117: 65-73.

Sakai, S., Antoku, K., Yamaguchi, T., Kawakami, K. (2008). Development of electrospun poly(vinyl alcohol) fibers immobilizing lipase highly activated by alkyl-silicate for flow-through reactors. J. Membr. Sci. 325: 454-459.

Samal, S., Das, R.R., Dey, R.K., Acharya, S. (2000) Chelating resins VI: chelating resins of formaldehyde condensed phenolic Schiff bases derived from 4,4-diaminodiphenyl ether with hydroxybenzaldehydes-synthesis, characterization, and metal ion adsorption studies. J. Appl. Polym. Sci. 77: 967-981.

Sampera, E., Rodrígueza, M., De la Rubia, M.A., Prats, D. (2009). Removal of metal ions at low concentration by micellar-enhanced ultrafiltration (MEUF) using sodium dodecyl sulfate (SDS) and linear alkylbenzene sulfonate (LAS). Sep. Purif. Technol. 65: 337-342.

Saracoglu, S., Soylak, M., Elc, L. (2003). Separation/preconcentration of trace heavy metals in urine, sediment and dyalisis concentrates by coprecipitation with samarium hydroxide for atomic absorption spectrometry. Talanta. 59: 287-293.

Sarı, A., Tuzen, M. (2009). Kinetic and equilibrium studies of biosorption of Pb(II) and Cd(II) from aqueous solution by macrofungus (*Amanita rubescens*) biomass. J. Hazard. Mater. 164: 1004-1011.

Sastre, J., Sahuquillo, A., Vidal, M., Rauret, G. (2002). Determination of Cd, Cu, Pb and Zn in environmental samples: microwave-assisted total digestion versus aqua regia and nitric acid extraction. Anal. Chim. Acta. 462: 59-72.

Schiewer, S., Patil, S.B. (2008). Modeling the effect of pH on biosorption of heavy metals by citrus peels. J. Hazard. Mater. 157: 8-17.

Schreuder-Gibson, H., Gibson, P., Senecal, K., Sennett, M., Walker, J., Yeomans, W., Ziegler, D., Tsai, P.P., (2002a). Protective textile materials based on electrospun nanofibers. J. Adv. Mater. 34(3): 44-55.

Senecal, K., Samuelson, L., Sennett, M., Schreuder-Gibson H., US patent application publication, US 2001/0045547.

Senecal, K.J., Ziegler, D.P., He, J., Mosurkal, R., Schreuder-Gibson, H., Samuelson, L.A. (2002) Materials Research Society Symposium Proceedings, 708 BB9.5.1.

Shahalam, A.M., Al-Harthy, A., Al-Zawhry, A. (2002). Feed water pretreatment in reverse osmosis systems in the Middle East. Desalination. 150: 235-245.

Shawon, J., Sung, C. M. (2004). Electrospinning of polycarbonate nanofibers with solvent mixtures THF and DMF. J. Mater. Sci. 39(14): 4605-4613.

Shenoy, S.L., Bates, W.D., Wnek, G. (2005a). Correlations between electrospinnability and physical gelation. Polymer. 46(21): 8990-9004.

Shevchenko, R.V., James, S.L., James, S.E. (2010). A review of tissue-engineered skin bioconstructs available for skin reconstruction. J. Royal Soc.: Interface 7: 229-258.

Shim, W.G., Kim, C., Lee, J.W., Yun, J.J., Jeong, Y., Moon, H., Yang, K.S. (2006). Adsorption Characteristics of Benzene on Electrospun-Derived Porous Carbon Nanofibers. J. Appl. Polym. Sci. 102: 2454-2462.

Shin, Y.M., Hohman, M.M. Brenner, M.P., Rutledge G.C. (2001b). Experimental characterization of electrospinning: the electrically forced jet and instabilities. Polymer. 42(25): 9955-9967.

Shin, Y.M., Hohman, M.M., Brenner, M.P., Rutledge, G.C. (2001a). Electrospinning: a whipping fluid jet generates submicron polymer fibers. Appl. Physic. Lett. 78(8): 1149-1151.

Shukla, S., Brinley, E., Cho, H.J., Seal, S. (2005). Electrospinning of hydroxypropyl cellulose fibers and their application in synthesis of nano and submicron tin oxide fibers. Polymer. 46(26): 12130-12145.

Shummer, P., Tebel, K.H. (1983). A new elongational rheometer for polymer solutions. J. Non-Newton. Fluid. 12: 331-347.

Simon-Deckers, A., Gouget, B., Mayne-L'Hermite, M., Herlin-Boime, N., Reynaud, C., Carrière, M., (2008). In vitro investigation of oxide nanoparticle and

carbonnanotubetoxicity and intracellular accumulation in A549 human pneumocytes. Toxicology 253 (1–3) 137–146.
Smit, E., Buttner, U., Sanderson R.D. (2005). Continuous yarns from electrospun fibers. Polymer 46(8): 2419-2423.
Son, W.K., Youk, J.H., Lee, T.S., Park, W.H. (2004d). The effects of solution properties and polyelectrolyte on electrospinning of ultrafine poly(ethylene oxide) fibers. Polymer. 45(9): 2959-2966.
Spasova, M., Manolova, N., Paneva, D., Rashkov, I. (2004). Preparation of chitosan-containing nanofibres by electrospinning of chitosan/poly(ethylene oxide) blend solutions. e-polymers, no. 056.
Spivak, A.F., Dzenis Y.A. (1998). Asymptotic decay of radius of a weakly conductive viscous jet in an external electric field. Appl. Physic. Lett. 73(21): 3067-3069.
Spivak, A.F., Dzenis, Y.A. (1999). A condition of the existence of a conductive liquid meniscus in an external electric field. J.Appl. Mechanic 66(4): 1026-1028.
Spivak, A.F., Dzenis, Y.A., Reneker D.H. (2000). A model of steady state jet in the electrospinning process. Mech. Res. Commun. 27(1): 37-42.
Srinivasan, G., Reneker D.H. (1995). Structure and morphology of small diameter electrospun aramid fibers. Polym. Int. 36(2): 195-201.
Srivastava, N.K., Majumder, C.B. (2008). Novel biofiltration methods for the treatment of heavy metals from industrial wastewater. J. Hazard. Mater. 151: 1-8.
Starvin, A.M., Rao, T.P. (2004). Removal and recovery of mercury(II) from hazardous wastes using 1-(2-thiazolylazo)-2-naphthol functionalized activated carbon as solid phase extractant. J. Hazard. Mater. 113: 75-79.
Stefánsson, A., Gunnarsson, I., Giroud, N. (2007). New methods for the direct determination of dissolved inorganic, organic and total carbon in natural waters by Reagent-Free Ion Chromatography and inductively coupled plasma atomic emission spectrometry. Anal. Chim. Acta. 582: 69-74.
Stumm, W. (1992). Chemistry of the Solid-Water Interface, John Wiley and Sons, New York.
Subbiah, T., Bhat, G.S., Tock, R.W., Parameswaran, S., Ramkumar, S.S. (2005). Electrospinning of nanofibers. J. Appl. Polym. Sci. 96(2): 557-569.
Subramanian, A., Vu, D., Larsen, G.F., Lin, H.Y. (2005). Preparation and evaluation of the electrospun chitosan/PEO fibers for potential applications in cartilage tissue engineering. J. Biomater. Sci. 16(7): 861-873.
Sud, D., Mahajan, G., Kaur, M.P. (2008). Agricultural waste material as potential adsorbent for sequestering heavy metal ions from aqueous solutions - A review. Bioresour. Technol. 99: 6017-6027.
Sukigara, S., Gandhi, M., Ayutsede, J., Micklus, M., Ko, F. (2003). Regeneration of Bombyx mori silk by electrospinning. Part 1. Processing parameters and geometric properties. Polymer. 44(19): 5721-5727.
Sun, B. (1994). Study on the mechanism of nylon-6,6 dissolving process using $CaCl_2$/MEOH as the solvent. Chin. J. Polym. Sci. 12(1): 57-65.
Sun, C.M., Qu, R.J., Ji, C.N., Wang, C.H., Sun, Y.Z., Yue, Z.W., Chang, G.X. (2006). Talanta.70: 14.
Supaphol, P., Mit-uppatham, C., Nithitanakul, M. (2005b). Ultrafine electrospun polyamide-6 fibers: effects of solvent system and emitting electrode polarity on morphology and average fiber diameter. Macromol. Mater. Eng. 290(9): 933-942.

Suvorov, D., Freer, R. (2001). Microwave materials and their applications. (2000). J. Eur. Ceramic Soc.. 21(15): 5-9.

Szécsényi, K.M., Leovac, V.M., Kovács, A., Pokol, G., Jacmovic, Z.K. (2005). Transition metal complexes with pyrazole-based ligands. J. Therm. Anal. Calorim. 1-5:

Takahashi, T., Taniguchi, M., Kawai, T. (2005). Fabrication of DNA nanofibers on a planar surface by electrospinning. Japan. J. Appl. Physic Part 2: 44(24-27): L860.

Tan, S.-H., Inai, R., Kotaki, M., Ramakrishna, S. (2005). Systematic parameter study for ultra-fine fiber fabrication via electrospinning process. Polymer. 46(16): 6128-6134.

Tang, Q., Tang, X., Hu, M., Li, Z., Chen, Y., Lou, P. (2010). Removal of Cd(II) from aqueous solution with activated Firmiana Simplex Leaf: Behaviors and affecting factors. J. Hazard. Mater. 179: 95-103.

Taylor, G. (1964). Disintegration of water drops in an electric field. Proceedings of the Royal Society of London. Series A, Mathematical and Physical Sciences 280(1382): 383-397.

Taylor, G. (1969). Electrically driven jets. Proceedings of the Royal Society of London. Series A, Mathematical and Physical Sciences. 313(1515): 453-475.

Teo, W.E., Ramakrishna, S. (2006). A review on electrospinning design and nanofibre assemblies. Nanotechnology. 17(14): 89-104.

Teo, W.E., Kotaki, M., Mo, X.M., Ramakrishna, S. (2005). Porous tubular structures with controlled fibre orientation using a modified electrospinning method. Nanotechnology. 16: 918-924.

Theron, S.A., Zussman, E., Yarin A.L. (2004). Experimental investigation of the governing parameters in the electrospinning of polymer solutions. Polymer. 45(6): 2017-2030.

Theron, S.A., Yarin, A.L., Zussman, E., Kroll, E. (2005). Multiple jets in electrospinning: experiment and modeling. Polymer. 46(9): 2889-2899.

Tokuyama, H., Hisaeda, J., Nii, S., Sakohara, S. (2010). Removal of heavy metal ions and humic acid from aqueous solutions by co-adsorption onto thermosensitive polymers. Sep. Purif. Technol. 71: 83-88.

Trofimov, B.A. in: Jones R.A. (editor), The Chemistry of Heterocyclic Compounds, Pyrroles, Vol. 48, J. Wiley, New York, 1992, Chap. 2, Vinylpyrroles, 131-298.

Tsai, P.P., Schreuder-Gibson, H., Gibson, P. (2002). Different electrostatic methods for making electret filters. J. Electrostat. 54(3-4): 333-341.

Tuzen, M., Parlar, K., Soylak, M. (2005). Enrichment/separation of cadmium(II) and lead(II) in environmental samples by solid phase extraction. J. Hazard. Mater. 121: 79-87.

U.S. Environmental Protection Agency. (2001). Trace elements in water, solids, and biosolids by inductively coupled plasma-atomic emission spectrometry. EPA-821-R-01-010. Method 200.7. New York.

Um, I.C., Fang, D.F., Hsiao, B.S., Okamoto, A., Chu, B. (2004). Electro-spinning and electro-blowing of hyaluronic acid. Biomacromol. 5(4): 1428-1436.

Uyama, Y., Kato, K., Deada, Y. (1998). Surface modification of polymers by grafting, Adv. Polym. Sci. 137: 1-39.

Vasiliev, A.N., Golovko, L.V., Trachevsky, V.V., Hall, G.S., Khinast, J.G. (2009). Adsorption of heavy metal cations by organic ligands grafted on porous materials. Micropor. Mesopor. Mater.118: 251-257.

Wan, Y.Q., He, J.H., Wu, Y., Yu, J.Y. (2007). Vibration-electrospinning for high-concentration poly(butylene succinate)/chloroform solution. International Journal of Electrospun Nanofibers and Applications 1(1): 17-28.

Wang, H.J., Zhou, A.L., Peng, F., Yu, H., Yang, J. (2007). Mechanism study on adsorption of acidified multiwalled carbon nanotubes to Pb(II). J. Colloid Interface Sci. 316: 277-283.

Wang, L.K., Hung, Y.T., Shammas, N.K. (2007). Advanced physicochemical treatment technologies. In: Handbook of Environmental Engineering, Vol. 5. Humana, New Jersey.

Wang, X., Min, M., Liu, Z., Yang, Y., Zhou, Z., Zhu, M., Chen, Y., Hsiao, B.S. (2011). Poly(ethyleneimine) nanofibrous affinity membrane fabricated via one step wet-electrospinning from poly(vinyl alcohol)-doped poly(ethyleneimine) solution system and its application. J. Membr. Sci. 379: 191-199.

Wang, X., Um, I.C., Fang, D., Okamoto, A., Hsiao, B.S., Chu, B. (2005). Formation of water-resistant hyaluronic acid nanofibers by blowing-assisted electro-spinning and non-toxic post treatments. Polymer. 46(13): 4853-4867.

Wang, Y., Hsieh, Y. (2003). Enzyme immobilization via electrospinning of polymer/enzyme blends. Polymer Preprints. 44(1): 1212-1213.

Wang, Y., Hsieh, Y. (2004). Enzyme immobilization to ultra-fine cellulose fibers via amphiphilic polyethylene glycol spacers. J. Polym. Sci. Part A: 42(17): 4289-4299.

Wang, Y., Hsieh, Y.L. (2008). Immobilization of lipase enzyme in polyvinyl alcohol (PVA) nanofibrous membranes. J. Membr. Sci. 309: 73-81.

Wang, Z.G., Xu, Z.K., Wan, L.S., Wu, J., Innocent, C., Seta, P. (2006). Nanofibrous membranes containing carbon nanotubes: electrospun for redox enzyme immobilization. Macromol. Rapid Commun. 27(7): 516-521.

Wannatong, L., Sirivat, A., Supaphol, P. (2004). Effects of solvents on electrospun polymeric fibers: preliminary study on polystyrene. Polym. Int. 53(11): 1851-1859.

Warner, S.B., Buer, A., Grimler, M., Ugbolue, S.C., Rutledge, G.C., Shin, M.Y. (1998). A fundamental investigation of the formation and properties of electrospun fibers. Annual Report, M98-D01, National Textile Center.

Waters, C.M., Noakes, T.J., Pavery, I., Hitomi C. (1992). US Patent 5088807.

Wei, M., Kang, B.W., Sung, C.M. and Mead, J. (2006a). Core-sheath structure in electrospun nanofibers from polymer blends. Macromol. Mater. Eng.291(11): 1307-1314.

Wei, M., Kang, B.W., Sung, C.M., Mead, J. (2006b). Preparation of nanofibers with controlled phase morphology from electrospinning of polybutadiene-polycarbonate blends. In: Polymeric Nanofibers. ACS Symposium Series 918. Edited by D. H. Reneker and H. Fong. Oxford University Press (USA), p. 149.

World Health Organization, Geneva. Guidelines for drinking water quality. 2nd ed. vol 2, Australia, 1996.

Wu, L., Yuan, X., Sheng, J. (2005). Immobilization of cellulase in nanofibrous PVA membranes by electrospinning J. Membr. Sci. 250: 167-173.

Wu, X.H., Wang, L., Yu, H., Huang, Y. (2005). Effect of solvent on morphology of electrospinning ethyl cellulose fibers. J. Appl. Polym. Sci. 97(3): 1292-1297.

Xin, Y., Huang, Z.H., Yan, E.Y., Zhang, W., Zhao, Q. (2006). Controlling poly(p phenylene vinylene)/poly(vinyl pyrrolidone) composite nanofibers in different morphologies by electrospinning. Appl. Physic Lett. 89(5): 053101.

Yamada, Y., Seno, Y., Masuoka, Y., Yamashita, K. (1998). Nitrogen oxides sensing characteristics of Zn_2SnO_4 thin film. Sensor Actuator. B: B49(3): 248-252.

Yan, X., Liu, G., Li, Z. (2004). Preparation and Phase Segregation of Block Copolymer Nanotube Multiblocks. J. Am. Chem. Soc. 126(32): 10059-10066.

Yan, X.H., Liu, G.J., Liu, F.T., Tang, B.Z., Peng, H., Pakhomov, A.B., Wong, C.Y. (2001). Superparamagnetic triblock copolymer/Fe_2O_3 hybrid nanofibers. Angew. Chem. Int. Ed., 40(19): 3593-3596.

Yanagisawa, H., Matsumoto, Y., Machida, M. (2010). Adsorption of Zn(II) and Cd(II) ions onto magnesium and activated carbon composite in aqueous solution. Appl. Surf. Sci. 256: 1619-1623.

Yang, F., Murugan, R., Wang, S., Ramakrishna, S. (2005). Electrospinning of nano/micro scale poly(L-lactic acid) aligned fibers and their potential in neural tissue engineering. Biomaterials. 26(15): 2603-2610.

Yang, G.C., Pan, Y., Gong, J., Shao, C.L., Wen, S.B., Shao, C., Qu, L.Y. (2004). Beaded fiber mats of PVA containing unsaturated heteropoly salt. Chin. Chem. Lett. 15(10): 1212-1214.

Yang, M., Xie, T., Peng, L., Zhao, Y., Wang, D. (2007). Fabrication and photoelectric oxygen sensing characteristics of electrospun Co doped ZnO nanofibres. Appl. Physic A: 89(2): 427-430.

Yao, L., Haas, T.W., Guiseppi-Elie, A., Bowlin, G.L., Simpson, D.G., Wnek, G.E. (2003). Electrospinning and stabilization of fully hydrolyzed poly(vinyl alcohol) fibers. Chem. Mater. 15(9): 1860-1864.

Yao, Y.Y., Zhu, P.X., Ye, H., Niu, A.J., Gao, X.S., Wu, D.C. (2005). Polysulfone nanofibers prepared by electrospinning and gas-jet/electrospinning. Acta Polymerica Sinica (5): 687-692.

Yarin, A.L., Koombhongse, S., Reneker, D.H. (2001b). Taylor cone and jetting from liquid droplets in electrospinning of nanofibers. J. Appl. Physic. 90(9): 4836-4846.

Yarin, A.L., Zussman, E. (2004). Upward needleless electrospinning of multiple nanofibers. Polymer. 45(9): 2977-2980.

Yarin, A.L., Koombhongse, S., Reneker, D.H. (2001a). Bending instability in electrospinning of nanofibers. J. Appl. Physic. 89(5): 3018-3026.

Yoshitake, H., Yokoi, T., Tatsumi, T. (2003). Adsorption behavior of arsenate at transition metal cations captured by amino-functionalized mesoporous silica, Chem. Mater. 15: 1713-1721.

You, Y., Lee, S.J., Min, B.M., Park, W.H. (2006). Effect of solution properties on nanofibrous structure of electrospun poly(lactic-co-glycolic acid). J. Appl. Polym. Sci. 99(3): 1214-1221.

Yu, J.H., Fridrikh, S.V., Rutledge, G.C. (2004). Production of submicrometer diameter fibers by two-fluid electrospinning. Adv. Mater. 16(17): 1562-1566.

Yuan, X.Y., Zhang, Y.Y., Dong, C.H., Sheng, J. (2004). Morphology of ultrafine polysulfone fibers prepared by electrospinning. Polymer International 53(11): 1704-1710.

Yun, K.S., Cho, B.W., Jo, S.M., Lee, W.I., Park, K.Y., Kim H.S., Kim, U.S., Ko, S.K., Chun S.W., Choi S.W. (2001). PCT/KR00/00501.

Zeng, J., Xu, X., Chen, X.S., Liang, Q., Bian, X., Yang, L., Jing, X. (2003b). Biodegradable electrospun fibers for drug delivery. Journal of Controlled Release 92(3): 227-231.

Zeng, J., Yang, L.X., Liang, Q.Z., Zhang, X.F., Guan, H.L., Xu, X.L., Chen, X.S., Jing, X.B. (2005). Influence of the drug compatibility with polymer solution on the release kinetics of electrospun fiber formulation. J. Control Release.105: 43-51.

Zhang, C.X., Yuan, X.Y., Wu, L.L., Sheng, J. (2005). Drug-loaded ultrafine poly(vinyl alcohol) fibre mats prepared by electrospinning. e-Polymers. 072.

Zhang, L.N., Wu, Y.J., Qu, X.Y., Li, Z.S., Ni, J.R. (2009). Mechanism of combination membrane and electro-winning process on treatment and remediation of Cu^{2+} polluted water body. J. Environ. Sci. 21: 764-769.

Zhang, Y., Qu, R., Sun, C., Chen, H., Wang, C., Ji, C., Yin, P. (2009). Comparison of synthesis of chelating resin silica-gel-supported diethylenetriamine and its removal properties for transition metal ions. J. Haz. Mater. 163: 127-135.

Zhao, S.L., Wu, X.H., Wang, L.G., Huang, Y. (2004). Electrospinning of ethyl cyanoethyl cellulose/tetrahydrofuran solutions. J. Appl. Polym. Sci. 91: 242-246.

Zhao, S.L., Wu, X.H., Wang, L.G., Huang, Y. (2004). Electrospinning of ethyl- cyanoethyl cellulose/tetrahydrofuran solutions. J. Appl. Polym. Sci. 91, pp. 242-246.

Zhou, L., Wang, Y., Liu, Z., Huang, Q. (2009). Characteristics of equilibrium, kinetics studies for adsorption of Hg(II), Cu(II), and Ni(II) ions by thiourea-modified magnetic chitosan microspheres. J. Hazard. Mater. 161: 995-1002.

Zhu, Y.B., Gao, C.Y., Liu, X.Y., Shen, J.C. (2002). Surface modification of polycaprolactone membrane via aminolysis and biomacromolecule immobilization for promoting cytocompatibility of human endothelial cells. Biomacromol. 3(6): 1312-1319.

Ziabari, M., Mottaghitalab, V., Haghi, A.K. (2009). Application of direct tracking method for measuring electrospun nanofiber diameter. Brazilian J. Chem. Eng. 26: 53 - 62.

Zolotov, Yu.A., Malofeeva, G.I., Petrukhin, O.M., Timerbaev, A.R. (1987). New methods for pre-concentration and determination of heavy metals in natural water. Pure Appl. Chem. 59: 497-504.

Zong, D.F., Kim, K., Ran, S., Hsiao, B.S., Chu, B., Brathwaite, C., Li, S., Chen, E. (2002). Nonwoven nanofiber membranes of poly(lactide) and poly(glycolide-co-lactide) via electrospinning and application for anti-adhesions. Polymer Preprints. 43:659-660.

Zong, X., Fang, D., Kim, K., Ran, S., Hsiao, B.S., Chu, B., Brathwaite, C., Li, S., Chen, E. (2002). Nonwoven nanofiber membranes of poly(lactide) and poly(glycolide-co-lactide) via electrospinning and application for anti-adhesions. Polymer Preprints. 43(2): 659-660.

Zong, X., Kim, K., Fang, D., Ran, S., Hsiao, B.S., Chu, B. (2002). Structure and process relationship of electrospun bioabsorbable nanofiber membranes. Polymer. 43(16): 4403-4412.

Zong, X., Li, S., Chen, E., Garlick, B., Kim, K., Fang, D., Chiu, J., Zimmerman, T., Brathwaite, C., Hsiao, B.S., Chu, B. (2004). Prevention of post surgery-induced abdominal adhesions by electrospun bioabsorbable nanofibrous poly(lactide-co-glycolide)-based membranes. Annals Surgery, 240(5): 910-915.

Zong, X.H., Kim, K., Fang, D., Ran, S.F., Hsiao, B.S., Chu, B. (2002). Structure and process relationship of electrospun bioabsorbable nanofiber membranes. Polymer. 43(16): 4403-4412.

Zussman, E., Rittel, D., Yarin, A.L. (2003). Failure modes of electrospun nanofibers. Applied Physic Lett. 82(22): 3958-3960.

Zussman, E., Yarin, A., Weihs, D. (2002). A micro-aerodynamic decelerator based on permeable surfaces of nanofiber mats. Experiments in Fluids 33(2): 315-320.